

# Perfectly Spherical Bloch Hyper-spheres from Quantum Matrix Geometry

Kazuki Hasebe

*National Institute of Technology, Sendai College, Ayashi, Sendai, 989-3128, Japan*

khasebe@sendai-nct.ac.jp

*June 26, 2024*

## Abstract

Exploiting analogies between the precessing quantum spin system and the charge-monopole system, we construct Bloch hyper-spheres with *exact* spherical symmetries in arbitrary dimensions. Such Bloch hyper-spheres are realized as a collection of the orbits of a precessing quantum spin. The geometry of Bloch hyper-spheres is exactly equal to the quantum Nambu geometry of higher dimensional fuzzy spheres. The stabilizer group symmetry of the Bloch hyper-sphere necessarily introduces degenerate spin-coherent states, giving rise to the Wilczek-Zee geometric phase of non-Abelian monopoles associated with the hyper-sphere holonomy. The degenerate spin-coherent states induce matrix-valued quantum geometric tensors. While the minimal spin Bloch hyper-spheres exhibit similar properties in even and odd dimensions, their large spin counterparts differ qualitatively depending on the parity of the dimensions. Exact correspondences between spin-coherent states and monopole harmonics in higher dimensions are established. We also investigate density matrices described by Bloch hyper-balls and elucidate their corresponding statistical and geometric properties, such as von Neumann entropies and Bures quantum metrics.

# Contents

<b>1</b>	<b>Introduction</b>	<b>2</b>
<b>2</b>	<b>Bloch sphere and the <math>SO(3)</math> Zeeman-Dirac model</b>	<b>4</b>
2.1	Minimal spin model . . . . .	4
2.2	Large spin model . . . . .	7
<b>3</b>	<b>Bloch four-sphere and the <math>SO(5)</math> Zeeman-Dirac model</b>	<b>10</b>
3.1	Minimal spin model . . . . .	11
3.2	Large spin model . . . . .	14
<b>4</b>	<b>Bloch three-sphere and <math>SO(4)</math> Zeeman-Dirac model</b>	<b>18</b>
4.1	Minimal spin model . . . . .	19
4.2	Large spin model . . . . .	20
<b>5</b>	<b>Bloch hyper-spheres in even higher dimensions</b>	<b>26</b>
5.1	General properties . . . . .	27
5.2	Irreducible representations . . . . .	28
5.3	$SO(2k + 1)$ Zeeman-Dirac model . . . . .	30
5.4	$SO(2k)$ Zeeman-Dirac model . . . . .	32
<b>6</b>	<b>Bloch hyper-balls and quantum statistics</b>	<b>34</b>
6.1	Bloch hyper-balls and density matrices . . . . .	34
6.2	von Neumann entropies . . . . .	35
6.3	Quantum statistical geometry . . . . .	36
<b>7</b>	<b>Summary</b>	<b>39</b>
<b>A</b>	<b>Examples of the generalized gamma matrices</b>	<b>41</b>
A.1	$SO(5)$ $\Gamma_a$ for $S = 1$ . . . . .	41
A.2	$SO(4)$ $\Gamma_\mu$ for $S = 3/2$ . . . . .	42
<b>B</b>	<b>Matrix-valued quantum geometric tensor</b>	<b>43</b>
<b>C</b>	<b><math>SO(4)</math> monopole harmonics from the <math>SO(4)</math> non-linear realization</b>	<b>44</b>
C.1	$SO(3)$ decomposition of the $SO(4)$ matrix generators . . . . .	44
C.2	$SO(4)$ monopole harmonics . . . . .	45
<b>D</b>	<b>Nested Bloch four-spheres from higher Landau levels</b>	<b>46</b>
<b>E</b>	<b><math>SO(d + 1)</math> minimal Zeeman-Dirac models</b>	<b>48</b>
E.1	$SO(d + 1)$ spinor representation matrices . . . . .	48
E.2	$SO(2k + 1)$ minimal spin model . . . . .	49
E.3	$SO(2k)$ minimal spin model . . . . .	50

# 1 Introduction

The geometry of quantum states provides an indispensable perspective for a deeper understanding of both quantum mechanics and quantum information [1, 2, 3, 4]. Its importance has also grown rapidly in recent advances in material science [5, 6]. The Bloch sphere [7] serves as the fundamental geometry of two-level quantum mechanics. In two-level quantum mechanics with conical degeneracy, Berry’s geometric phase [8] was recognized in the adiabatic evolution of the energy eigenstate [9]. Soon after Berry’s work, Wilczek and Zee introduced a non-Abelian version of the geometric phase for degenerate energy levels [10]. As the Bloch sphere illustrates the underlying geometry of such a two-level quantum mechanics and Berry’s geometric phase, higher dimensional Bloch spheres (Bloch hyper-spheres) realize a paradigmatic example of the geometry of multi-level quantum mechanics and the Wilczek-Zee non-Abelian phase. In the recent developments of quantum matter [11], higher dimensional topological phases can be accessed through the concept of synthetic dimensions [12, 13, 14, 15], and higher dimensional topologies have attracted increasing attention. In particular, the non-Abelian geometric phases have recently been observed by state-of-the-art tabletop experiments [16, 17, 19, 18, 20].

A two-level Hamiltonian for qubit is introduced as

$$H = \sum_{i=1}^3 x_i \cdot \frac{1}{2} \sigma_i. \quad (1.1)$$

Its eigenstates are referred to as the spin-coherent states or Bloch coherent states [21, 22, 23, 24]. In the context of quantum information, the qubit state is first given, and then the Bloch vector  $x_i$  is determined to visualize the geometry of the qubit. Meanwhile, in quantum physics, a quantum mechanical Hamiltonian is usually given first, and quantum states follow as its eigenstates. The Hamiltonian (1.1) is ubiquitous in the quantum world and plays a crucial role in various contexts of physics: When  $x_i$  represent the direction of an applied magnetic field, the Hamiltonian (1.1) is called the Zeeman magnetic interaction term. Meanwhile, if  $x_i$  are taken to be a crystal momentum, the Hamiltonian is known in material science as the Dirac (or Weyl) Hamiltonian where the spin index of the Pauli matrices signifies the two-band index.<sup>1</sup> For these reasons, we refer to the Hamiltonian (1.1) as the ( $SO(3)$ ) Zeeman-Dirac Hamiltonian in this paper. The Bloch sphere emerges as the underlying geometry behind all of the physical systems described by the Zeeman-Dirac Hamiltonian. For a large spin model, such as nuclear spin, we employ the Zeeman-Dirac Hamiltonian of  $SU(2)$  spin matrices with spin magnitude  $S(= 1/2, 1, 3/2, \dots)$ :

$$H = \sum_{i=1}^3 x_i \cdot S_i, \quad (1.2)$$

which accommodates *equally* spaced  $2S + 1$  energy levels. As demonstrated by Berry [8], the geometric phase associated with the adiabatic evolution of the spin-coherent state of the Hamiltonian (1.2) is identical to the  $U(1)$  phase accounted for by the Dirac magnetic monopole with magnetic charge  $S$  [25, 26]. For a general  $N$  level system with *arbitrary* level spacing or an  $N$ -qudit, the corresponding Hamiltonian is represented by the  $N \times N$  Hermitian matrix expanded by the  $SU(N)$  matrix generators (apart from the trivial  $U(1)$  unit matrix corresponding to an overall energy shift). The  $SO(3)$  Zeeman-Dirac Hamiltonian of  $S = \frac{N-1}{2}$  (1.2) is realized as a special case of such  $SU(N)$  Hamiltonians. The study of the  $SU(N)$  generalization of the Zeeman-Dirac model has a rather long history [27, 28, 29, 30, 31], and the  $SU(N)$  spin-coherent states have been constructed in Refs.[32, 33, 34]. The  $SU(N)$  spin magnetism is crucial for quantum information processing using alkaline-earth atoms [35]. The underlying geometry of such  $SU(N)$  models is described by an  $SU(N)$  generalized Bloch “sphere”, *i.e.*,  $\mathbb{C}P^{N-1}$  geometry [31, 36, 37, 38], as

---

<sup>1</sup>For the real spin  $\frac{1}{2}\sigma_i$  and momentum  $x_i$ , (1.1) simply stands for the helicity.

it reproduces the Bloch sphere in the special  $N = 2$  case,  $\mathbb{C}P^1 \simeq S^2$ . The  $SU(4)$  generalization of the Bloch sphere has recently been implemented experimentally in a photonic device [39]. However, it should be noted that this  $SU(N)$  generalization leads to unitarily symmetric manifolds rather than spherically symmetric ones as just mentioned.

Another extension of the  $SO(3)$  Zeeman-Dirac Hamiltonian, and perhaps even more interesting in some sense, is the time-reversal symmetric  $S = 3/2$  quadrupole Hamiltonian [40]. This  $S = 3/2$  quadrupole Hamiltonian is equivalent to the  $SO(5)$  Zeeman-Dirac Hamiltonian made of the  $SO(5)$  gamma matrices<sup>2</sup>  $\gamma_a$  [41, 42]:

$$H = \sum_{a=1}^5 x_a \cdot \frac{1}{2} \gamma_a. \quad (1.3)$$

While this Hamiltonian is a special case of the  $SU(4)$  Hamiltonian, it is important in its own right. The  $SO(5)$  model is closely related to special Jahn-Teller systems [43, 44] and an ultra-cold atom system of spin  $3/2$  fermions [45]<sup>3</sup>. The Hamiltonian (1.3) also plays a crucial role as the parent Hamiltonian of topological insulator [47]. This  $SO(5)$  Hamiltonian exhibits two energy levels of equal magnitude but opposite sign, similar to the  $SO(3)$  Hamiltonian (1.1). Each of the energy levels accommodates double degeneracy attributed to the existence of time-reversal symmetry (the Kramers theorem). The adiabatic evolution of the doubly degenerate  $SO(5)$  spin-coherent states in each energy level naturally induces the Wilczek-Zee non-Abelian connection [48, 49, 50], which is identified as the gauge field of Yang's  $SU(2)$  monopole [51, 52] or the BPST instanton [53]. Very recently, the  $SO(5)$  Zeeman-Dirac Hamiltonian has been implemented in cold atom systems and meta-materials, in which the physical consequences peculiar to the  $SU(2)$  monopole have been observed experimentally [18, 19].

The  $SO(3)$  Zeeman-Dirac Hamiltonians of large spins were readily constructed by replacing the Pauli matrices with general  $SU(2)$  spin matrices. However, it is far from obvious how to generalize the  $SO(5)$  Hamiltonian for arbitrarily large spins. This is because the gamma matrices themselves are *not* generators of the  $SO(5)$  group (but their commutators are), and we cannot adopt  $SO(5)$  generators of large spins for this purpose. To construct the gamma matrices of large spins, we utilize the analogy between the charge-monopole system on a sphere (known as the Landau model) and the precession of the quantum spin (Fig.1): The trajectories of the precessing spin on the Bloch sphere can be interpreted as the cyclotron orbits of a charged particle on a two-sphere in the Dirac monopole background [26, 54] (Fig.1). We exploit

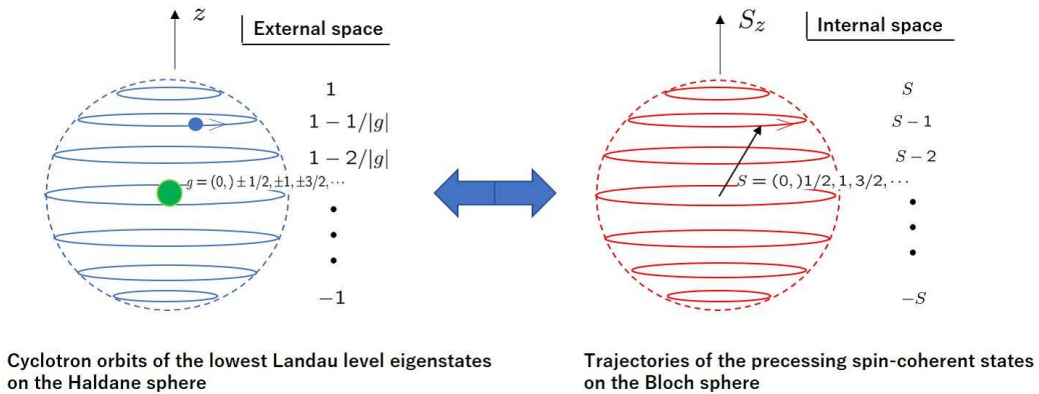


Figure 1: Analogies between the electron cyclotron orbits of the Landau model [54] (left) and the orbits of the quantum spin precession (right).

<sup>2</sup>Recall that the Pauli matrices are equivalent to the gamma matrices of  $SO(3)$ .

<sup>3</sup>See [46] for conical singularities in various contexts of physics.

this observation to construct the generalized gamma matrices of large spins. This idea is in line with recent developments of non-commutative geometry [55, 56, 57, 58, 59, 59, 60, 61, 62, 63, 64, 65, 66], in particular from the quantum matrix geometry of the higher dimensional fuzzy spheres [66, 63, 61, 57, 56].<sup>4</sup> We present a systematic construction of exactly spherical Bloch hyper-spheres and investigate their unique properties. We will see that higher dimensional Zeeman-Dirac models necessarily exhibit energy level degeneracies and realize the Wilczek-Zee connections of non-Abelian monopoles. We also construct Bloch hyper-balls and address their implications in quantum statistics and quantum statistical geometry.

This paper is organized as follows. In Sec.2, we review the original Bloch sphere and the spin-coherent states. Section 3 discusses the  $SO(5)$  Zeeman-Dirac models and their geometric structures. In Sec.4, we construct  $SO(4)$  Zeeman-Dirac models and clarify their properties. We analyze the Zeeman-Dirac models in arbitrary dimensions in Sec.5. In Sec.6, we introduce the density matrices associated with Bloch hyper-balls and exploit their statistical properties, such as von Neumann entropy and Bures information metric. Sec.7 is devoted to summary and discussion.

## 2 Bloch sphere and the $SO(3)$ Zeeman-Dirac model

As a warm-up, we review the Bloch sphere and the spin-coherent states with emphasis on their relation to the  $SO(3)$  Zeeman-Dirac model. We will clarify the relationship between the spin-coherent states and the Landau level eigenstates.

### 2.1 Minimal spin model

We introduce the  $SO(3)$  minimal Zeeman-Dirac model:

$$H = \sum_{i=1}^3 x_i \cdot \frac{1}{2} \sigma_i, \quad (2.1)$$

where  $x_i$  are the coordinates on  $S^2$  or the components of the Bloch vector:

$$x_1 = \cos \phi \sin \theta, \quad x_2 = \sin \phi \sin \theta, \quad x_3 = \cos \theta. \quad (2.2)$$

It is easy to solve the eigenvalue problem of this  $2 \times 2$  matrix Hamiltonian (2.1):

$$H\Phi^{(\lambda)} = \lambda \cdot \Phi^{(\lambda)}, \quad (2.3)$$

where the eigenvalues are given by

$$\lambda = +1/2, -1/2. \quad (2.4)$$

The corresponding eigenstates are known as the spin-coherent states

$$\Phi^{(+\frac{1}{2})} = \frac{1}{\sqrt{2(1+x_3)}} \begin{pmatrix} 1+x_3 \\ x_1+ix_2 \end{pmatrix} = \begin{pmatrix} \cos(\frac{\theta}{2}) \\ \sin(\frac{\theta}{2})e^{i\phi} \end{pmatrix}, \quad \Phi^{(-\frac{1}{2})} = \frac{1}{\sqrt{2(1+x_3)}} \begin{pmatrix} -x_1+ix_2 \\ 1+x_3 \end{pmatrix} = \begin{pmatrix} -\sin(\frac{\theta}{2})e^{-i\phi} \\ \cos(\frac{\theta}{2}) \end{pmatrix}, \quad (2.5)$$

which are normalized as

$$\Phi^{(+\frac{1}{2})\dagger} \Phi^{(+\frac{1}{2})} = \Phi^{(-\frac{1}{2})\dagger} \Phi^{(-\frac{1}{2})} = 1, \quad \Phi^{(+\frac{1}{2})\dagger} \Phi^{(-\frac{1}{2})} = 0. \quad (2.6)$$

Notice that the eigenvalues (2.4) are the diagonal components of  $\frac{1}{2}\sigma_3$ . In other words, the eigenstates (2.5) carry the quantum numbers of the  $U(1)$  sub-algebra of  $SU(2)$ . The eigenvalues  $\lambda = \pm 1/2$  have a

---

<sup>4</sup>The quantum geometry of the fuzzy sphere is now being applied to various branches of physics [67, 68, 69, 70, 71].

nice geometric meaning as the latitudes on the Bloch sphere where the spin-coherent states are oriented (see the left of Fig.2). We can generate the spin-coherent states by the following well-known geometric manipulation. The projection of the Bloch vector  $x_i$  onto the  $xy$ -plane is given by

$$y_1 = \cos \phi, \quad y_2 = \sin \phi. \quad (2.7)$$

The spin-coherent state with  $\lambda = +1/2$  can be obtained by rotating the north-pole oriented spin-coherent state about the  $\epsilon_{\mu\nu}y_\nu$ -axis by  $\theta$  (see the right of Fig.2).

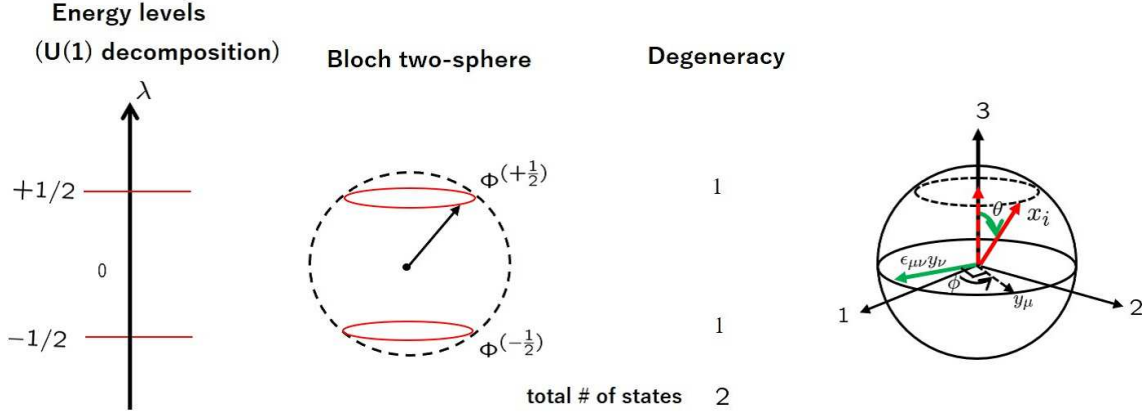


Figure 2: The eigenvalues and the eigenstates of the  $SO(3)$  Zeeman-Dirac model (left and middle) and the rotation of the spin (right).

Such a manipulation is demonstrated by the non-linear realization matrix

$$\Phi = e^{-i\theta \sum_{\mu,\nu=1}^2 \epsilon_{\mu\nu} y_\mu \frac{1}{2} \sigma_\nu}, \quad (2.8)$$

which is expanded as

$$\begin{aligned} \Phi &= \cos\left(\frac{\theta}{2}\right) 1_2 - i \sin\left(\frac{\theta}{2}\right) \sum_{\mu,\nu=1}^2 \epsilon_{\mu\nu} y_\mu \sigma_\nu = \begin{pmatrix} \cos \frac{\theta}{2} & -\sin \frac{\theta}{2} e^{-i\phi} \\ \sin \frac{\theta}{2} e^{i\phi} & \cos \frac{\theta}{2} \end{pmatrix} \\ &= \frac{1}{\sqrt{2(1+x_3)}} ((1+x_3)1_2 - i\epsilon_{\mu\nu} x_\mu \sigma_\nu) = \frac{1}{\sqrt{2(1+x_3)}} \begin{pmatrix} 1+x_3 & -x_1+ix_2 \\ x_1+ix_2 & 1+x_3 \end{pmatrix}. \end{aligned} \quad (2.9)$$

The spin-coherent states (2.5) are indeed obtained from  $\Phi$  as

$$\Phi^{(+\frac{1}{2})} = \Phi \begin{pmatrix} 1 \\ 0 \end{pmatrix}, \quad \Phi^{(-\frac{1}{2})} = \Phi \begin{pmatrix} 0 \\ 1 \end{pmatrix} \quad (2.10)$$

or

$$\Phi = \left( \Phi^{(+\frac{1}{2})} \quad \Phi^{(-\frac{1}{2})} \right). \quad (2.11)$$

Since  $\Phi$  has a clear geometrical meaning and simultaneously contains the two spin-coherent states as its columns, we will use the non-linear realization matrix (2.8) instead of the spin-coherent states themselves. Obviously,  $\Phi$  denotes a unitary matrix that diagonalizes the Zeeman-Dirac Hamiltonian:

$$\Phi^\dagger H \Phi = \frac{1}{2} \sigma_3. \quad (2.12)$$

It is important to note that the diagonalization can be justified solely from the group theoretical properties of the  $SU(2)$ . Solving eigenvalue problems for large-sized matrix Hamiltonians is generally laborious. However, the geometric method makes it feasible, since the properties of the  $SU(2)$  group are universal regardless of the magnitude of spin. Non-linear realization matrix  $\Phi$  (2.8) is factorized as<sup>5</sup>

$$\Phi = e^{-i\frac{\phi}{2}\sigma_3} e^{-i\frac{\theta}{2}\sigma_2} e^{i\frac{\phi}{2}\sigma_3}. \quad (2.13)$$

A similar factorization holds for non-linear realizations of arbitrary spin matrices. This factorization significantly reduces numerical computation time in using  $\Phi$ , especially for large spin matrices. As noted in (2.12),  $\Phi$  enjoys the  $U(1)$  degrees of freedom (apart from the overall  $U(1)$ )

$$\Phi \rightarrow \Phi \cdot e^{i\frac{\chi}{2}\sigma_3}, \quad (2.14)$$

which corresponds to the degrees of freedom for the relative phase of two spin-coherent states. For the original Hamiltonian (2.1), this  $U(1)$  symmetry acts as

$$e^{-i\frac{\chi}{2}\tilde{\sigma}_3} H e^{i\frac{\chi}{2}\tilde{\sigma}_3} = H, \quad (2.15)$$

where

$$\tilde{\sigma}_3 \equiv \Phi\sigma_3\Phi^\dagger = \sum_{i=1}^3 x_i\sigma_i (= 2H). \quad (2.16)$$

The  $U(1)$  transformation,  $e^{i\frac{\chi}{2}\tilde{\sigma}_3} = e^{i\chi\sum_{i=1}^3 x_i\frac{1}{2}\sigma_i}$ , stands for the  $SO(2)$  rotation of  $\chi$  about the direction pointed by the Bloch vector, and so the geometric origin of the  $U(1)$  symmetry is understood as the  $SO(2)$  stabilizer group of the two-sphere,  $S^2 \simeq SO(3)/SO(2)$ . It is obvious that any rotations about the direction pointed by the Bloch vector do not change the  $SO(3)$  Hamiltonian (2.1). An invariant quantity under the  $U(1)$  transformation (2.14) is given by

$$\Phi^{(\pm 1/2)\dagger} \sigma_i \Phi^{(\pm 1/2)} = \pm x_i, \quad (2.17)$$

which is nothing but the Bloch vector (2.2). The Berry connections of the spin-coherent states are derived as [8]

$$A^{(\pm 1/2)} = -i\Phi^{(\pm 1/2)\dagger} d\Phi^{(\pm 1/2)} = \pm \frac{1}{2}(1 - \cos\theta)d\phi = \mp \frac{1}{2(1+x_3)}\epsilon_{ij3}x_j dx_i, \quad (2.18)$$

which are realized as the diagonal components of the pure  $SU(2)$  gauge field:

$$-i\Phi^\dagger d\Phi = \begin{pmatrix} A^{(+1/2)} & * \\ * & A^{(-1/2)} \end{pmatrix}. \quad (2.19)$$

The  $U(1)$  degrees of freedom (2.12) formally correspond to the  $U(1)$  gauge transformations through (2.19):

$$A^{(\pm 1/2)} \rightarrow A^{(\pm 1/2)} \pm \frac{1}{2}d\chi. \quad (2.20)$$

The Berry connection (2.18) is exactly equal to the monopole gauge field with magnetic charge  $\lambda = \pm 1/2$ . A natural question may arise about the relationship between the Zeeman-Dirac model and the Landau model. Let us recall the  $SO(3)$  Landau model in the  $U(1)$  monopole background (see [55] for instance). The

---

<sup>5</sup>The factorization (2.13) implies that  $\Phi$  is a special case of Wigner's  $D$  function (see Chap.3 of Ref.[72], for instance),  $\Phi = e^{-i\frac{\phi}{2}\sigma_3} e^{-i\frac{\theta}{2}\sigma_2} e^{-i\frac{\chi}{2}\sigma_3}|_{\chi=-\phi}$ .

degenerate lowest Landau level eigenstates of monopole charge  $\pm 1/2$  are given by the monopole harmonics [26]<sup>6</sup>

$$\lambda = +\frac{1}{2} : \phi_1^{(+\frac{1}{2})} = \cos\left(\frac{\theta}{2}\right), \quad \phi_2^{(+\frac{1}{2})} = \sin\left(\frac{\theta}{2}\right) e^{-i\phi}, \quad (2.22a)$$

$$\lambda = -\frac{1}{2} : \phi_1^{(-\frac{1}{2})} = -\sin\left(\frac{\theta}{2}\right) e^{i\phi}, \quad \phi_2^{(-\frac{1}{2})} = \cos\left(\frac{\theta}{2}\right). \quad (2.22b)$$

Interestingly, these lowest Landau level eigenstates constitute the spin-coherent states (2.5):

$$\Phi^{(+\frac{1}{2})} = \begin{pmatrix} \phi_1^{(+\frac{1}{2})*} \\ \phi_2^{(+\frac{1}{2})*} \end{pmatrix}, \quad \Phi^{(-\frac{1}{2})} = \begin{pmatrix} \phi_1^{(-\frac{1}{2})*} \\ \phi_2^{(-\frac{1}{2})*} \end{pmatrix}. \quad (2.23)$$

## 2.2 Large spin model

We extend the previous discussion to arbitrary  $SU(2)$  spin matrices ( $S = 0, 1/2, 1, 3/2, \dots$ ), which satisfy  $[S_i, S_j] = i\epsilon_{ijk}S_k$  and

$$\sum_{i=1}^3 S_i S_i = S(S+1)\mathbf{1}_{2S+1}. \quad (2.24)$$

The matrix components of the spin matrices are given by

$$\begin{aligned} (S_x)_{mn} &= \frac{1}{2}(\sqrt{(S+m)(S-n)} \delta_{m-1,n} + \sqrt{(S-m)(S+n)} \delta_{m,n-1}), \\ (S_y)_{mn} &= i\frac{1}{2}(\sqrt{(S+m)(S-n)} \delta_{m-1,n} - \sqrt{(S-m)(S+n)} \delta_{m,n-1}), \\ (S_z)_{mn} &= m\delta_{m,n} \quad (m, n = S, S-1, S-2, \dots, -S). \end{aligned} \quad (2.25)$$

The  $S_z$  takes a diagonal form,

$$S_z = \begin{pmatrix} S & 0 & 0 & 0 & 0 \\ 0 & S-1 & 0 & 0 & 0 \\ 0 & 0 & S-2 & 0 & 0 \\ 0 & 0 & 0 & \ddots & 0 \\ 0 & 0 & 0 & 0 & -S \end{pmatrix}. \quad (2.26)$$

The  $SO(3)$  Hamiltonian (2.1) is simply generalized as

$$H = \sum_{i=1}^3 x_i S_i. \quad (2.27)$$

As indicated before, we apply the geometric method to solve the eigenvalue problem of (2.27):

$$\Phi^\dagger H \Phi = S_3, \quad (2.28)$$

where  $\Phi$  denotes the non-linear realization matrix

$$\Phi = e^{-i\theta \sum_{\mu,\nu=1}^2 \epsilon_{\mu,\nu} y_\mu S_\nu} = e^{-i\phi S_3} e^{-i\theta S_2} e^{i\phi S_3}. \quad (2.29)$$

---

<sup>6</sup>The monopole harmonics are defined on a two-sphere and their orthonormal relations are given by

$$\int_{S^2} d\theta d\phi \sin\theta \phi_\alpha^{(\lambda)*} \phi_\beta^{(\lambda')} = 2\pi \delta_{\alpha\beta} \delta_{\lambda\lambda'}. \quad (2.21)$$



In the notation

$$\Phi \equiv (\Phi^{(S)} \ \Phi^{(S-1)} \ \Phi^{(S-2)} \ \dots \ \Phi^{(-S)}), \quad (2.30)$$

(2.28) is restated as

$$H\Phi^{(\lambda)} = \lambda \cdot \Phi^{(\lambda)}, \quad (2.31)$$

where

$$\lambda = S, S-1, S-2, \dots, -S. \quad (2.32)$$

The  $SO(3)$  spin-coherent state<sup>7</sup>  $\Phi^{(\lambda)}$  is realized as the  $\lambda$ th column of (2.30) and denotes the spin coherent state oriented to the latitude  $\lambda$  on the Bloch sphere. Note that the spectra of  $H$  are nicely illustrated as the latitudes on the Bloch sphere (Fig.3). As  $\Phi$  is a unitary matrix, the  $\Phi^{(\lambda)}$  apparently satisfy the ortho-normal relations

$$\Phi^{(\lambda)\dagger} \Phi^{(\lambda')} = \delta_{\lambda\lambda'}. \quad (2.33)$$

Equation (2.28) is invariant under the  $U(1)$  transformation

$$\Phi \rightarrow \Phi \cdot e^{i\chi S_3} \quad (2.34)$$

or

$$\Phi^{(\lambda)} \rightarrow \Phi^{(\lambda)} e^{i\lambda\chi}. \quad (2.35)$$

In the following, we discuss several important  $U(1)$  invariant quantities. The Bloch vector is a  $U(1)$ -invariant quantity, as implied by the equation

$$\Phi^{(\lambda)\dagger} S_i \Phi^{(\lambda)} = \lambda \cdot x_i. \quad (2.36)$$

Another important  $U(1)$  invariant quantity is the quantum geometric tensor [73]<sup>8</sup>

$$\chi_{\mu\nu}^{(\lambda)} = \partial_{\theta_\mu} \Phi^{(\lambda)\dagger} \partial_{\theta_\nu} \Phi^{(\lambda)} - \partial_{\theta_\mu} \Phi^{(\lambda)\dagger} \Phi^{(\lambda)} \Phi^{(\lambda)\dagger} \partial_{\theta_\nu} \Phi^{(\lambda)} \quad (\theta_\mu = \theta, \phi). \quad (2.37)$$

Using the spin matrices (2.25) and mathematical software,<sup>9</sup> we can easily show that the symmetric part of  $\chi_{\mu\nu}^{(\lambda)}$  provides the two-sphere metric:

$$g_{\theta_\mu\theta_\nu}^{(\lambda)} = \frac{1}{2}(\chi_{\theta_\mu\theta_\nu}^{(\lambda)} + \chi_{\theta_\nu\theta_\mu}^{(\lambda)}) = \frac{1}{2}(S(S+1) - \lambda^2) g_{\theta_\mu\theta_\nu}^{(S_2)} \quad (2.38)$$

with

$$g_{\theta_\mu\theta_\nu}^{(S_2)} = \text{diag}(g_{\theta\theta}^{S_2}, g_{\phi\phi}^{S_2}) = \text{diag}(1, \sin^2\theta). \quad (2.39)$$

The Berry phase associated with the spin-coherent state  $\Phi^{(\lambda)}$  can be derived as

$$-i\Phi^\dagger d\Phi = \begin{pmatrix} A^{(S)} & * & * & * \\ * & A^{(S-1)} & * & * \\ * & * & \ddots & * \\ * & * & * & A^{(-S)} \end{pmatrix} \quad (2.40)$$

or

$$A^{(\lambda)} = -i\Phi^{(\lambda)\dagger} d\Phi^{(\lambda)} = -\lambda \frac{1}{1+x_3} \epsilon_{ij3} x_j dx_i = \lambda(1 - \cos\theta) d\phi. \quad (2.41)$$

<sup>7</sup>Since  $S$  takes both half-integer and integer values,  $\Phi^{(\lambda)}$  may be more appropriately called the  $SU(2)$  spin-coherent states rather than the  $SO(3)$ .

<sup>8</sup>The quantum geometric tensor appears as the second order term of the expansion of overlapped wave-functions. For even higher order geometric tensors, see Refs.[74, 75].

<sup>9</sup>We checked the validity of (2.38) up to  $S = 7/2$ .

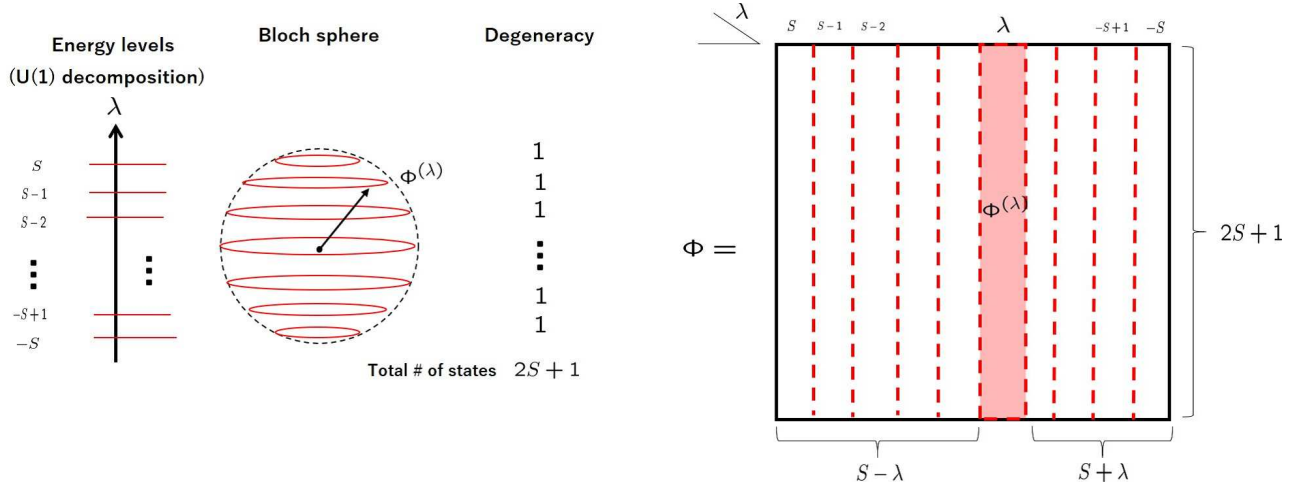


Figure 3: The Bloch sphere with large spin  $S$  and the  $SO(3)$  spin-coherent state  $\Phi^{(\lambda)}$  in  $\Phi$ .

Note that the energy eigenvalue  $\lambda$  appears as the monopole charge in (2.41). The corresponding field strength  $F^{(\lambda)} = dA^{(\lambda)} = \frac{1}{2}F_{\theta_\mu\theta_\nu}^{(\lambda)}d\theta_\mu \wedge d\theta_\nu$  is equal to the anti-symmetric part of the quantum geometric tensor:

$$F_{\theta_\mu\theta_\nu}^{(\lambda)} = -i(\chi_{\theta_\mu\theta_\nu}^{(\lambda)} - \chi_{\theta_\nu\theta_\mu}^{(\lambda)}) = \lambda \sin(\theta)\epsilon_{\mu\nu}, \quad (2.42)$$

which is also a  $U(1)$  gauge invariant quantity. The corresponding first Chern number is evaluated as

$$\text{ch}_1^{(\lambda)} = \frac{1}{2\pi} \int F^{(\lambda)} = 2\lambda = \text{sgn}(\lambda) \cdot D_{SO(3)}(|\lambda| - \frac{1}{2}) = -\text{ch}_1^{(-\lambda)}, \quad (2.43)$$

where

$$D_{SO(3)}(S) \equiv 2S + 1. \quad (2.44)$$

It is known that the Landau level eigenstates are also embedded in the non-linear realization matrix  $\Phi$  [63]. Assume that  $g$  denotes the monopole charge and  $N$  signifies the Landau level index. For the  $SU(2)$  spin index, we have the identification

$$S = N + |g|, \quad (2.45)$$

and for the  $U(1)$  index,

$$S - \lambda = N - g + |g|. \quad (2.46)$$

The quantities on the left-hand sides of (2.45) and (2.46) come from the  $SO(3)$  Zeeman-Dirac model, while those on the right-hand sides come from the  $SO(3)$  Landau model. From (2.45) and (2.46), we have

$$N = S - |\lambda|, \quad g = \lambda. \quad (2.47)$$

Take  $\phi_1^{(g)}, \phi_2^{(g)}, \dots, \phi_{2S+1}^{(g)}$  for the  $N = (S - |g|)$ th Landau level eigenstates in the  $U(1)$  monopole background

with magnetic charge  $g$  (Fig.4)<sup>10</sup>, then the  $SO(3)$  spin-coherent state is represented as

$$\Phi^{(\lambda)} = \begin{pmatrix} \phi_1^{(\lambda)*} \\ \phi_2^{(\lambda)*} \\ \vdots \\ \phi_{2S+1}^{(\lambda)*} \end{pmatrix}, \quad (2.50)$$

which signifies the exact relation between the spin-coherent states and the monopole harmonics: The spin-coherent states of large spin  $S$  consist of the  $(2S+1)$ -fold degenerate Landau level eigenstates of  $N = S - |\lambda|$  in the monopole background with magnetic charge  $\lambda$  (Fig.4).

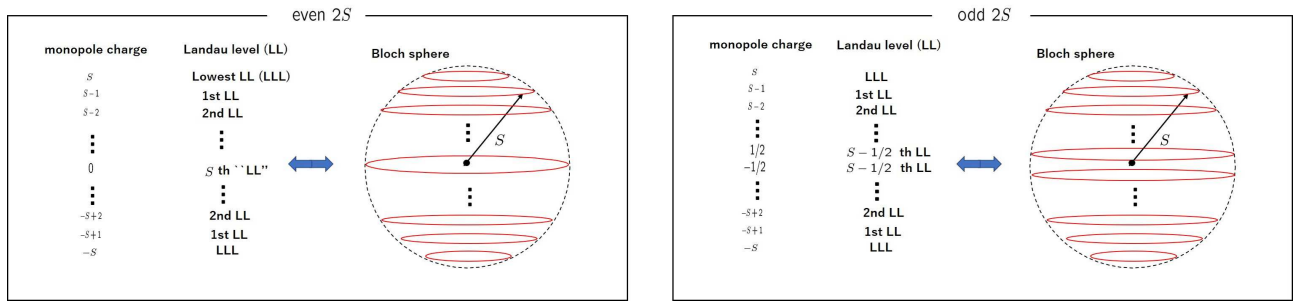


Figure 4: Correspondence between the monopole harmonics and the  $SO(3)$  spin-coherent states.

In the above discussions, we started from the Zeeman-Dirac model and later addressed the relationship to the Landau model. However, we can reverse the flow of the argument. Suppose that the  $SO(3)$  Landau model is first given and the Landau level eigenstates are known. We can generate the large spin matrices  $S_i$  by the following formula

$$\int_{S^2} d\Omega_2 \phi_\alpha^{(\lambda)*} x_i \phi_\beta^{(\lambda)} = \frac{4\pi\lambda}{S(S+1)(2S+1)} (S_i)_{\alpha\beta}. \quad (2.51)$$

In the present  $SO(3)$  case, since arbitrary spin matrices were already known, the construction of spin matrices from the Landau level eigenstates was unnecessary. However, in the case of  $SO(5)$  and other higher dimensional groups, this procedure is crucial when constructing large spin gamma matrices.

### 3 Bloch four-sphere and the $SO(5)$ Zeeman-Dirac model

Here, we extend the results of Sec.2 to the  $SO(5)$  Zeeman-Dirac model. The basic idea comes from the analogy between the cyclotron motion on a four-sphere and the  $SO(5)$  spin precession in internal space.

<sup>10</sup>The monopole harmonics satisfy

$$\int_{S^2} d\Omega_2 \phi_\alpha^{(\lambda)*} \phi_\beta^{(\lambda)} = A(S^2) \frac{1}{D_{SO(3)}(S)} \delta_{\alpha\beta} = \frac{4\pi}{2S+1} \delta_{\alpha\beta}, \quad (2.48)$$

with  $d\Omega_2 = \sin\theta d\theta d\phi$ ,  $D_{SO(3)}(S) = 2S+1$  and  $A(S^2) = \int_{S^2} d\Omega_2 = 4\pi$ . The monopole configuration (2.41) is represented as

$$A^{(\lambda)} = -i \sum_{\alpha=1}^{2S+1} \phi_\alpha^{(\lambda)} d\phi_\alpha^{(\lambda)*}. \quad (2.49)$$

### 3.1 Minimal spin model

The geometric phase of the minimal  $SO(5)$  Zeeman-Dirac model [41, 42] has been investigated in Refs.[48, 49, 50]. Here, we reproduce the previous results using the group theoretical method.

We adopt the following  $SO(5)$  gamma matrices

$$\gamma_{\mu=1,2,3,4} = \begin{pmatrix} 0 & \bar{q}_\mu \\ q_\mu & 0 \end{pmatrix}, \quad \gamma_5 = \begin{pmatrix} \mathbf{1}_2 & 0 \\ 0 & -\mathbf{1}_2 \end{pmatrix} \quad (q_\mu = \{-i\sigma_i, \mathbf{1}_2\}, \quad \bar{q}_\mu = \{i\sigma_i, \mathbf{1}_2\}). \quad (3.1)$$

These satisfy

$$\{\gamma_a, \gamma_b\} = 2\delta_{ab}\mathbf{1}_4 \quad (a, b = 1, 2, 3, 4, 5) \quad (3.2)$$

and yield the  $SO(5)$  generators as

$$\sigma_{ab} = -i\frac{1}{4}[\gamma_a, \gamma_b], \quad (3.3)$$

or

$$\sigma_{\mu\nu} = \frac{1}{2} \begin{pmatrix} \eta_{\mu\nu}^{(+i)} \sigma_i & 0 \\ 0 & \eta_{\mu\nu}^{(-i)} \sigma_i \end{pmatrix}, \quad \sigma_{\mu 5} = i\frac{1}{2} \begin{pmatrix} 0 & \bar{q}_\mu \\ -q_\mu & 0 \end{pmatrix} = -\sigma_{5\mu}. \quad (3.4)$$

Here,  $\eta_{\mu\nu}^{(\pm)i}$  denote the 't Hooft tensors,

$$\eta_{\mu\nu}^{(\pm)i} \equiv \epsilon_{\mu\nu i 4} \pm \delta_{\mu i} \delta_{\nu 4} \mp \delta_{\nu i} \delta_{\mu 4}. \quad (3.5)$$

The minimal  $SO(5)$  Zeeman-Dirac Hamiltonian is given by the following  $4 \times 4$  matrix<sup>11</sup>

$$H = \sum_{a=1}^5 x_a \cdot \frac{1}{2} \gamma_a \quad \left( \sum_{a=1}^5 x_a x_a = 1 \right), \quad (3.8)$$

where  $x_a$  denote the coordinates of a four-sphere:

$$\begin{aligned} x_1 &= \cos \phi \sin \theta \sin \chi \sin \xi, & x_2 &= \sin \phi \sin \theta \sin \chi \sin \xi, & x_3 &= \cos \theta \sin \chi \sin \xi, \\ x_4 &= \cos \chi \sin \xi, & x_5 &= \cos \xi. \end{aligned} \quad (3.9)$$

The parameter  $\xi$  signifies the azimuthal angle on  $S^4$ . Due to the property (3.2), the square of  $H$  (3.8) becomes

$$H^2 = \frac{1}{4} \sum_{a=1}^5 x_a x_a \mathbf{1}_4 = \frac{1}{4} \mathbf{1}_4, \quad (3.10)$$

which implies that the eigenvalues of  $H$  are

$$\lambda = \pm \frac{1}{2}. \quad (3.11)$$

Each eigenvalue is doubly degenerate. In the above diagonalization, we utilized the specific properties of the gamma matrices (3.2) that  $SO(5)$  gamma matrices of large spin do not respect. For later convenience, we

<sup>11</sup>A four-level matrix Hamiltonian is generally given by

$$H = \sum_{A=1}^{15} n_A \cdot \frac{1}{2} \lambda_A, \quad (3.6)$$

where  $\lambda_A$  are  $SU(4)$  Gell-Mann matrices. The minimal  $SO(5)$  Hamiltonian (3.8) is realized in the special case

$$n_A = \sum_{a=1}^5 \eta_{a6}^A x_a \quad (3.7)$$

where  $\eta_{ab}^A$  denote the  $SU(4)$  generalized 't Hooft symbol [76].

develop a geometric method for the present case. To orient the  $SO(5)$  spin-coherent state to the direction  $x_a$ , we introduce the  $SO(5)$  non-linear realization matrix [61, 63]:

$$\Psi = e^{i\xi \sum_{\mu=1}^4 y_\mu \sigma_{\mu 5}}, \quad (3.12)$$

where  $y_\mu$  denote the coordinates of the  $S^3$ -latitude on the four-sphere at the azimuthal angle  $\xi$ :

$$y_1 = \cos \phi \sin \theta \sin \chi, \quad y_2 = \sin \phi \sin \theta \sin \chi, \quad y_3 = \cos \theta \sin \chi, \quad y_4 = \cos \chi. \quad (3.13)$$

Note the resemblance between (2.8) and (3.12). The matrix  $\Psi$  is represented by the  $S^4$  coordinates as

$$\Psi = \cos\left(\frac{\xi}{2}\right)\mathbf{1}_4 + 2i \sin\left(\frac{\xi}{2}\right) \sum_{\mu=1}^4 y_\mu \sigma_{\mu 5} = \frac{1}{\sqrt{2(1+x_5)}} \begin{pmatrix} (1+x_5)\mathbf{1}_2 & -x_\mu \bar{q}_\mu \\ x_\mu q_\mu & (1+x_5)\mathbf{1}_2 \end{pmatrix}, \quad (3.14)$$

which is factorized as

$$\Psi = N(\chi, \theta, \phi)^\dagger \cdot e^{i\xi \sigma_{45}} \cdot N(\chi, \theta, \phi) \quad (3.15)$$

where

$$N(\chi, \theta, \phi) \equiv e^{i\chi \sigma_{43}} e^{i\theta \sigma_{31}} e^{i\phi \sigma_{12}}. \quad (3.16)$$

It is not difficult to check that (3.14) diagonalizes the  $SO(5)$  Hamiltonian,

$$\Psi^\dagger H \Psi = \frac{1}{2} \gamma_5, \quad (3.17)$$

or

$$H \Psi = \Psi \frac{1}{2} \gamma_5. \quad (3.18)$$

In the notation

$$\Psi = \left( \Psi^{(+\frac{1}{2})} : \Psi^{(-\frac{1}{2})} \right) = \left( \Psi_1^{(+\frac{1}{2})} \Psi_2^{(+\frac{1}{2})} : \Psi_1^{(-\frac{1}{2})} \Psi_2^{(-\frac{1}{2})} \right), \quad (3.19)$$

the eigenvalue equation (3.18) is restated as

$$H \Psi_\sigma^{(\lambda)} = \lambda \Psi_\sigma^{(\lambda)}, \quad (3.20)$$

where  $\sigma = 1, 2$  for each of  $\lambda = +1/2, -1/2$ . The identification (3.19) indeed reproduces the  $SO(5)$  spin-coherent states in the previous literature [48, 49, 50]:

$$\Psi_1^{(+\frac{1}{2})} = \frac{1}{\sqrt{2(1+x_5)}} \begin{pmatrix} 1+x_5 \\ 0 \\ x_4 - ix_3 \\ x_2 - ix_1 \end{pmatrix}, \quad \Psi_2^{(+\frac{1}{2})} = \frac{1}{\sqrt{2(1+x_5)}} \begin{pmatrix} 0 \\ 1+x_5 \\ -x_2 - ix_1 \\ x_4 + ix_3 \end{pmatrix}, \quad (3.21a)$$

$$\Psi_1^{(-\frac{1}{2})} = \frac{1}{\sqrt{2(1+x_5)}} \begin{pmatrix} -x_4 - ix_3 \\ x_2 - ix_1 \\ 1+x_5 \\ 0 \end{pmatrix}, \quad \Psi_2^{(-\frac{1}{2})} = \frac{1}{\sqrt{2(1+x_5)}} \begin{pmatrix} -x_2 - ix_1 \\ -x_4 + ix_3 \\ 0 \\ 1+x_5 \end{pmatrix}. \quad (3.21b)$$

See Fig.5 also. Since  $\gamma_5$  is immune to the  $SO(4)$  rotations generated by  $\sigma_{\mu\nu}$ , Eq.(3.17) implies the existence of the  $SO(4)$  symmetry:

$$\Psi \rightarrow \Psi \cdot e^{i\frac{1}{2} \omega_{\mu\nu} \sigma_{\mu\nu}} \quad (3.22)$$

or

$$\Psi^{(\pm 1/2)} \rightarrow \Psi^{(\pm 1/2)} \cdot e^{i\frac{1}{4} \eta_{\mu\nu}^{(\pm)} \omega_{\mu\nu} \sigma_i}. \quad (3.23)$$

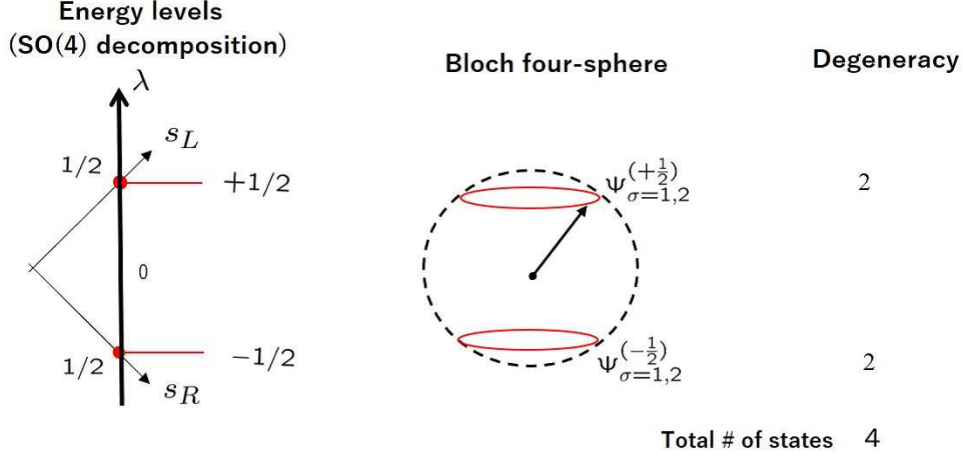


Figure 5: The eigenvalues and the eigenstates of the minimal  $SO(5)$  Zeeman-Dirac model.

For the original Hamiltonian (3.8), the  $SO(4)$  symmetry is represented as

$$e^{-i\frac{1}{2}\omega_{\mu\nu}\tilde{\sigma}_{\mu\nu}} H e^{i\frac{1}{2}\omega_{\mu\nu}\tilde{\sigma}_{\mu\nu}} = H, \quad (3.24)$$

where  $\tilde{\sigma}_{\mu\nu}$  denote the  $SO(4)$  matrix generators of the form

$$\tilde{\sigma}_{\mu\nu} \equiv \Psi \sigma_{\mu\nu} \Psi^\dagger. \quad (3.25)$$

Such an  $SO(4)$  symmetry is considered to be the “internal” symmetry of the  $SO(5)$  Zeeman-Dirac Hamiltonian in the sense that the  $SO(4)$  transformation does not change the direction of the Bloch vector  $x_a$ , and the double degeneracy in each energy level is a consequence of such an  $SO(4)$  symmetry. The Bloch vector represents an  $SO(4)$  invariant quantity:

$$\Psi_\sigma^{(\pm\frac{1}{2})\dagger} \gamma_a \Psi_\tau^{(\pm\frac{1}{2})} = \pm x_a \delta_{\sigma\tau}. \quad (3.26)$$

The Wilczek-Zee connections associated with the  $SO(5)$  spin-coherent states are derived as

$$A^{(+\frac{1}{2})} = -i\Psi^{(+\frac{1}{2})\dagger} d\Psi^{(+\frac{1}{2})} = -\frac{1}{2(1+x_5)} \eta_{\mu\nu}^{(+i)} \sigma_i x_\nu dx_\mu, \quad (3.27a)$$

$$A^{(-\frac{1}{2})} = -i\Psi^{(-\frac{1}{2})\dagger} d\Psi^{(-\frac{1}{2})} = -\frac{1}{2(1+x_5)} \eta_{\mu\nu}^{(-i)} \sigma_i x_\nu dx_\mu, \quad (3.27b)$$

which are exactly equal to the gauge field configuration of Yang’s  $SU(2)$  monopoles [51, 77]. This implies a close relation to the  $SO(5)$  Landau model [61, 63]. Take  $\psi_{\alpha=1,2,3,4}^{(\pm 1/2)}$  for the lowest Landau level eigenstates in the  $SU(2)$  monopole/anti-monopole with the second Chern number  $+1/-1$ .<sup>12</sup> They are embedded in

<sup>12</sup>The lowest Landau level eigenstates are explicitly given by

$$\begin{aligned} \psi_1^{(+\frac{1}{2})} &= \sqrt{\frac{1+x_5}{2}} \begin{pmatrix} 1 \\ 0 \end{pmatrix}, \quad \psi_2^{(+\frac{1}{2})} = \sqrt{\frac{1+x_5}{2}} \begin{pmatrix} 0 \\ 1 \end{pmatrix}, \quad \psi_3^{(+\frac{1}{2})} = \frac{1}{\sqrt{2(1+x_5)}} \begin{pmatrix} x_4 + ix_3 \\ -x_2 + ix_1 \end{pmatrix}, \quad \psi_4^{(+\frac{1}{2})} = \frac{1}{\sqrt{2(1+x_5)}} \begin{pmatrix} x_2 + ix_1 \\ x_4 - ix_3 \end{pmatrix}, \\ \psi_1^{(-\frac{1}{2})} &= \frac{1}{\sqrt{2(1+x_5)}} \begin{pmatrix} -x_4 + ix_3 \\ -x_2 + ix_1 \end{pmatrix}, \quad \psi_2^{(-\frac{1}{2})} = \frac{1}{\sqrt{2(1+x_5)}} \begin{pmatrix} x_2 + ix_1 \\ -x_4 - ix_3 \end{pmatrix}, \quad \psi_3^{(-\frac{1}{2})} = \sqrt{\frac{1+x_5}{2}} \begin{pmatrix} 1 \\ 0 \end{pmatrix}, \quad \psi_4^{(-\frac{1}{2})} = \sqrt{\frac{1+x_5}{2}} \begin{pmatrix} 0 \\ 1 \end{pmatrix}. \end{aligned} \quad (3.28)$$

$\Psi$  (3.19) as

$$\Psi^\dagger = \begin{pmatrix} \psi_1^{(+\frac{1}{2})} & \psi_2^{(+\frac{1}{2})} & \psi_3^{(+\frac{1}{2})} & \psi_4^{(+\frac{1}{2})} \\ \psi_1^{(-\frac{1}{2})} & \psi_2^{(-\frac{1}{2})} & \psi_3^{(-\frac{1}{2})} & \psi_4^{(-\frac{1}{2})} \end{pmatrix} \quad (3.29)$$

or

$$\Psi^{(+\frac{1}{2})} = (\Psi_1^{(+\frac{1}{2})} \ \Psi_2^{(+\frac{1}{2})}) = \begin{pmatrix} \psi_1^{(+\frac{1}{2})\dagger} \\ \psi_2^{(+\frac{1}{2})\dagger} \\ \psi_3^{(+\frac{1}{2})\dagger} \\ \psi_4^{(+\frac{1}{2})\dagger} \end{pmatrix}, \quad \Psi^{(-\frac{1}{2})} = (\Psi_1^{(-\frac{1}{2})} \ \Psi_2^{(-\frac{1}{2})}) = \begin{pmatrix} \psi_1^{(-\frac{1}{2})\dagger} \\ \psi_2^{(-\frac{1}{2})\dagger} \\ \psi_3^{(-\frac{1}{2})\dagger} \\ \psi_4^{(-\frac{1}{2})\dagger} \end{pmatrix}. \quad (3.30)$$

### 3.2 Large spin model

Now we explore  $SO(5)$  Zeeman-Dirac models with large spin. To construct large-spin  $SO(5)$  gamma matrices, we utilize the Landau level eigenstates of the  $SO(5)$  Landau model [66]. We take the matrix elements of the four-sphere coordinates with the (lowest) Landau level eigenstates

$$(\Gamma_a)_{\alpha\beta} = 2(S+2) \int_{S^4} d\Omega_4 \psi_\alpha^\dagger x_a \psi_\beta, \quad (3.31)$$

where  $\alpha$  runs from 1 to

$$D_{SO(5)}(S) = \frac{1}{3}(S+1)(2S+1)(2S+3). \quad (3.32)$$

The explicit matrix forms of  $\Gamma_a$  are given by

$$(\Gamma_\mu)_{(s'_L, m'_L, s'_R, m'_R; s_L, m_L, s_R, m_R)} = -2 \left( \sqrt{(S-\lambda+1)(S+\lambda+2)} Y_\mu^{(+,-)}(s_L, s_R)_{(m'_L, m'_R; m_L, m_R)} \delta_{s'_L, s_L + \frac{1}{2}} \delta_{s'_R, s_R - \frac{1}{2}} \right. \\ \left. + \sqrt{(S+\lambda+1)(S-\lambda+2)} Y_\mu^{(-,+)}(s_L, s_R)_{(m'_L, m'_R; m_L, m_R)} \delta_{s'_L, s_L - \frac{1}{2}} \delta_{s'_R, s_R + \frac{1}{2}} \right), \quad (3.33a)$$

$$(\Gamma_5)_{(s'_L, m'_L, s'_R, m'_R; s_L, m_L, s_R, m_R)} = 2\lambda \delta_{s'_L, s_L} \delta_{s'_R, s_R} \delta_{m'_L, m_L} \delta_{m'_R, m_R}, \quad (3.33b)$$

where  $s_L, s_R, s'_L$  and  $s'_R$  are non-negative integers or half-integers subject to  $s'_L + s'_R = s_L + s_R = S$  and  $\lambda \equiv s_L - s_R$ . The quantities,  $Y_\mu^{(+,-)}(s_L, s_R)$  and  $Y_\mu^{(-,+)}(s_L, s_R)$ , are defined in [61]. For  $S = 1/2$ ,  $\Gamma_a$  (3.33) are reduced to the original  $SO(5)$  gamma matrices (3.1). For  $S = 1$ , see Appendix A.

The matrices  $\Gamma_a$  (3.33) can be regarded as a natural generalization of the gamma matrices, as they satisfy<sup>13</sup>

$$\sum_{a=1}^5 \Gamma_a \Gamma_a = 4S(S+2) \mathbf{1}_{D_{SO(5)}(S)}, \quad (3.36a)$$

$$[\Gamma_a, \Gamma_b, \Gamma_c, \Gamma_d] = -16(S+1) \epsilon_{abcde} \Gamma_e, \quad (3.36b)$$

<sup>13</sup>While (3.36) is a natural generalization of the basic properties of the gamma matrices

$$\sum_{a=1}^5 \gamma_a \gamma_a = 5 \cdot \mathbf{1}_4, \quad [\gamma_a, \gamma_b, \gamma_c, \gamma_d] = -4! \epsilon_{abcde} \gamma_e, \quad (3.34)$$

$\Gamma_a$  ( $S \geq 1$ ) fail to have a similar property to (3.2):

$$\Gamma_a \Gamma_a \not\propto \mathbf{1} \quad (\text{no sum for } a), \quad \Gamma_a \Gamma_b \neq -\Gamma_b \Gamma_a \quad (a \neq b). \quad (3.35)$$

where  $[\ , \ , \ ]$  represents the Nambu four-bracket, which denotes the total antisymmetric combination of the four entities inside the bracket. These relations (3.36) are exactly equal to the definition of the fuzzy four-sphere [78, 79]. The  $SO(5)$  matrix generators  $\Sigma_{ab}$  with matrix dimension (3.32) can be obtained from the commutators of the  $\Gamma_a$ s:

$$\Sigma_{ab} = -i\frac{1}{4}[\Gamma_a, \Gamma_b]. \quad (3.37)$$

The matrices  $\Gamma_a$  transform as an  $SO(5)$  vector,

$$[\Sigma_{ab}, \Gamma_c] = i\delta_{ac}\Gamma_b - i\delta_{bc}\Gamma_a, \quad (3.38)$$

or

$$\Gamma_a \rightarrow R_{ab}\Gamma_b, \quad (3.39)$$

where  $R_{ab} \equiv e^{i\frac{1}{2}\omega_{ab}\Sigma_{ab}^{(\text{vec})}}$  ( $(\Sigma_{ab}^{(\text{vec})})_{cd} \equiv -i\delta_{ac}\delta_{bd} + i\delta_{ad}\delta_{bc}$ ) denote  $SO(5)$  group elements,

$$R_{ac}R_{bc} = \delta_{ab}, \quad \epsilon_{abcde}R_{aa'}R_{bb'}R_{cc'}R_{dd'} = \epsilon_{a'b'c'd'e'}R_{ee'}. \quad (3.40)$$

It is obvious that (3.36) are  $SO(5)$  covariant equations, demonstrating the  $SO(5)$  spherical symmetry of the present system. In the large  $S$  limit, Eq.(3.36a) becomes  $\sum_{a=1}^5 \frac{1}{2}\Gamma_a \cdot \frac{1}{2}\Gamma_a \sim S^2 \mathbf{1}_{D_{SO(5)}(S)}$ , which implies that  $\frac{1}{2}\Gamma_a$  represent quantum spin matrices of spin  $S$ . The diagonal matrix  $\frac{1}{2}\Gamma_5$  (3.33b) is given by

$$\frac{1}{2}\Gamma_5 = \begin{pmatrix} S\mathbf{1}_{2S+1} & 0 & 0 & 0 & 0 \\ 0 & (S-1)\mathbf{1}_{4S} & 0 & 0 & 0 \\ 0 & 0 & (S-2)\mathbf{1}_{3(2S-1)} & 0 & 0 \\ 0 & 0 & 0 & \ddots & 0 \\ 0 & 0 & 0 & 0 & -S\mathbf{1}_{2S+1} \end{pmatrix} = \bigoplus_{\lambda=-S}^S \lambda \mathbf{1}_{D_{SO(4)}(s_L, s_R)}, \quad (3.41)$$

where

$$D_{SO(4)}(s_L, s_R) = (2s_L + 1)(2s_R + 1) = (S + \lambda + 1)(S - \lambda + 1) \quad (3.42)$$

with bi-spin index of  $SU(2)_L \otimes SU(2)_R \simeq SO(4)$ :

$$s_L \equiv \frac{S}{2} + \frac{\lambda}{2}, \quad s_R \equiv \frac{S}{2} - \frac{\lambda}{2}. \quad (3.43)$$

Note that  $\frac{1}{2}\Gamma_5$  (3.41) is exactly equal to  $S_z$  (2.26) up to the degeneracies.

We now introduce the  $SO(5)$  large-spin Zeeman-Dirac Hamiltonian as

$$H = \sum_{a=1}^5 x_a \cdot \frac{1}{2}\Gamma_a \quad \left( \sum_{a=1}^5 x_a x_a = 1 \right). \quad (3.44)$$

Since the  $\Gamma_a$  behave as an  $SO(5)$  vector, we can safely use the group-theoretic method to diagonalize this Hamiltonian. Replacing  $\sigma_{ab}$  with  $\Sigma_{ab}$  (3.37), we readily obtain

$$\Psi = e^{i\xi \sum_{\mu=1}^4 y_\mu \Sigma_{\mu 5}} = N(\chi, \theta, \phi)^\dagger \cdot e^{-i\xi \Sigma_{45}} \cdot N(\chi, \theta, \phi) \quad (N(\chi, \theta, \phi) \equiv e^{i\chi \Sigma_{43}} e^{i\theta \Sigma_{31}} e^{i\phi \Sigma_{12}}), \quad (3.45)$$

which diagonalizes the Hamiltonian,

$$\Psi^\dagger H \Psi = \frac{1}{2}\Gamma_5. \quad (3.46)$$

The eigenvalues of the  $SO(5)$  Hamiltonian range from  $-S$  to  $S$ , with each interval between the adjacent eigenvalues being 1. The degeneracy  $D_{SO(4)}(s_L, s_R)$  takes a convex form with a peak at the equation  $x_5 = 0$  (Fig.6). The explicit degenerate eigenstates can be identified from the non-linear realization matrix (Fig.7):



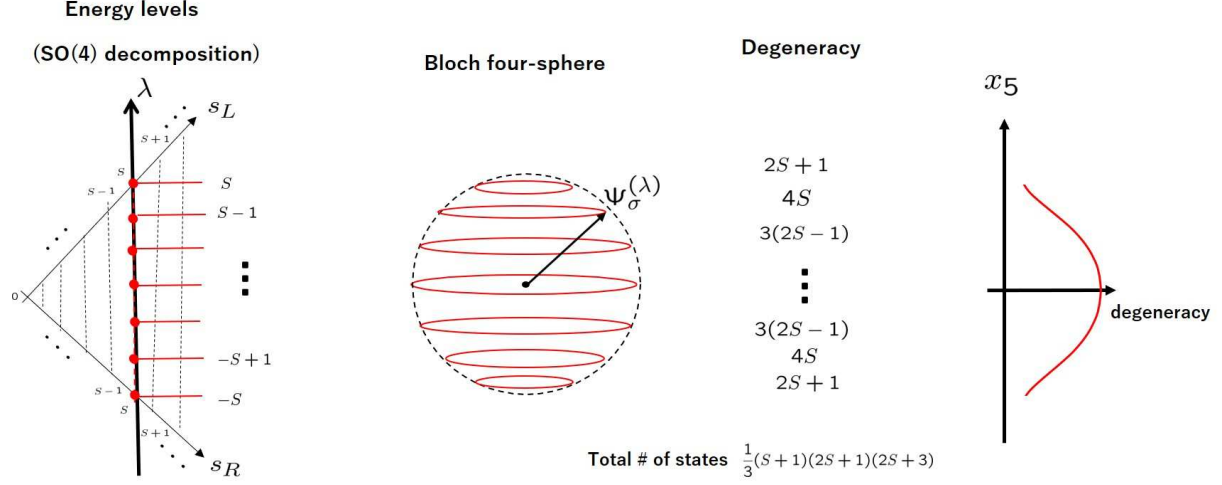


Figure 6: The  $SO(5)$  Zeeman-Dirac model with large spin  $S$ .

$$\begin{aligned} \Psi &= \left( \Psi^{(S)} \vdots \Psi^{(S-1)} \vdots \Psi^{(S-2)} \vdots \dots \vdots \Psi^{(-S)} \right) \\ &= \left( \Psi_1^{(S)} \dots \Psi_{2S+1}^{(S)} \vdots \Psi_1^{(S-1)} \dots \Psi_{4S}^{(S-1)} \vdots \Psi_1^{(S-2)} \dots \Psi_{3(2S-1)}^{(S-2)} \vdots \dots \vdots \Psi_1^{(-S)} \dots \Psi_{2S+1}^{(-S)} \right). \end{aligned} \quad (3.47)$$

The columns  $\Psi_\sigma^{(\lambda)}$  ( $\lambda = S, S-1, \dots, -S$ ,  $\sigma = 1, 2, \dots, D_{SO(4)}(s_L, s_R)$ ) denote the  $SO(5)$  spin-coherent states that satisfy

$$\sum_{a=1}^5 (x_a \cdot \frac{1}{2} \Gamma_a) \Psi_\sigma^{(\lambda)} = \lambda \Psi_\sigma^{(\lambda)} \quad (\sigma = 1, 2, \dots, D_{SO(4)}(s_L, s_R)). \quad (3.48)$$

Their ortho-normal relations are given by

$$\Psi_\sigma^{(\lambda)\dagger} \Psi_\tau^{(\lambda')} = \delta_{\sigma\tau} \delta_{\lambda\lambda'}. \quad (3.49)$$

Since  $\Gamma_5$  is immune to the  $SO(4)$  transformations,  $[\Gamma_5, \Sigma_{\mu\nu}] = 0$ , there exist  $SO(4)$  degrees of freedom in (3.46):

$$\Psi \rightarrow \Psi \cdot e^{i\frac{1}{2}\omega_{\mu\nu}\Sigma_{\mu\nu}}. \quad (3.50)$$

The Bloch vector is an  $SO(4)$  invariant quantity:

$$\Psi^{(\lambda)\dagger} \Gamma_a \Psi^{(\lambda)} = 2\lambda \cdot x_a \mathbf{1}_{D_{SO(4)}(s_L, s_R)}. \quad (3.51)$$

Unlike the previous  $SO(3)$  case (2.37), the quantum geometric tensor becomes a matrix-valued tensor, which transforms as an  $SO(4)$  covariant quantity (not an  $SO(4)$  invariant quantity):

$$\chi_{\theta_\mu\theta_\nu}^{(\lambda)} = \partial_{\theta_\mu} \Psi^{(\lambda)\dagger} \partial_{\theta_\nu} \Psi^{(\lambda)} - \partial_{\theta_\mu} \Psi^{(\lambda)\dagger} \Psi^{(\lambda)} \Psi^{(\lambda)\dagger} \partial_{\theta_\nu} \Psi^{(\lambda)} \quad (\theta_\mu, \theta_\nu = \xi, \chi, \theta, \phi). \quad (3.52)$$

(See Appendix B for more details on matrix-valued quantum geometric tensors.) The trace of its symmetric part gives rise to the four-sphere metric:<sup>14</sup>

$$g_{\theta_\mu\theta_\nu}^{(\lambda)} = \frac{1}{2} \text{tr}(\chi_{\theta_\mu\theta_\nu}^{(\lambda)} + \chi_{\theta_\nu\theta_\mu}^{(\lambda)}) \propto g_{\theta_\mu\theta_\nu}^{(S^4)} = \text{diag}(1, \sin^2 \xi, \sin^2 \xi \sin^2 \chi, \sin^2 \xi \sin^2 \chi \sin^2 \theta). \quad (3.53)$$

<sup>14</sup>Using a mathematical software, we checked the validity of (3.53) up to  $S = 2$ . Similar calculations have been performed in the context of the Landau models [63, 58].

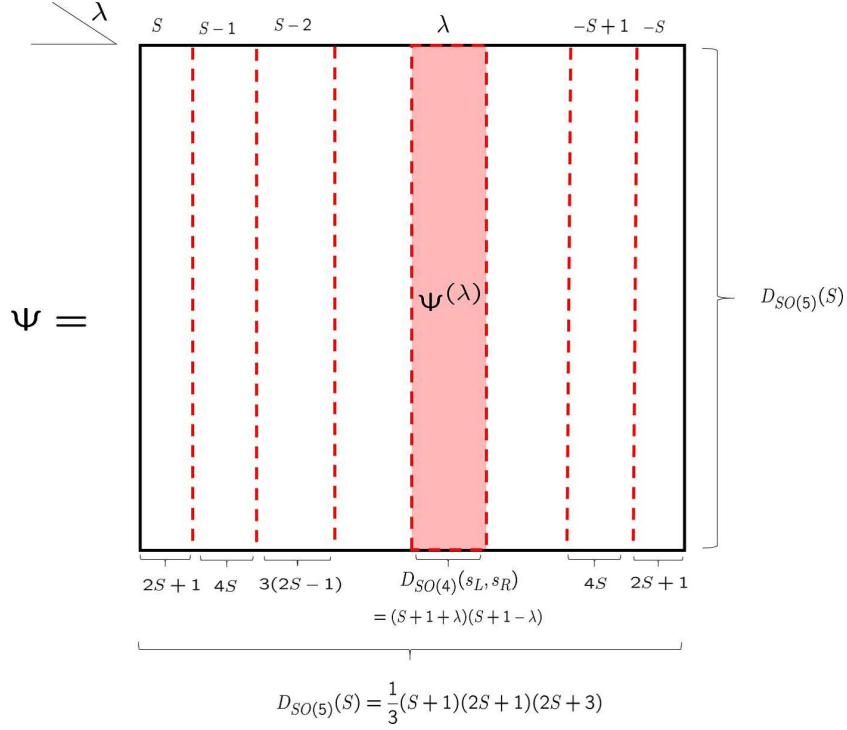


Figure 7: The  $SO(5)$  spin-coherent state matrix  $\Psi^{(\lambda)}$  in  $\Psi$ .

The dependence of  $S$  and  $|\lambda|$  is accounted for by the proportionality coefficient omitted in (3.53).

Following a similar calculation in [63], the Wilczek-Zee connections are derived as

$$-i\Psi^\dagger d\Psi = \begin{pmatrix} A^{(S)} & * & * & * & * \\ * & A^{(S-1)} & * & * & * \\ * & * & \ddots & * & * \\ * & * & * & A^{(-S+1)} & * \\ * & * & * & * & A^{(-S)} \end{pmatrix}, \quad (3.54)$$

where

$$A^{(\lambda)} = -i\Psi^{(\lambda)\dagger} d\Psi^{(\lambda)} = -\frac{1}{1+x_5} \Sigma_{\mu\nu}^{(s_L, s_R)} x_\nu dx_\mu = \frac{1}{2} \omega_{\mu\nu\theta\rho} \Sigma_{\mu\nu}^{(s_L, s_R)} d\theta_\rho. \quad (3.55)$$

Here,  $\omega_{\mu\nu\theta\rho}$  denote the spin-connection of  $S^4$  [61] and  $\Sigma_{\mu\nu}^{(s_L, s_R)}$  signify the  $SO(4)$  matrix generators

$$\Sigma_{\mu\nu}^{(s_L, s_R)} \equiv \eta_{\mu\nu}^{(+i)} S_i^{(s_L)} \otimes \mathbf{1}_{2s_R+1} + \mathbf{1}_{2s_L+1} \otimes \eta_{\mu\nu}^{(-i)} S_i^{(s_R)}, \quad (3.56)$$

with 't Hooft tensors  $\eta_{\mu\nu}^{(\pm i)}$  (3.5). The Wilczek-Zee connections  $A^{(\lambda)}$  in (3.55) coincide with the gauge fields of the  $SO(4)$  monopoles [63].<sup>15</sup> The corresponding curvature,  $F_{\theta_\mu\theta_\nu} = \partial_{\theta_\mu} A_{\theta_\nu} - \partial_{\theta_\nu} A_{\theta_\mu} + i[A_{\theta_\mu}, A_{\theta_\nu}]$ , is equal to the antisymmetric part of (3.52):

$$F_{\theta_\mu\theta_\nu}^{(\lambda)} = -i(\chi_{\theta_\mu\theta_\nu}^{(\lambda)} - \chi_{\theta_\nu\theta_\mu}^{(\lambda)}) = \frac{1}{2} e_{\theta_\mu}^{\mu'} \wedge e_{\theta_\nu}^{\nu'} \Sigma_{\mu'\nu'}^{(s_L, s_R)}, \quad (3.58)$$

<sup>15</sup>The stereographic projection of the  $SO(4)$  monopole is given by the  $SO(4)$  BPST instanton configuration on  $\mathbb{R}^4$ :

$$A_\mu = -\frac{2}{x^2+1} \Sigma_{\mu\nu}^{(s_L, s_R)} x_\nu, \quad F_{\mu\nu} = -\frac{4}{(x^2+1)^2} \Sigma_{\mu\nu}^{(s_L, s_R)}, \quad (3.57)$$

which does not satisfy either the self- or the anti-self dual equation, but realizes a solution of the pure Yang-Mills field equation.

where  $e^{\mu'}_{\theta\mu}$  denote the vierbein of  $S^4$  [61]. The  $SO(4)$  monopole is essentially the composite of the  $SU(2)$  monopole and the  $SU(2)$  anti-monopole to have two topological invariants, the second Chern number and a generalized Euler number [63]:

$$\text{ch}_2^{(\lambda)} \equiv \frac{1}{8\pi^2} \int_{S^4} \text{tr}(F \wedge F) = \frac{1}{8\pi^2} \int_{S^4} \text{tr}(\mathcal{F} \wedge \mathcal{F}) = \frac{2}{3}(S+1)\lambda(S+1+\lambda)(S+1-\lambda), \quad (3.59a)$$

$$\tilde{c}_2^{(\lambda)} \equiv \frac{1}{8\pi^2} \int_{S^4} \text{tr}(F \wedge \mathcal{F}) = \frac{1}{8\pi^2} \int_{S^4} \text{tr}(\mathcal{F} \wedge F) = \frac{1}{3}(S(S+2)+\lambda^2)(S+1+\lambda)(S+1-\lambda), \quad (3.59b)$$

where  $\mathcal{F}$  stands for the dual field strength of  $F$  with the replacement of the  $SO(4)$  matrix generators  $\Sigma_{\mu\nu}^{(s_L, s_R)}$  in (3.58) by  $\frac{1}{2}\epsilon_{\mu\nu\rho\sigma}\Sigma_{\rho,\sigma}^{(s_L, s_R)}$ . The topological numbers (3.59) exhibit the reflection symmetry:

$$\text{ch}_2^{(\lambda)} = -\text{ch}_2^{(-\lambda)}, \quad \tilde{c}_2^{(\lambda)} = +\tilde{c}_2^{(-\lambda)}. \quad (3.60)$$

The Atiyah-Singer index theorem tells that [63]

$$\text{ch}_2^{(\lambda)} = \text{sgn}(\lambda) \cdot D_{SO(5)}(S - \frac{1}{2}, |\lambda| - \frac{1}{2}) = -\text{ch}_2^{(-\lambda)}, \quad (3.61)$$

where  $\text{sgn}(0) \equiv 0$  and

$$D_{SO(5)}(S - \frac{1}{2}, |\lambda| - \frac{1}{2}) \equiv \frac{2}{3}(S+1)|\lambda|(S+|\lambda|+1)(S-|\lambda|+1). \quad (3.62)$$

The  $SO(5)$  spin-coherent state matrices in (3.47) are represented as

$$\Psi^{(\lambda)} = \left( \Psi_1^{(\lambda)} \quad \Psi_2^{(\lambda)} \quad \dots \quad \Psi_{D_{SO(4)}(s_L, s_R)}^{(\lambda)} \right) = \begin{pmatrix} \psi_1^{(\lambda)\dagger} \\ \psi_2^{(\lambda)\dagger} \\ \psi_3^{(\lambda)\dagger} \\ \vdots \\ \psi_{D_{SO(5)}(S)}^{(\lambda)} \end{pmatrix}^\dagger, \quad (3.63)$$

where  $\psi_\alpha^{(\lambda)}$  are the  $SO(5)$  Landau level eigenstates of the  $SO(4)$  monopole background with bi-spin index  $(s_L, s_R) = (\frac{S}{2} + \frac{\lambda}{2}, \frac{S}{2} - \frac{\lambda}{2})$  (3.43) (see Fig.8).<sup>16</sup> The correspondence between the spin-coherent states and the Landau level eigenstates is given as follows:

$D_{SO(5)}(S)$  : Dimension of the spin-coherent states = Degeneracy of the Landau level eigenstates  
 $D_{SO(4)}(s_L, s_R)$  : Degeneracy of the spin-coherent states = Dimension of the Landau level eigenstates

## 4 Bloch three-sphere and $SO(4)$ Zeeman-Dirac model

This section discusses the  $SO(4)$  Zeeman-Dirac models. The properties of the large-spin  $SO(4)$  Zeeman-Dirac models are quite different from those of the  $SO(3)$  and  $SO(5)$  models.

<sup>16</sup>The orthonormal relations for the  $SO(5)$  monopole harmonics are given by

$$\int_{S^4} d\Omega_4 \psi_\alpha^{(\lambda)\dagger} \psi_\beta^{(\lambda)} = A(S^4) \frac{D_{SO(4)}(s_L, s_R)}{D_{SO(5)}(S)} = 8\pi^2 \frac{(S+\lambda+1)(S-\lambda+1)}{(S+1)(2S+1)(2S+3)} \quad (\alpha, \beta = 1, 2, \dots, D_{SO(5)}(S)), \quad (3.64)$$

where  $A(S^4) = \frac{8\pi^2}{3}$ . The  $SO(4)$  monopole gauge field (3.55) can also be represented as

$$A^{(\lambda)} = -i \sum_{\alpha=1}^{D_{SO(5)}(S)} \psi_\alpha^{(\lambda)} d\psi_\alpha^{(\lambda)\dagger}. \quad (3.65)$$

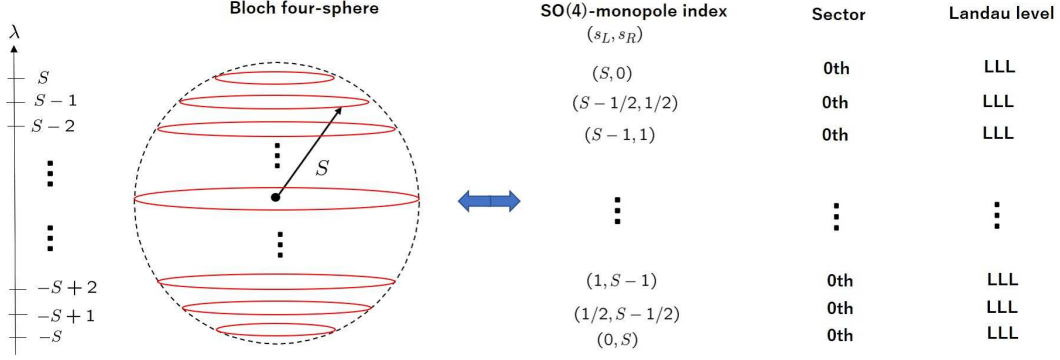


Figure 8: The Bloch four-sphere and the  $SO(5)$  Landau level eigenstates.

#### 4.1 Minimal spin model

With the  $SO(4)$  gamma matrices  $\gamma_\mu$  (3.1), we construct the minimal  $SO(4)$  Zeeman-Dirac model,

$$H = \sum_{\mu=1}^4 x_\mu \cdot \frac{1}{2} \gamma_\mu = \frac{1}{2} \begin{pmatrix} 0 & \sum_{\mu=1}^4 x_\mu \bar{q}_\mu \\ \sum_{\mu=1}^4 x_\mu q_\mu & 0 \end{pmatrix} \quad \left( \sum_{\mu=1}^4 x_\mu x_\mu = 1 \right). \quad (4.1)$$

As the  $SO(5)$  minimal Hamiltonian (3.8) is reduced to (4.1) on the  $S^3$ -equator ( $\xi = \frac{\pi}{2}$ ) of the four-sphere, they share similar properties, such as  $H^2 = \frac{1}{4} \mathbf{1}_4$ . With the  $S^3$ -coordinates

$$x_1 = \sin \theta \cos \phi \sin \chi, \quad x_2 = \sin \theta \sin \phi \sin \chi, \quad x_3 = \cos \theta \sin \chi, \quad x_4 = \cos \chi, \quad (4.2)$$

we introduce a unitary matrix in a similar manner to (3.12)<sup>17</sup>

$$\Psi(\chi, \theta, \phi) = e^{i\chi \sum_{i=1}^3 y_i \sigma_{i4}} = \begin{pmatrix} U(\chi, \theta, \phi) & 0 \\ 0 & U(\chi, \theta, \phi)^\dagger \end{pmatrix} \quad (y_{i=1,2,3} \equiv \frac{1}{\sin \chi} x_i), \quad (4.4)$$

where

$$U(\chi, \theta, \phi) \equiv e^{i\frac{\chi}{2} y_i \sigma_i} = \frac{1}{\sqrt{2(1+x_4)}} ((1+x_4) \mathbf{1}_2 + i x_i \sigma_i). \quad (4.5)$$

The unitary matrix  $\Psi$  transforms the  $SO(4)$  minimal Hamiltonian into the form

$$\Psi^\dagger H \Psi = \frac{1}{2} \gamma_4. \quad (4.6)$$

Applying another unitary transformation

$$V \equiv e^{i\frac{\pi}{2} \sigma_{45}} = \frac{1}{\sqrt{2}} \begin{pmatrix} \mathbf{1}_2 & -\mathbf{1}_2 \\ \mathbf{1}_2 & \mathbf{1}_2 \end{pmatrix} \quad (V^\dagger \gamma_4 V = \gamma_5), \quad (4.7)$$

we can diagonalize the  $SO(4)$  Hamiltonian (4.1) as

$$\tilde{\Psi}^\dagger H \tilde{\Psi} = \frac{1}{2} \gamma_5, \quad (4.8)$$

<sup>17</sup>Using (3.15), we can factorize (4.4) as

$$\Psi(\chi, \theta, \phi) = N(\theta, \phi)^\dagger \cdot e^{i\chi \sigma_{34}} \cdot N(\theta, \phi) \quad (N(\theta, \phi) \equiv e^{i\theta \sigma_{31}} e^{i\phi \sigma_{12}}). \quad (4.3)$$

where

$$\tilde{\Psi} \equiv \Psi V = \frac{1}{\sqrt{2}} \begin{pmatrix} U & -U \\ U^\dagger & U^\dagger \end{pmatrix}. \quad (4.9)$$

Therefore, the  $SO(4)$  spin-coherent states that satisfy

$$H\tilde{\Psi}_\sigma^{(\pm\frac{1}{2})} = \pm\frac{1}{2}\tilde{\Psi}_\sigma^{(\pm\frac{1}{2})} \quad (\sigma = 1, 2) \quad (4.10)$$

are obtained as

$$\tilde{\Psi} = ( \tilde{\Psi}_1^{(+\frac{1}{2})} \tilde{\Psi}_2^{(+\frac{1}{2})} ; \tilde{\Psi}_1^{(-\frac{1}{2})} \tilde{\Psi}_2^{(-\frac{1}{2})} ) \quad (4.11)$$

where

$$\begin{aligned} \tilde{\Psi}_1^{(+\frac{1}{2})} &= \frac{1}{2\sqrt{1+x_4}} \begin{pmatrix} 1+x_4+ix_3 \\ -x_2+ix_1 \\ 1+x_4-ix_3 \\ x_2-ix_1 \end{pmatrix}, & \tilde{\Psi}_2^{(+\frac{1}{2})} &= \frac{1}{2\sqrt{1+x_4}} \begin{pmatrix} x_2+ix_1 \\ 1+x_4-ix_3 \\ -x_2-ix_1 \\ 1+x_4+ix_3 \end{pmatrix}, \\ \tilde{\Psi}_1^{(-\frac{1}{2})} &= \frac{1}{2\sqrt{1+x_4}} \begin{pmatrix} -1-x_4-ix_3 \\ x_2-ix_1 \\ 1+x_4-ix_3 \\ x_2-ix_1 \end{pmatrix}, & \tilde{\Psi}_2^{(-\frac{1}{2})} &= \frac{1}{2\sqrt{1+x_4}} \begin{pmatrix} -x_2-ix_1 \\ -1-x_4+ix_3 \\ -x_2-ix_1 \\ 1+x_4+ix_3 \end{pmatrix}. \end{aligned} \quad (4.12)$$

See Fig.9. The eigenvalues and the degeneracies of the  $SO(4)$  minimal model are equal to those of the  $SO(5)$  minimal model. Equation (4.6) is invariant under the  $SO(3)$  transformation

$$\Psi \rightarrow \Psi \cdot e^{i\frac{1}{2}\omega_{ij}\sigma_{ij}}, \quad (4.13)$$

where  $\sigma_{ij} = \frac{1}{2}\epsilon_{ijk} \begin{pmatrix} \sigma_k & 0 \\ 0 & \sigma_k \end{pmatrix}$  are the  $SO(3)$  matrix generators that commute with  $\gamma_4$ . This symmetry brings the  $SO(3)$  degeneracy to each energy level. As an  $SO(3)$  gauge invariant quantity, the  $SO(4)$  Bloch vector satisfies

$$(\tilde{\Psi}_\sigma^{(\pm\frac{1}{2})})^\dagger \gamma_\mu \tilde{\Psi}_\tau^{(\pm\frac{1}{2})} = \pm x_\mu \delta_{\sigma\tau}. \quad (4.14)$$

In the present case, the doubly degenerate  $SO(4)$  spin-coherent states in the upper and lower energy levels provide the identical Wilczek-Zee connection

$$A \equiv -i\tilde{\Psi}_1^\dagger d\tilde{\Psi}_1 = -i\tilde{\Psi}_2^\dagger d\tilde{\Psi}_2 = -i\frac{1}{2}(U^\dagger dU + UdU^\dagger) = -\frac{1}{2(1+x_4)}\epsilon_{ijk}x_j dx_i \sigma_k, \quad (4.15)$$

which exactly coincides with the  $SU(2)$  spin-connection of  $S^3$  [80, 81].

## 4.2 Large spin model

The construction of the  $SO(4)$  large-spin Zeeman-Dirac model is rather tricky. One might consider to adopt  $\Gamma_{\mu=1,2,3,4}$  (3.33) as the  $SO(4)$  large spin gamma matrices, but  $\Gamma_\mu$  are not good enough for this purpose. This is because the sum of the squares of  $\Gamma_\mu$  is not proportional to the unit matrix:

$$\sum_{\mu=1}^4 \Gamma_\mu \Gamma_\mu \not\propto \mathbf{1}. \quad (4.16)$$

The generalized gamma matrices with the desired property,  $\sum_{\mu=1}^4 \Gamma_\mu \Gamma_\mu \propto \mathbf{1}$ , can be constructed from the  $SO(4)$  Landau model [66, 57, 80] in the subspace [82, 83, 84, 85] (Fig.10):

$$(s_L, s_R) = \left(\frac{S}{2} + \frac{1}{4}, \frac{S}{2} - \frac{1}{4}\right) \oplus \left(\frac{S}{2} - \frac{1}{4}, \frac{S}{2} + \frac{1}{4}\right) \quad (2S : \text{odd}). \quad (4.17)$$

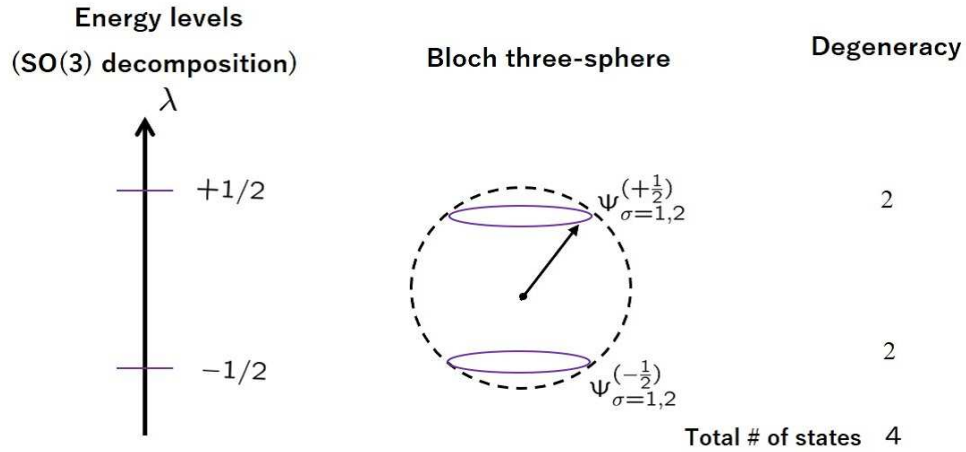


Figure 9:  $SO(4)$  minimal Zeeman-Dirac model.

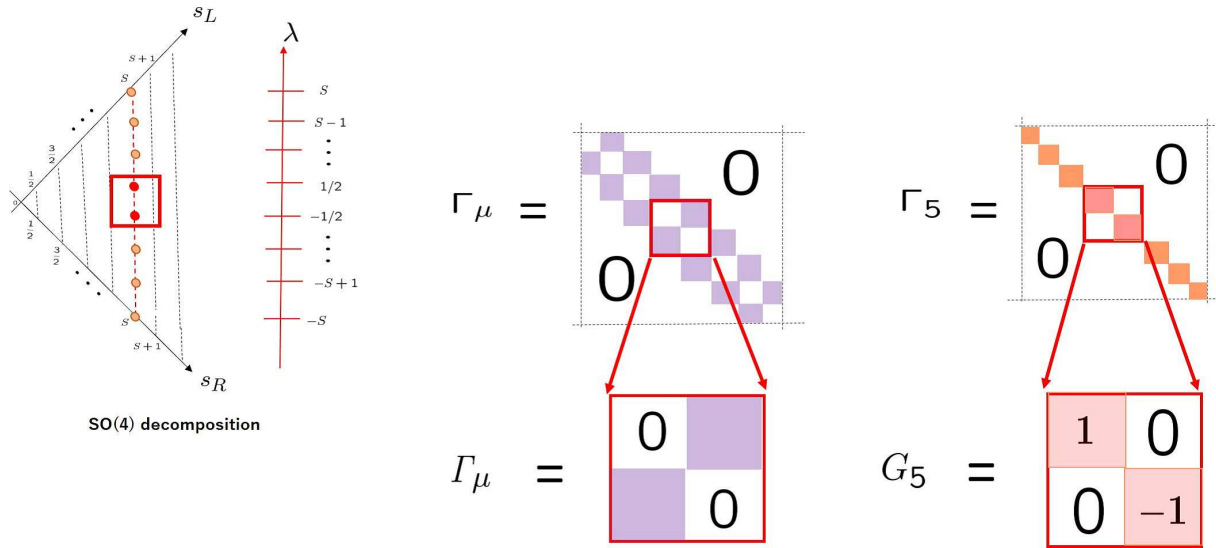


Figure 10: The  $SO(4)$  subspace of  $(s_L, s_R) = (\frac{2S+1}{4}, \frac{2S-1}{4}) \oplus (\frac{2S-1}{4}, \frac{2S+1}{4})$ , with dimension,  $2 \cdot \frac{2S+3}{2} \cdot \frac{2S+1}{2} = \frac{1}{2}(2S+3)(2S+1)$ .

The subspace (4.17) geometrically corresponds to the two latitudes adjacent to the equator of the Bloch four-sphere. The restriction to a sub-space obviously reduces the  $SO(5)$  covariance to the  $SO(4)$  covariance. Note that  $S$  must be a half-integer value in the  $SO(4)$  models, so that  $s_{L/R}$  (4.17) takes integer or half-integer values. The matrix elements of  $\Gamma_\mu$  in the subspace (4.17) are given by

$$\Gamma_\mu = -(2S+3) \begin{pmatrix} 0 & Y_\mu^{(+,-)}(\frac{2S-1}{4}, \frac{2S+1}{4}) \\ Y_\mu^{(-,+)}(\frac{2S+1}{4}, \frac{2S-1}{4}) & 0 \end{pmatrix} \quad (2S : \text{odd}), \quad (4.18)$$

where  $Y_\mu^{(+,-)}(\frac{2S-1}{4}, \frac{2S+1}{4})$  are  $\frac{1}{4}(2S+1)(2S+3) \times \frac{1}{4}(2S+1)(2S+3)$  square matrices and  $Y_\mu^{(-,+)}(\frac{2S+1}{4}, \frac{2S-1}{4})$  are their Hermitian conjugates.<sup>18</sup> For  $S = 1/2$ , (4.18) is equal to  $\gamma_\mu$ . For  $S = 3/2$ , see Appendix A.2.

With (4.19), we can explicitly show that  $\Gamma_\mu$  (4.18) satisfy [66, 57]<sup>19</sup>

$$\sum_{\mu=1}^4 \Gamma_\mu \Gamma_\mu = \frac{1}{2}(2S+1)(2S+3) \mathbf{1}_{\frac{1}{2}(2S+1)(2S+3)}, \quad (4.22a)$$

$$[[\Gamma_\mu, \Gamma_\nu, \Gamma_\rho]] = 16(S+1) \epsilon_{\mu\nu\rho\sigma} \Gamma_\sigma, \quad (4.22b)$$

where  $[[\ , \ , \ ]]$  signifies the Nambu “three-bracket” defined by

$$[[\Gamma_\mu, \Gamma_\nu, \Gamma_\rho]] \equiv [\Gamma_\mu, \Gamma_\nu, \Gamma_\rho, G_5] = 4[\Gamma_\mu, \Gamma_\nu, \Gamma_\rho] G_5 \quad (4.23)$$

with

$$G_5 \equiv \begin{pmatrix} \mathbf{1}_{\frac{1}{4}(2S+3)(2S+1)} & 0 \\ 0 & -\mathbf{1}_{\frac{1}{4}(2S+3)(2S+1)} \end{pmatrix}. \quad (4.24)$$

Equations (4.22) denote the definition of fuzzy three-sphere [83, 84]. The corresponding  $SO(4)$  matrix generators are given by

$$\Sigma_{\mu\nu} \equiv \bigoplus_{\lambda=-\frac{1}{2}}^{\frac{1}{2}} \Sigma_{\mu\nu}^{(\frac{s}{2}+\frac{\lambda}{2}, \frac{s}{2}-\frac{\lambda}{2})} = \begin{pmatrix} \Sigma_{\mu\nu}^{(\frac{2S+1}{4}, \frac{2S-1}{4})} & 0 \\ 0 & \Sigma_{\mu\nu}^{(\frac{2S-1}{4}, \frac{2S+1}{4})} \end{pmatrix}. \quad (4.25)$$

---

<sup>18</sup>Explicitly,  $Y_\mu^{(+,-)}$  are given by [57]

$$\begin{aligned} Y_{\mu=1,2}^{(+,-)}(\frac{2S-1}{4}, \frac{2S+1}{4})_{(m'_L, m'_R; m_L, m_R)} &= \frac{1}{2S+3} (-i)^\mu \times \\ &\left( \delta_{m'_L, m_L + \frac{1}{2}} \delta_{m'_R, m_R + \frac{1}{2}} \sqrt{\left(\frac{2S+3}{4} + m_L\right)\left(\frac{2S+1}{4} - m_R\right)} - (-1)^\mu \delta_{m'_L, m_L - \frac{1}{2}} \delta_{m'_R, m_R - \frac{1}{2}} \sqrt{\left(\frac{2S+3}{4} - m_L\right)\left(\frac{2S+1}{4} + m_R\right)} \right), \\ Y_{\mu=3,4}^{(+,-)}(\frac{2S-1}{4}, \frac{2S+1}{4})_{(m'_L, m'_R; m_L, m_R)} &= -\frac{1}{2S+3} (-i)^\mu \times \\ &\left( \delta_{m'_L, m_L + \frac{1}{2}} \delta_{m'_R, m_R - \frac{1}{2}} \sqrt{\left(\frac{2S+3}{4} + m_L\right)\left(\frac{2S+1}{4} + m_R\right)} + (-1)^\mu \delta_{m'_L, m_L - \frac{1}{2}} \delta_{m'_R, m_R + \frac{1}{2}} \sqrt{\left(\frac{2S+3}{4} - m_L\right)\left(\frac{2S+1}{4} - m_R\right)} \right), \end{aligned} \quad (4.19)$$

with  $-\frac{2S+1}{4} \leq m'_L, m_R \leq \frac{2S+1}{4}$  and  $-\frac{2S-1}{4} \leq m_L, m'_R \leq \frac{2S-1}{4}$ , and

$$Y_\mu^{(-,+)}(\frac{2S+1}{4}, \frac{2S-1}{4}) = Y_\mu^{(+,-)}(\frac{2S-1}{4}, \frac{2S+1}{4})^\dagger. \quad (4.20)$$

<sup>19</sup>Equation (4.22) realizes a natural generalization of the properties of the  $SO(4)$  gamma matrices,

$$\sum_{\mu=1}^4 \gamma_\mu \gamma_\mu = 4 \cdot \mathbf{1}_4, \quad [\gamma_\mu, \gamma_\nu, \gamma_\rho, \gamma_5] = 4! \epsilon_{\mu\nu\rho\sigma} \gamma_\sigma. \quad (4.21)$$

Notice that, while the commutators between  $\Gamma_\mu$  do not yield  $SO(4)$  matrix generators (4.25) (except for  $S = 1/2$ )<sup>20</sup>

$$[\Gamma_\mu, \Gamma_\nu] \neq 4i\Sigma_{\mu\nu}, \quad (4.26)$$

$\Gamma_\mu$  behave as an  $SO(4)$  vector under the transformation generated by  $\Sigma_{\mu\nu}$ :

$$[\Sigma_{\mu\nu}, \Gamma_\rho] = i\delta_{\mu\rho}\Gamma_\nu - i\delta_{\nu\rho}\Gamma_\mu. \quad (4.27)$$

The matrix  $G_5$  (4.24) obviously satisfies  $[\Sigma_{\mu\nu}, G_5] = 0$  and is immune to the  $SO(4)$  transformations generated by  $\Sigma_{\mu\nu}$ . These properties imply that (4.22) are  $SO(4)$  covariant equations. Note that any of  $\Gamma_\mu$  is diagonalized as

$$\begin{aligned} \Gamma_\mu &\rightarrow \Gamma_{\text{diag}} \equiv \begin{pmatrix} S\mathbf{1}_{2S+1} & 0 & 0 & 0 & 0 \\ 0 & (S-1)\mathbf{1}_{2S-1} & 0 & 0 & 0 \\ 0 & 0 & (S-2)\mathbf{1}_{2S-3} & 0 & 0 \\ 0 & 0 & 0 & \ddots & 0 \\ 0 & 0 & 0 & 0 & -S\mathbf{1}_{2S+1} \end{pmatrix} + \frac{1}{2}G_5 \\ &= \bigoplus_{\lambda=-S}^S (\lambda + \frac{1}{2}\text{sgn}(\lambda)) \mathbf{1}_{2|\lambda|+1}. \end{aligned} \quad (4.28)$$

We checked the validity of (4.28) using the explicit form of  $\Gamma_\mu$  for  $S = 1/2, 3/2, 5/2$  and  $7/2$ , though we do not have a general proof of (4.28) for arbitrary  $S$ . However, it may be reasonable to assume that (4.28) holds for arbitrary  $S$ , since the parent  $SO(5)$  gamma matrices are diagonalized to take the same form  $\Gamma_5$  (3.41) regardless of spin magnitude. One may find a resemblance between  $\Gamma_{\text{diag}}$  (4.28) and  $\frac{1}{2}\Gamma_5$  (3.41). We now introduce the large-spin  $SO(4)$  Zeeman-Dirac Hamiltonian as

$$H = \sum_{\mu=1}^4 x_\mu \cdot \frac{1}{2}\Gamma_\mu. \quad (4.29)$$

With the  $SO(4)$  covariance, the Hamiltonian (4.29) can be transformed as

$$\Psi^\dagger \cdot H \cdot \Psi = \frac{1}{2}\Gamma_4, \quad (4.30)$$

where

$$\Psi = e^{i\chi \sum_{i=1}^3 y_i \Sigma_{i4}} = \begin{pmatrix} e^{i\chi \sum_{i=1}^3 y_i \Sigma_{i4}^{(\frac{2S+1}{4}, \frac{2S-1}{4})}} & 0 \\ 0 & e^{i\chi \sum_{i=1}^3 y_i \Sigma_{i4}^{(\frac{2S-1}{4}, \frac{2S+1}{4})}} \end{pmatrix}. \quad (4.31)$$

The matrix  $\Psi$  is factorized as

$$\Psi(\chi, \theta, \phi) = \mathcal{N}(\theta, \phi)^\dagger e^{i\chi \Sigma_{34}} \mathcal{N}(\theta, \phi), \quad (4.32)$$

with

$$\mathcal{N}(\theta, \phi) = e^{i\theta \Sigma_{31}} e^{i\phi \Sigma_{12}}. \quad (4.33)$$

Equation (4.30) obviously has the  $SO(3)$  symmetry generated by  $\Sigma_{ij}$ , and so each energy level accommodates the  $2|\lambda| + 1$  degeneracy, accordingly.

---

<sup>20</sup>See also Appendix A.2.



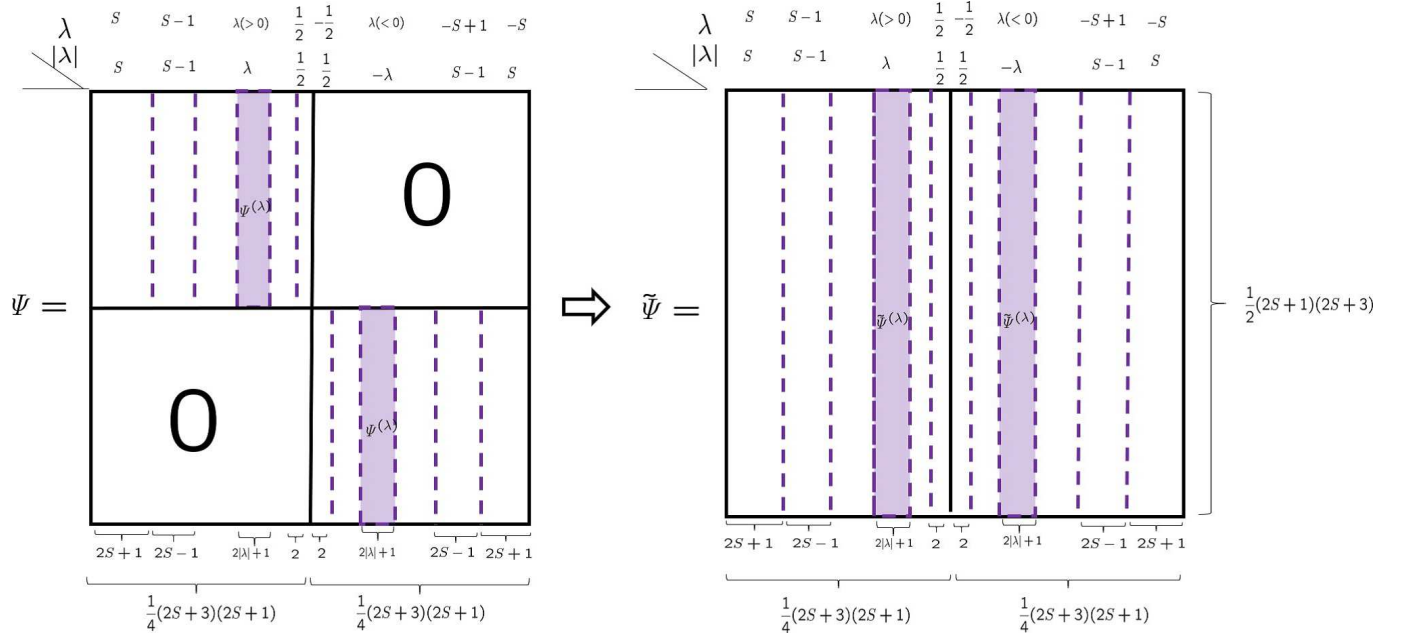


Figure 11: (Left)  $\Psi$  (4.32). For positive/negative  $\lambda$ ,  $\Psi^{(\lambda)}$  appears in the up-left/down-right block of  $\Psi$ . (Right)  $\tilde{\Psi}$  (4.36). For positive/negative  $\lambda$ ,  $\tilde{\Psi}^{(\lambda)}$  appears in the left/right block of  $\tilde{\Psi}$ .

The rectangular matrices  $\Psi^{(\lambda)}$  in Fig.11 are made of the  $SO(4)$  monopole harmonics  $\phi_\alpha^{(\lambda)} \equiv \phi_\alpha^{(s_L, s_R) = (\frac{S}{2} + \frac{1}{4} \text{sgn}(\lambda), \frac{S}{2} - \frac{1}{4} \text{sgn}(\lambda))}$  (C.22) as<sup>21</sup>

$$\Psi^{(\lambda)} \equiv \begin{pmatrix} \Psi_1^{(\lambda)} & \Psi_2^{(\lambda)} & \dots & \Psi_{2|\lambda|+1}^{(\lambda)} \end{pmatrix} = \begin{pmatrix} \phi_1^{(\lambda)\dagger} \\ \phi_2^{(\lambda)\dagger} \\ \phi_3^{(\lambda)\dagger} \\ \vdots \\ \phi_{(S+\frac{3}{2})(S+\frac{1}{2})}^{(\lambda)\dagger} \end{pmatrix}. \quad (4.34)$$

See Fig.12 also.

With an appropriate unitary matrix  $\mathcal{V}$ ,  $\Gamma_4$  is diagonalized as in (4.28):

$$\mathcal{V}^\dagger \Gamma_4 \mathcal{V} = \Gamma_{\text{diag}}. \quad (4.35)$$

Therefore, with

$$\tilde{\Psi} \equiv \Psi \mathcal{V}, \quad (4.36)$$

we can diagonalize  $H$  (4.29) as

$$\tilde{\Psi}^\dagger H \tilde{\Psi} = \frac{1}{2} \Gamma_{\text{diag}} = \begin{pmatrix} \frac{S}{2} \mathbf{1}_{2S+1} & 0 & 0 & 0 & 0 \\ 0 & (\frac{S}{2} - \frac{1}{2}) \mathbf{1}_{2S-1} & 0 & 0 & 0 \\ 0 & 0 & (\frac{S}{2} - 1) \mathbf{1}_{2S-3} & 0 & 0 \\ 0 & 0 & 0 & \ddots & 0 \\ 0 & 0 & 0 & 0 & -\frac{S}{2} \mathbf{1}_{2S+1} \end{pmatrix} + \frac{1}{4} G_5. \quad (4.37)$$

<sup>21</sup>See Appendix C for more details on the  $SO(4)$  monopole harmonics. Here,  $\phi_\alpha^{(\lambda)}$  denote the lowest sub-band eigenstates of  $S - |\lambda|$ th Landau level with the chirality  $\text{sgn}(\lambda)$  in the background of the  $SU(2)$  monopole with the spin index  $|\lambda|$ .

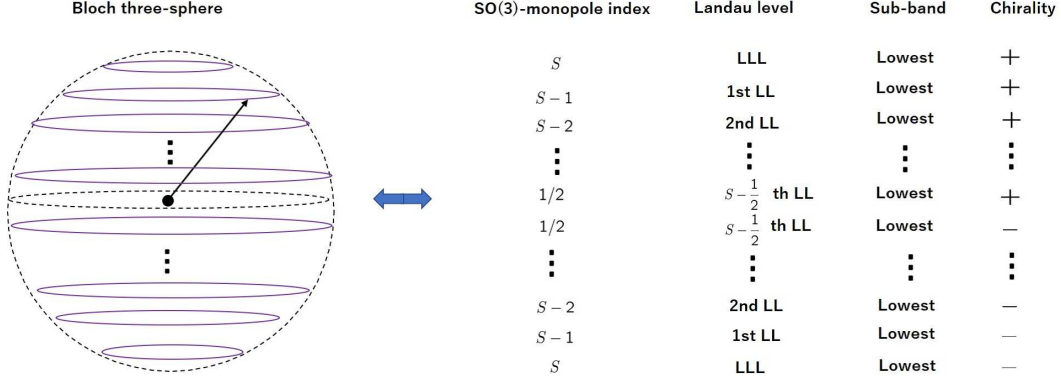


Figure 12: Bloch three-sphere and the  $SO(4)$  Landau level eigenstates

The eigenvalues rang from  $-(\frac{S}{2} + \frac{1}{4})$  to  $+\frac{S}{2} + \frac{1}{4}$ , equally spaced by  $1/2$ , except for the spacing 1 between  $1/2$  and  $-1/2$  (Fig.13).

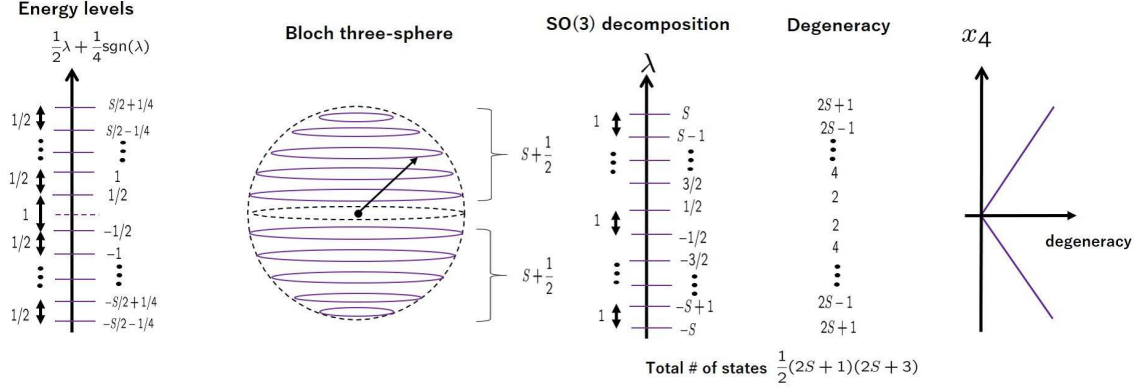


Figure 13: For odd  $2S$ , there are  $2S + 1$  energy levels. Note that zero-energy state is void.

The  $SO(4)$  spin-coherent states  $\tilde{\Psi}_\sigma^{(\lambda)}$  are realized in  $\tilde{\Psi}$  as (Fig.11):

$$\begin{aligned} \tilde{\Psi} &= \left( \tilde{\Psi}^{(S)} \vdots \tilde{\Psi}^{(S-1)} \vdots \dots \vdots \tilde{\Psi}^{(1/2)} \vdots \tilde{\Psi}^{(-1/2)} \vdots \dots \vdots \tilde{\Psi}^{(-S+1)} \vdots \tilde{\Psi}^{(-S)} \right) \\ &= \left( \tilde{\Psi}_S^{(S)} \dots \tilde{\Psi}_{-S}^{(S)} \vdots \tilde{\Psi}_{S-1}^{(S-1)} \dots \tilde{\Psi}_{-(S-1)}^{(S-1)} \vdots \dots \vdots \tilde{\Psi}_{1/2}^{(1/2)} \tilde{\Psi}_{-1/2}^{(1/2)} \vdots \tilde{\Psi}_{1/2}^{(-1/2)} \tilde{\Psi}_{-1/2}^{(-1/2)} \vdots \dots \vdots \tilde{\Psi}_{S-1}^{(-S+1)} \dots \tilde{\Psi}_{-(S-1)}^{(-S+1)} \vdots \tilde{\Psi}_S^{(-S)} \dots \tilde{\Psi}_{-S}^{(-S)} \right), \end{aligned} \quad (4.38)$$

and they satisfy

$$H \tilde{\Psi}_\sigma^{(\lambda)} = \frac{1}{2} \left( \lambda + \frac{1}{2} \text{sgn}(\lambda) \right) \cdot \tilde{\Psi}_\sigma^{(\lambda)} \quad \left( \sigma = \overbrace{|\lambda|, |\lambda| - 1, |\lambda| - 2, \dots, -|\lambda|}^{=2|\lambda|+1} \right). \quad (4.39)$$

Their ortho-normal relations are given by

$$(\tilde{\Psi}_\sigma^{(\lambda)})^\dagger \tilde{\Psi}_\tau^{(\lambda')} = \delta_{\sigma\tau} \delta_{\lambda\lambda'}. \quad (4.40)$$

Note that the energy levels of the  $SO(5)$  and  $SO(4)$  Zeeman-Dirac models are equal only for the  $S = 1/2$  case, but are generally different. (Compare Fig.13 with Fig.6). As the energy level approaches zero by  $1/2$ ,

the corresponding degeneracy decreases by 2, leading to the absence of a zero-energy state (Fig.13). As usual, an  $SO(3)$  gauge invariant quantity is given by the Bloch vector:

$$(\tilde{\Psi}^{(\lambda)})^\dagger \Gamma_\mu \tilde{\Psi}^{(\lambda)} = (\lambda + \frac{1}{2} \text{sgn}(\lambda)) \cdot x_\mu \mathbf{1}_{2|\lambda|+1}. \quad (4.41)$$

The quantum geometric tensor is given by a matrix-valued  $SO(3)$  covariant quantity,

$$\chi_{\theta_i \theta_j}^{(\lambda)} \equiv \partial_{\theta_i} (\tilde{\Psi}^{(\lambda)})^\dagger \partial_{\theta_j} \tilde{\Psi}^{(\lambda)} - \partial_{\theta_j} (\tilde{\Psi}^{(\lambda)})^\dagger \partial_{\theta_i} \tilde{\Psi}^{(\lambda)} \quad (\tilde{\Psi}^{(\lambda)})^\dagger \partial_{\theta_j} \tilde{\Psi}^{(\lambda)} \quad (\theta_i, \theta_j = \chi, \theta, \phi), \quad (4.42)$$

and the trace of its symmetric part gives rise to the three-sphere metric,

$$g_{\theta_i \theta_j}^{(\lambda)} = \frac{1}{2} \text{tr}(\chi_{\theta_i \theta_j}^{(\lambda)} + \chi_{\theta_j \theta_i}^{(\lambda)}) \propto g_{\theta_i \theta_j}^{(S^3)} = \text{diag}(1, \sin^2 \chi, \sin^2 \chi \sin^2 \theta). \quad (4.43)$$

We checked (4.43) for  $S = 1/2, 3/2$  and  $5/2$ . The proportionality coefficients omitted in (4.43) depend on both  $S$  and  $|\lambda|$ . The Wilczek-Zee connection is derived as

$$-i \tilde{\Psi}^\dagger d \tilde{\Psi} = \mathcal{V}^\dagger (-i \Psi^\dagger d \Psi) \mathcal{V} = \begin{pmatrix} A^{(S)} & * & * & * & | & * & * & * & * \\ * & A^{(S-1)} & * & * & | & * & * & * & * \\ * & * & \ddots & * & | & * & * & * & * \\ * & * & * & A^{(1/2)} & | & * & * & * & * \\ \hline * & * & * & * & | & A^{(-1/2)} & * & * & * \\ * & * & * & * & | & * & \ddots & * & * \\ * & * & * & * & | & * & * & A^{(-S+1)} & * \\ * & * & * & * & | & * & * & * & A^{(-S)} \end{pmatrix}, \quad (4.44)$$

where

$$A^{(\lambda)} = -i (\tilde{\Psi}^{(\lambda)})^\dagger d \tilde{\Psi}^{(\lambda)} = -\frac{1}{1+x_4} \epsilon_{ijk} x_j S_k^{(|\lambda|)} dx_i = -i \frac{1}{2} (U^{(|\lambda|)\dagger} dU^{(|\lambda|)} + U^{(|\lambda|)} dU^{(|\lambda|)\dagger}) = A^{(-\lambda)}, \quad (4.45)$$

with

$$U^{(|\lambda|)} \equiv e^{i\chi \sum_{i=1}^3 y_i S_i^{(|\lambda|)}}. \quad (4.46)$$

We explicitly evaluated (4.45) for  $S = 1/2, 3/2, 5/2$  and  $7/2$  to have

$$A^{(\lambda)} = \frac{1}{2} \omega_{ij\theta_k} \epsilon_{ijk'} S_{k'}^{(|\lambda|)} d\theta_k, \quad (4.47)$$

where  $\omega_{ij\theta_k}$  denote the spin-connection of  $S^3$ . The corresponding curvature  $F_{\theta_i \theta_j} = \partial_{\theta_i} A_{\theta_j} - \partial_{\theta_j} A_{\theta_i} + i[A_{\theta_i}, A_{\theta_j}]$  is the antisymmetric part of (4.42):

$$F_{\theta_i \theta_j}^{(\lambda)} = -i(\chi_{\theta_i \theta_j}^{(\lambda)} - \chi_{\theta_j \theta_i}^{(\lambda)}) = \frac{1}{2} e^{i'}_{\theta_i} \wedge e^{j'}_{\theta_j} \epsilon_{i'j'k'} S_{k'}^{(S)}, \quad (4.48)$$

where  $e^{i'}_{\theta_i}$  denote the dreibein of  $S^3$  [57].

## 5 Bloch hyper-spheres in even higher dimensions

This section discusses how the previous discussions are generalized in arbitrary dimensions. While  $SO(d+1)$  large-spin gamma matrices can in principle be derived using the Landau level eigenstates of higher dimensional Landau models [86, 87, 88], the evaluation of their explicit matrix forms is a formidable task. We therefore deduce general results from a group theoretical analysis.

## 5.1 General properties

As discussed in the previous sections, the  $SO(5)$  Zeeman-Dirac model and the  $SO(4)$  model respect the  $SO(4)$  symmetry and the  $SO(3)$  symmetry, respectively. These symmetries introduce degeneracies and the Wilczek-Zee connections equivalent to the  $SO(4)$  and  $SO(3)$  monopole gauge fields. We will discuss how these features can be understood geometrically and extended to arbitrary dimensions. Let us consider the  $SO(d+1)$  Zeeman-Dirac model

$$H = \sum_{a=1}^{d+1} x_a \cdot \frac{1}{2} \Gamma_a \quad \left( \sum_{a=1}^{d+1} x_a x_a = 1 \right), \quad (5.1)$$

where  $x_a$  are given parameters that denote the Bloch vector. In general, the  $SO(d+1)$  Hamiltonian (5.1) has an  $SO(d)$  symmetry,<sup>22</sup>

$$U^\dagger H U = H \quad (U \in SO(d)). \quad (5.2)$$

Each of the energy levels accommodates the degeneracy attributed to the  $SO(d)$  symmetry. The geometric origin of this  $SO(d)$  symmetry is explained as follows. Suppose that  $S_{ab} \in SO(d)$  denotes the rotation about the direction of the Bloch vector (Fig.14). Under such a transformation, the Bloch vector is apparently

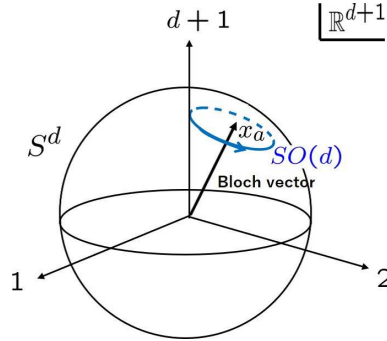


Figure 14:  $SO(d)$  stabilizer group that does not transform the point  $x_a$  (Bloch vector) on  $S^d$ .

invariant

$$x_a \rightarrow S_{ab} x_b = x_a \quad (S_{ab} \in SO(d)). \quad (5.3)$$

This transformation that does not change a point on manifold is known as the stabilizer group. The  $SO(d)$  stabilizer group appears as the denominator of the coset  $S^d \simeq SO(d+1)/SO(d)$ . The  $SO(d)$  invariance of the Bloch vector can be reinterpreted as a symmetry of the Hamiltonian (5.1):

$$H = \sum_{a=1}^{d+1} x_a \cdot \frac{1}{2} \Gamma_a \rightarrow \sum_a \left( \sum_b S_{ab} x_b \right) \cdot \frac{1}{2} \Gamma_a = \sum_a x_a \cdot \frac{1}{2} \overbrace{\left( \sum_b S_{ba} \Gamma_b \right)}^{=U^\dagger \Gamma_a U} = U^\dagger H U. \quad (5.4)$$

Thus, the  $SO(d)$  symmetry of the  $SO(d+1)$  Zeeman-Dirac Hamiltonian originates from the stabilizer group of the Bloch hyper-sphere. This  $SO(d)$  symmetry necessarily introduces a corresponding degeneracy to each energy level. Next, we clarify the geometric origin of the  $SO(d)$  monopole gauge field. Through adiabatic evolution, an  $SO(d+1)$  spin-coherent state experiences transitions among the degenerate states within each energy level, giving rise to the Wilczek-Zee connection. This Wilczek-Zee connection is attributed to the  $SO(d)$  holonomy of  $S^d$ , which is identical to the gauge field of the  $SO(d)$  non-Abelian monopole. The above mechanics is summarized in Fig.15. In the following, we confirm these speculations through more

<sup>22</sup>Meanwhile, the  $SO(d+1)$  Landau model has the  $SO(d+1)$  symmetry and each of the Landau levels exhibits degeneracy due to the  $SO(d+1)$  symmetry. The degenerate Landau level eigenstates constitute an irreducible representation of  $SO(d+1)$ .

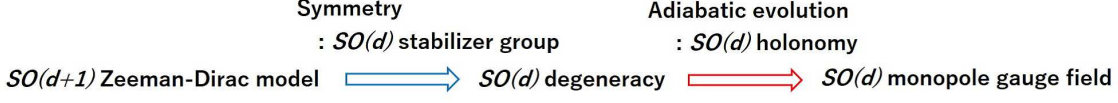


Figure 15: Emergence of the  $SO(d)$  monopole gauge field from the  $SO(d+1)$  Zeeman-Dirac model

concrete analyses.

## 5.2 Irreducible representations

Before going to details, we present a general argument about the representations of the orthogonal groups. Suppose that  $[l_1, l_2, \dots, l_k]_{SO(2k+1)}$  and  $[l_1, l_2, \dots, l_k]_{SO(2k)}$  signify the Young tableaux of the groups  $SO(2k+1)$  and  $SO(2k)$ , respectively [89].<sup>23</sup> The representations of our interest are designated as

$$[\lambda]_{SO(2k+1)} \equiv [S, \lambda]_{SO(2k+1)} \equiv \overbrace{[S, S, \dots, S, \lambda]}^k_{SO(2k+1)} \quad (0 \leq \lambda \leq S), \quad (5.7)$$

$$[\lambda]_{SO(2k)} \equiv [S, \lambda]_{SO(2k)} \equiv \overbrace{[S, S, \dots, S, \lambda]}^k_{SO(2k)} \quad (-S \leq \lambda \leq S), \quad (5.8)$$

with dimensions

$$D_{SO(2k+1)}(\lambda) \equiv D_{SO(2k+1)}(S, \lambda) \equiv \frac{2\lambda+1}{2S+1} \prod_{j=1}^{k-1} \frac{S-\lambda+k-j}{k-j} \frac{S+\lambda+k-j+1}{2S+k-j+1} \cdot \prod_{l=1}^k \prod_{i=1}^l \frac{2S+l+i-1}{l+i-1}, \quad (5.9a)$$

$$D_{SO(2k)}(\lambda) \equiv D_{SO(2k)}(S, \lambda) \equiv \prod_{j=1}^{k-1} \frac{(S+j)^2 - \lambda^2}{j^2} \cdot \prod_{l=1}^{k-2} \prod_{i=1}^{k-l-1} \frac{2S+2l+i}{2l+i} = D_{SO(2k)}(-\lambda). \quad (5.9b)$$

<sup>23</sup>For  $SO(5)$ , the index  $(p, q)$  in Appendix D is related to  $[l_1, l_2]_{SO(5)}$  as

$$p = l_1 + l_2, \quad q = l_1 - l_2. \quad (5.5)$$

For  $SO(4)$ , the bi-spin index  $(s_L, s_R)$  is related to  $[l_1, l_2]_{SO(4)}$  as

$$s_L = \frac{l_1 + l_2}{2}, \quad s_R = \frac{l_1 - l_2}{2}. \quad (5.6)$$

In particular,<sup>24</sup>

$$D_{SO(2k+1)}(S) = D_{SO(2k+2)}(\pm S) = \prod_{l=1}^k \prod_{i=1}^l \frac{2S+l+i-1}{l+i-1} \sim S^{\frac{1}{2}k(k+1)} \sim S \cdot D_{SO(2k)(1/2)} = S^1, S^3, S^6, S^{10}, \dots, \quad (5.12a)$$

$$D_{SO(2k)}(1/2) = D_{SO(2k)}(-1/2) = \prod_{j=1}^{k-1} \frac{(2S+2j)^2-1}{(2j)^2} \cdot \prod_{l=1}^{k-2} \prod_{i=1}^{k-l-1} \frac{2S+2l+i}{2l+i} \sim S^{\frac{1}{2}(k+2)(k-1)} = S^0, S^2, S^5, S^9, \dots. \quad (5.12b)$$

As we will see in Secs.5.3 and 5.4,  $D_{SO(2k+1)}(\lambda)/D_{SO(2k)}(\lambda)$  indicates the degeneracy of the energy level indexed by  $\lambda$  of the  $SO(2k+2)/SO(2k+1)$  model. The degeneracies (5.9) are shown in Fig.16. There are

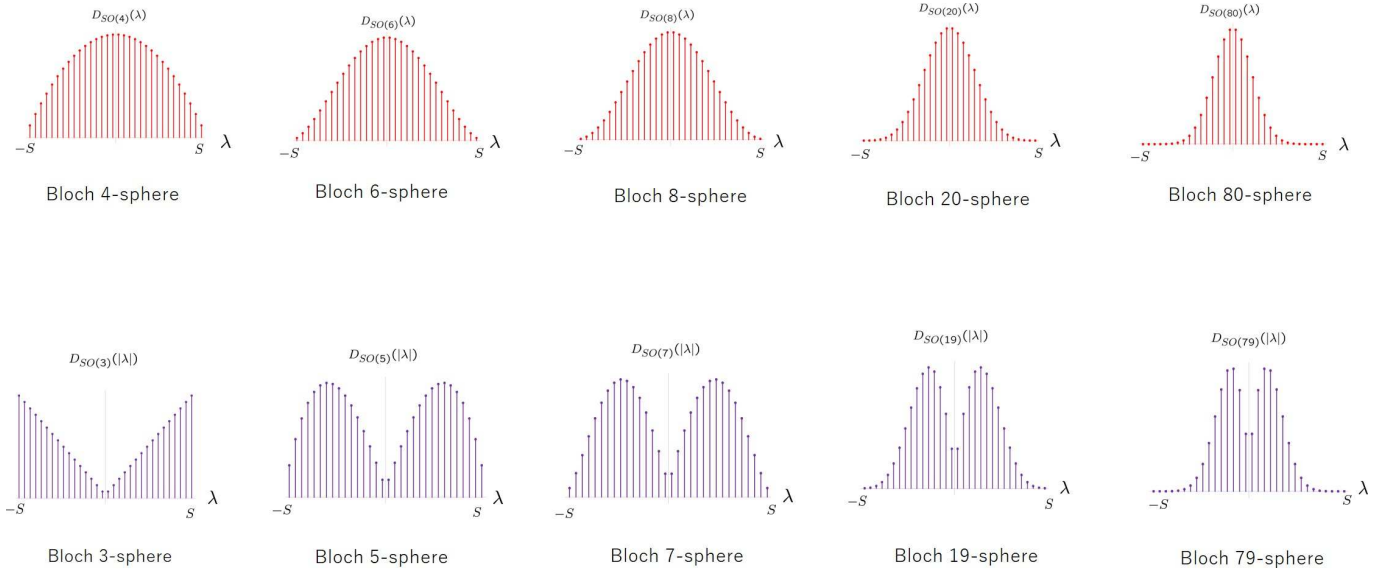


Figure 16: The upper/lower figure represents the distributions of the degeneracies of the  $SO(2k+1)/SO(2k)$  Zeeman-Dirac model for  $2S = 31$ .

<sup>24</sup>For instance,

$$D_{SO(3)}(S) = 2S+1, \quad D_{SO(5)}(S) = \frac{1}{3}(S+1)(2S+1)(2S+3), \quad D_{SO(7)}(S) = \frac{1}{90}(S+1)(S+2)(2S+1)(2S+3)^2(2S+5),$$

$$D_{SO(9)}(S) = \frac{1}{18900}(S+1)(S+2)^2(S+3)(2S+1)(2S+3)^2(2S+5)^2(2S+7), \quad (5.10)$$

and

$$D_{SO(2)}(1/2) = 1, \quad D_{SO(4)}(1/2) = \frac{1}{4}(2S+1)(2S+3), \quad D_{SO(6)}(1/2) = \frac{1}{192}(2S+1)(2S+3)^3(2S+5),$$

$$D_{SO(8)}(1/2) = \frac{1}{69120}(S+2)(2S+1)(2S+3)^3(2S+5)^3(2S+7). \quad (5.11)$$

interesting relations between adjacent dimensions:

$$D_{SO(2k+1)}(S) = \sum_{\lambda=-S}^S D_{SO(2k)}(\lambda), \quad (5.13a)$$

$$D_{SO(2k)}(1/2) = \sum_{\lambda=\frac{1}{2}}^S D_{SO(2k-1)}(\lambda) = \sum_{\lambda=-S}^{-\frac{1}{2}} D_{SO(2k-1)}(-\lambda) = D_{SO(2k)}(-1/2) \quad (2S : \text{odd}), \quad (5.13b)$$

which imply

$$\Sigma_{\mu\nu}^{[S]SO(2k+1)} = \bigoplus_{\lambda=-S}^S \Sigma_{\mu\nu}^{[\lambda]SO(2k)} \quad (\mu, \nu = 1, 2, \dots, 2k), \quad (5.14a)$$

$$\Sigma_{ij}^{[1/2]SO(2k)} = \bigoplus_{\lambda=1/2}^S \Sigma_{ij}^{[\lambda]SO(2k-1)} \quad (i, j = 1, 2, \dots, 2k-1). \quad (5.14b)$$

Notice that (5.13b) holds *only* for odd  $2S$ , not for even  $2S$ . (Recall that odd dimensional Bloch hyperspheres are defined only for half-integer  $S$ .) Equation (5.13) implies the dimensional hierarchies between even and odd dimensions.<sup>25</sup>

### 5.3 $SO(2k+1)$ Zeeman-Dirac model

As in the  $SO(5)$  case, there exist large spin gamma matrices for arbitrary  $SO(2k+1)$  groups (see Refs.[90, 91] for reviews and references therein). Using such gamma matrices, we can construct the large spin  $SO(2k+1)$  Zeeman-Dirac model. For a better understanding, we analyze the  $SO(2k+1)$  minimal model in Appendix E.2.

The  $SO(2k+1)$  large-spin gamma matrices satisfy two basic equations<sup>26</sup>

$$\sum_{a=1}^{2k+1} \Gamma_a \Gamma_a = 4S(S+k) \mathbf{1}_{D_{SO(2k+1)}(S)}, \quad (5.16a)$$

$$[\Gamma_{a_1}, \Gamma_{a_2}, \dots, \Gamma_{a_{2k}}] = i^k \frac{(2k)!! (2S+2k-2)!!}{(2S)!!} \epsilon_{a_1 a_2 \dots a_{2k+1}} \Gamma_{a_{2k+1}}, \quad (5.16b)$$

where  $[\ , \ , \dots, \ ]$  is called the  $2k$ -bracket that signifies totally antisymmetric combination of the  $2k$  quantities inside the bracket. The matrices  $\Gamma_a$  thus satisfy the quantum Nambu geometry [92, 93] and act as the coordinates of a fuzzy  $2k$ -sphere. The commutators between  $\Gamma_a$ s yield the  $SO(2k+1)$  generators of symmetric representation<sup>27</sup>

$$\Sigma_{ab}^{[S]SO(2k+1)} = -i \frac{1}{4} [\Gamma_a, \Gamma_b]. \quad (5.18)$$

<sup>25</sup>Such a dimensional hierarchy has been observed in the Landau models [88, 87, 86] and also in the non-linear sigma models [76].

<sup>26</sup>The matrices  $\Gamma_a$  satisfy the orthonormal relations:

$$\text{tr}(\Gamma_a \Gamma_b) = 4 \frac{S(S+k)}{2k+1} D_{SO(2k+1)}(S) \delta_{ab}. \quad (5.15)$$

<sup>27</sup>The sum of the squares of (5.18) is given by

$$\sum_{a < b=1}^{2k+1} \Sigma_{ab}^{[S]SO(2k+1)} \Sigma_{ab}^{[S]SO(2k+1)} = kS(S+k) \mathbf{1}_{D_{SO(2k+1)}(S)}. \quad (5.17)$$

The  $SO(2k+1)$  covariance of  $\Gamma_a$  is represented as  $[\Sigma_{ab}^{[S]SO(2k+1)}, \Gamma_c] = i\delta_{ac}\Gamma_b - i\delta_{bc}\Gamma_a$ . The  $SO(2k+1)$  Zeeman-Dirac Hamiltonian

$$H = \sum_{a=1}^{2k+1} x_a \cdot \frac{1}{2}\Gamma_a \quad \left( \sum_{a=1}^{2k+1} x_a x_a = 1 \right) \quad (5.19)$$

is diagonalized as

$$\Psi^\dagger H \Psi = \frac{1}{2}\Gamma_{2k+1} = \bigoplus_{\lambda=-S}^S \lambda \mathbf{1}_{D_{SO(2k)}(\lambda)}, \quad (5.20)$$

where

$$\Psi = e^{i\theta_{2k} \sum_{\mu=1}^{2k} y_\mu \Sigma_{\mu, 2k+1}^{[S]SO(2k+1)}} = N^\dagger \cdot e^{i\theta_{2k} \Sigma_{2k, 2k+1}^{[S]SO(2k+1)}} \cdot N \quad \left( y_{\mu=1, 2, \dots, 2k} = \frac{1}{\sin \theta_{2k}} x_\mu, \quad x_{2k+1} = \cos \theta_{2k} \right), \quad (5.21)$$

with

$$N = e^{i\theta_{2k-1} \Sigma_{2k, 2k-1}^{[S]SO(2k+1)}} e^{i\theta_{2k-2} \Sigma_{2k-1, 2k-2}^{[S]SO(2k+1)}} \dots e^{i\theta_4 \Sigma_{54}^{[S]SO(2k+1)}} e^{i\theta_3 \Sigma_{43}^{[S]SO(2k+1)}} e^{i\theta \Sigma_{31}^{[S]SO(2k+1)}} e^{i\phi \Sigma_{12}^{[S]SO(2k+1)}}. \quad (5.22)$$

As shown in (5.20), the  $SO(2k+1)$  Hamiltonian exhibits  $2S+1$  energy levels

$$\lambda = S, S-1, S-2, \dots, -S, \quad (5.23)$$

with degeneracies  $D_{SO(2k)}(\lambda)$  (5.9b). The spectrum (5.23) is symmetric with respect to the origin, and the geometric picture of the Bloch  $2k$ -sphere is similar to that of the Bloch four-sphere (Fig.6), up to the energy level degeneracy.

This  $SO(2k)$  degeneracy comes from the  $SO(2k)$  symmetry of (5.20)

$$\Psi \rightarrow \Psi \cdot e^{i\frac{1}{2}\omega_{\mu\nu} \Sigma_{\mu\nu}^{[S]SO(2k+1)}}. \quad (5.24)$$

The  $SO(2k)$  decomposition (5.13a) and the analyses of Appendix E.2 suggest that the Wilczek-Zee  $SO(2k)$  connection is given by the  $SO(2k)$  monopole gauge field,

$$A^{(\lambda)} = -\frac{1}{1+x_{2k+1}} \Sigma_{\mu\nu}^{[\lambda]SO(2k)} x_\nu dx_\mu, \quad (5.25)$$

where  $\Sigma_{\mu\nu}^{[\lambda]SO(2k)}$  denote the  $SO(2k)$  generators of  $[\lambda]_{SO(2k)}$ . For  $k=2$ , (5.25) reproduces the  $SO(4)$  monopole connection (3.55). We also checked the validity of (5.25) using generalized  $SO(7)$  gamma matrices for  $S=1/2, 1$  and  $3/2$ . The non-trivial topology of the  $SO(2k)$  monopole field configuration is specified by the  $k$ th Chern number

$$\text{ch}_k = \frac{1}{k!(2\pi)^k} \int_{S^{2k}} \text{tr}(F^k), \quad (5.26)$$

which is equivalent to the homotopy map from the equator of  $S^{2k}$  to the  $SO(2k)$  transition function,

$$\pi_{2k-1}(SO(2k)) \simeq \mathbb{Z}. \quad (5.27)$$

For the monopole field configuration (5.25), the  $k$ th Chern number is evaluated as

$$\text{ch}_k^{[\lambda]SO(2k)} = \text{sgn}(\lambda) \cdot D_{SO(2k+1)}(S - \frac{1}{2}, |\lambda| - \frac{1}{2}) = -\text{ch}_k^{[-\lambda]SO(2k)} \quad (5.28)$$

with  $\text{sgn}(0) \equiv 0$ . Equation (5.28) is an apparent generalization of the previous  $k=2$  case (3.61). Two opposite energy levels with respect to the zero-energy have the same magnitude of Chern numbers with opposite signs.



## 5.4 $SO(2k)$ Zeeman-Dirac model

The  $SO(2k)$  large-spin gamma matrices are realized in the subspace  $\lambda = (+1/2) \oplus (-1/2)$  of the  $SO(2k+1)$  large-spin gamma matrices [83, 85]. The spin magnitude  $S$  should be a half-integer for the same reason as in the  $SO(4)$  model. Analysis of the  $SO(2k)$  minimal model is presented in Appendix E.3.

The  $SO(2k)$  large spin gamma matrices are given by the following off-diagonal block matrices,

$$\Gamma_\mu = \begin{pmatrix} 0 & \mathcal{Y}_\mu^\dagger \\ \mathcal{Y}_\mu & 0 \end{pmatrix} \quad (\mu = 1, 2, \dots, 2k). \quad (5.29)$$

They satisfy the two equations:<sup>28</sup>

$$\sum_{\mu=1}^{2k} \Gamma_\mu \Gamma_\mu = \frac{1}{2}(2S+1)(2S+2k-1) \mathbf{1}_{2D_{SO(2k)}(1/2)}, \quad (5.33a)$$

$$[[\Gamma_{\mu_1}, \Gamma_{\mu_2}, \dots, \Gamma_{\mu_{2k-1}}]] = -i^k \frac{(2k)!! (2S+2k-2)!!}{(2S)!!} \epsilon_{\mu_1 \mu_2 \dots \mu_{2k}} \Gamma_{\mu_{2k}}, \quad (5.33b)$$

where

$$[[\Gamma_{\mu_1}, \Gamma_{\mu_2}, \dots, \Gamma_{\mu_{2k-1}}]] \equiv [\Gamma_{\mu_1}, \Gamma_{\mu_2}, \dots, \Gamma_{\mu_{2k-1}}, G_{2k+1}] = 2k [\Gamma_{\mu_1}, \Gamma_{\mu_2}, \dots, \Gamma_{\mu_{2k-1}}] G_{2k+1}. \quad (5.34)$$

Equation (5.33a) was derived in Ref.[83]. The matrix  $G_{2k+1}$  is a diagonal matrix

$$G_{2k+1} = \begin{pmatrix} \mathbf{1}_{D_{SO(2k)}(1/2)} & 0 \\ 0 & -\mathbf{1}_{D_{SO(2k)}(1/2)} \end{pmatrix}, \quad (5.35)$$

which anti-commutes with all  $\Gamma_\mu$ s:

$$\{\Gamma_\mu, G_{2k+1}\} = 0. \quad (5.36)$$

With such  $\Gamma_\mu$ s, we construct the  $SO(2k)$  Zeeman-Dirac Hamiltonian as

$$H = \sum_{\mu=1}^{2k} x_\mu \cdot \frac{1}{2} \Gamma_\mu = \frac{1}{2} \begin{pmatrix} 0 & Q^{(-)} \\ Q^{(+)} & 0 \end{pmatrix} \quad \left( \sum_{\mu=1}^{2k} x_\mu x_\mu = 1 \right), \quad (5.37)$$

where

$$Q^{(+)} \equiv \sum_{\mu=1}^{2k} x_\mu \mathcal{Y}_\mu, \quad Q^{(-)} \equiv Q^{(+)\dagger} = \sum_{\mu=1}^{2k} x_\mu \mathcal{Y}_\mu^\dagger. \quad (5.38)$$

The Hamiltonian (5.37) obviously respects the chiral symmetry:

$$\{H, G_{2k+1}\} = 0. \quad (5.39)$$

---

<sup>28</sup>Together with

$$\Gamma_{2k+1} = \sqrt{\frac{(2S+1)(2S+2k-1)}{4k}} G_{2k+1}, \quad (5.30)$$

$\Gamma_{a=1,2,\dots,2k+1}$  satisfy the orthonormal relations,

$$\text{tr}(\Gamma_a \Gamma_b) = \frac{(2S+1)(2S+2k-1)}{2k} D_{SO(2k)}(1/2) \delta_{ab}, \quad (5.31)$$

and the quantum Nambu algebra,

$$[\Gamma_{a_1}, \Gamma_{a_2}, \dots, \Gamma_{a_{2k}}] = i^k \sqrt{\frac{(2S+1)(2S+2k-1)}{4k}} \frac{(2k)!! (2S+2k-2)!!}{(2S)!!} \epsilon_{a_1 a_2 \dots a_{2k+1}} \Gamma_{a_{2k+1}}. \quad (5.32)$$

While the commutators between  $\Gamma_\mu$ s do not realize  $SO(2k)$  generators,  $\Gamma_\mu$  transform as a vector under the  $SO(2k)$  transformations generated by the following  $SO(2k)$  generators [66],

$$\Sigma_{\mu\nu} \equiv \begin{pmatrix} \Sigma_{\mu\nu}^{[+1/2]SO(2k)} & 0 \\ 0 & \Sigma_{\mu\nu}^{[-1/2]SO(2k)} \end{pmatrix}. \quad (5.40)$$

The non-linear realization matrix is constructed as

$$\Psi = e^{i\theta_{2k-1} \sum_{i=1}^{2k-1} y_i \Sigma_{i,2k}} = \mathcal{N}^\dagger e^{i\theta_{2k-1} \Sigma_{2k-1,2k}} \mathcal{N} = \begin{pmatrix} \mathcal{U}^{[+1/2]} & 0 \\ 0 & \mathcal{U}^{[-1/2]} \end{pmatrix}, \quad (5.41)$$

where

$$y_{i=1,2,\dots,2k-1} = \frac{1}{\sin(\theta_{2k-1})} x_i \quad x_{2k} = \cos(\theta_{2k-1}), \quad (5.42a)$$

$$\mathcal{N} = e^{i\theta_{2k-2} \Sigma_{2k-1,2k-2}} e^{i\theta_{2k-3} \Sigma_{2k-2,2k-3}} \dots e^{i\theta_4 \Sigma_{54}} e^{i\theta_3 \Sigma_{43}} e^{i\theta \Sigma_{31}} e^{i\phi \Sigma_{12}}, \quad (5.42b)$$

$$\mathcal{U}^{[\pm 1/2]} \equiv e^{i\theta_{2k-1} \sum_{i=1}^{2k-1} y_i \Sigma_{i,2k}^{[\pm 1/2]SO(2k)}}. \quad (5.42c)$$

The matrix  $\Psi$  transforms the  $SO(2k)$  Hamiltonian (5.37) into the form

$$\Psi^\dagger H \Psi = \frac{1}{2} \Gamma_{2k}. \quad (5.43)$$

With an appropriate unitary matrix  $\mathcal{V}$ ,  $\Gamma_{2k}$  is diagonalized as<sup>29</sup>

$$\mathcal{V}^\dagger \Gamma_{2k} \mathcal{V} = \Gamma_{\text{diag}} \equiv \bigoplus_{\lambda=-S}^S (\lambda + \frac{1}{2} \text{sgn}(\lambda)) \mathbf{1}_{D_{SO(2k-1)}(|\lambda|)} = \bigoplus_{\lambda=-S}^S \lambda \mathbf{1}_{D_{SO(2k-1)}(|\lambda|)} + \frac{1}{2} G_{2k+1}. \quad (5.44)$$

In other words, we can diagonalize the Hamiltonian with  $\tilde{\Psi} = \Psi \mathcal{V}$  as

$$\tilde{\Psi}^\dagger H \tilde{\Psi} = \frac{1}{2} \Gamma_{\text{diag}} = \bigoplus_{\lambda=-S}^S \frac{1}{2} (\lambda + \frac{1}{2} \text{sgn}(\lambda)) \mathbf{1}_{D_{SO(2k-1)}(|\lambda|)}. \quad (5.45)$$

Apparently there are  $SO(2k-1)$  degrees of freedom in (5.43):

$$\Psi \rightarrow \Psi \cdot e^{i\frac{1}{2} \sum_{i,j=1}^{2k-1} \omega_{ij} \Sigma_{ij}} \quad (5.46)$$

or

$$\tilde{\Psi} \rightarrow \tilde{\Psi} \cdot e^{i\frac{1}{2} \sum_{i,j=1}^{2k-1} \omega_{ij} \tilde{\Sigma}_{ij}} \quad (\tilde{\Sigma}_{ij} \equiv \mathcal{V}^\dagger \Sigma_{ij} \mathcal{V}). \quad (5.47)$$

For a Hamiltonian with chiral symmetry, we can define the winding number [47]

$$\nu^{(\pm)} \equiv (-i)^{k-1} \frac{1}{(2\pi)^k} \frac{(k-1)!}{(2k-1)!} \int_{S^{2k-1}} \text{tr}((-iQ^{(\mp)} dQ^{(\pm)})^{2k-1}) = \pm D_{SO(2k+1)}(S - \frac{1}{2}, 0) = \text{ch}_k^{[\pm \frac{1}{2}]SO(2k)}, \quad (5.48)$$

which corresponds to the homotopy map

$$\pi_{2k-1}(SO(2k)) \simeq \mathbb{Z}. \quad (5.49)$$

The analysis of the  $SO(2k)$  spinor representation (Appendix E.3) and the  $SO(2k-1)$  decomposition (5.13b) suggest that the diagonal blocks of  $-i\tilde{\Psi}^\dagger d\tilde{\Psi}$  may yield the  $SO(2k-1)$  Wilczek-Zee connection in a similar fashion to (4.44):

$$A^{(\lambda)} = -\frac{1}{1+x_{2k}} \sum_{ij}^{[|\lambda|]SO(2k-1)} x_j dx_i. \quad (5.50)$$

For  $k=2$ , (5.50) is reduced to the  $SO(3)$  monopole connection (4.47).

The obtained results are illustrated in Fig.17.

<sup>29</sup>We can check the validity of (5.44) using the explicit matrix form of  $\Gamma_{2k}$ .

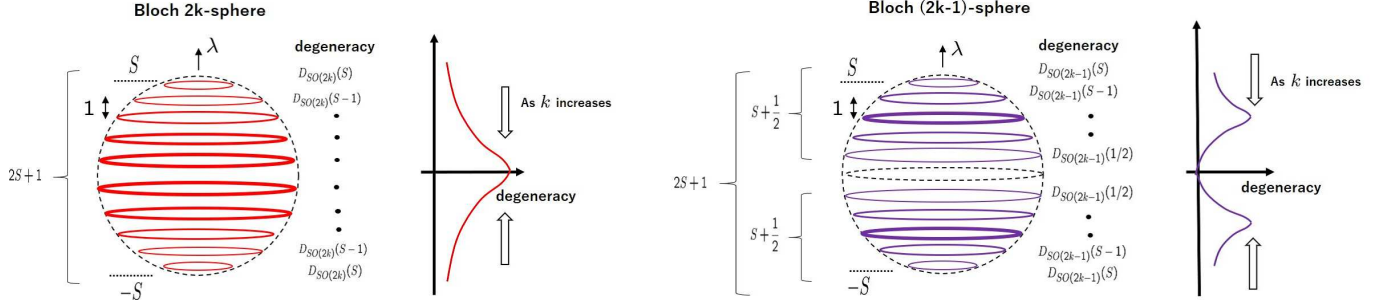


Figure 17: The Bloch  $2k$ -sphere (left) and the Bloch  $(2k-1)$ -sphere (right). In both cases, there are  $2S+1$  energy levels. For the Bloch  $2k$ -spheres, the degeneracies increase toward the equator: As  $k$  increases, the peak at the equator becomes sharper (see also the upper figures of Fig.16). For the Bloch  $(2k-1)$ -spheres, the degeneracies have two peaks in the northern and southern hemispheres: As  $k$  increases, the two peaks approach the equator (see also the lower figures of Fig.16.)

## 6 Bloch hyper-balls and quantum statistics

We refer to the  $d+1$  dimensional hyper-volume region surrounded by the Bloch hyper-sphere  $S^d$  as the Bloch hyper-ball,  $B^{d+1}$ . Here, we consider  $2S+1$ -level density matrices whose parameters are given by the coordinates of  $B^{d+1}$  and investigate the corresponding von Neumann entropies and the Bures information metrics.

### 6.1 Bloch hyper-balls and density matrices

Arbitrary  $2 \times 2$  density matrix is represented as

$$\rho = \frac{1}{2}(\mathbf{1}_2 + r \sum_{i=1}^3 x_i \sigma_i) \quad (0 \leq r \leq 1, \quad \sum_{i=1}^3 x_i x_i = 1), \quad (6.1)$$

which is formally equivalent to

$$\rho = \frac{1}{2}\mathbf{1}_2 + rH. \quad (6.2)$$

Here,  $H$  denotes the  $SO(3)$  Zeeman-Dirac Hamiltonian (2.1). The parameters  $rx_i$  indicate a position inside the Bloch three-ball to specify the density matrix (6.1).

In the following, we explore the density matrix made of the  $SO(d+1)$  Zeeman-Dirac Hamiltonian  $H$ :

$$\rho = \alpha \mathbf{1} + \beta H, \quad (6.3)$$

where  $\alpha$  and  $\beta$  are quantities to be determined so that  $\rho$  satisfies the necessary conditions for density matrix:

1.  $\rho$  is Hermitian
2.  $\text{tr}(\rho) = 1$
3. The eigenvalues of  $\rho$  are non-negative.

The first condition implies that  $\alpha$  and  $\beta$  should be real parameters. The second condition gives  $\alpha = \frac{1}{\text{tr}\mathbf{1}}$ , provided that  $H$  is a traceless matrix as in the case of the Zeeman-Dirac Hamiltonian. The third condition yields  $0 \leq \beta \leq \alpha/(h_1 \equiv \text{Max}(\text{eigenvalues of } H))$  when the spectrum of  $H$  is symmetric with respect to the zero-energy, as in the present case. Consequently, we have

$$\alpha = \frac{1}{\text{tr}\mathbf{1}}, \quad \beta = \frac{\alpha}{h_1} r, \quad (0 \leq r \leq 1) \quad (6.4)$$

and (6.3) becomes

$$\rho = \frac{1}{\text{tr}\mathbf{1}}\left(\mathbf{1} + \frac{1}{h_1}rH\right). \quad (6.5)$$

The present density matrix represents a special multi-level density matrix. See Refs.[28, 29] for a general multi-level density matrix. In such a general model, the geometry of the allowed parameter region is much more intricate than the simple volume region of a hyper-ball.

For the case of the  $SO(2k+1)$  model, the parameters are identified as  $\alpha = D_{SO(2k+1)}(S)$  and  $h_1 = S$ . Therefore, the density matrix becomes

$$\rho = \frac{1}{D_{SO(2k+1)}(S)}\left(\mathbf{1}_{D_{SO(2k+1)}(S)} + r\frac{1}{S}\sum_{a=1}^{2k+1}x_a \cdot \frac{1}{2}\Gamma_a\right) \quad (0 \leq r \leq 1, \quad \sum_{a=1}^{2k+1}x_ax_a = 1). \quad (6.6)$$

The inequality  $0 \leq r \leq 1$  indicates the region occupied by the Bloch  $2k+1$ -ball, and the density matrix is defined at each point inside the  $B^{2k+1}$ .

Similarly, for the  $SO(2k)$  model, the parameters are identified as  $\alpha = 2D_{SO(2k)}(1/2)$  and  $h_1 = \frac{1}{2}(S + \frac{1}{2})$ . The density matrix is then given by

$$\rho = \frac{1}{2D_{SO(2k)}(1/2)}\left(\mathbf{1}_{2D_{SO(2k)}(1/2)} + r\frac{4}{2S+1}\sum_{\mu=1}^{2k}x_\mu \cdot \frac{1}{2}\Gamma_\mu\right) \quad (2S : \text{odd}, \quad 0 \leq r \leq 1, \quad \sum_{\mu=1}^{2k}x_\mu x_\mu = 1). \quad (6.7)$$

## 6.2 von Neumann entropies

With a given density matrix  $\rho$ , the von Neumann entropy is defined as

$$S_{vN} = -\text{tr}(\rho \ln \rho) = -\sum_{\lambda} D(\lambda) \rho_{\lambda} \ln \rho_{\lambda} \quad (\text{tr}\rho = \sum_{\lambda} D(\lambda) \rho_{\lambda} = 1), \quad (6.8)$$

where  $\rho_{\lambda}$  denote the eigenvalues of  $\rho$  with degeneracy  $D(\lambda)$ . For the present models, they are given by

$$B^{2k+1} : \rho_{\lambda}(r) = \frac{1}{D_{SO(2k+1)}(S)}\left(1 + \frac{\lambda}{S}r\right), \quad D(\lambda) = D_{SO(2k)}(\lambda), \quad (6.9a)$$

$$B^{2k} : \rho_{\lambda}(r) = \frac{1}{2D_{SO(2k)}(1/2)}\left(1 + \frac{2\lambda + \text{sgn}(\lambda)}{2S+1}r\right), \quad D(\lambda) = D_{SO(2k-1)}(|\lambda|). \quad (6.9b)$$

Using (5.13), we can readily confirm that (6.9) satisfies  $\text{tr}\rho = \sum_{\lambda=-S}^S D(\lambda)\rho_{\lambda}(r) = 1$ . Their von Neumann entropies (6.8) are evaluated as

$$B^{2k+1} : S_{vN}(r) = \ln(D_{SO(2k+1)}(S)) - \frac{1}{D_{SO(2k+1)}(S)}\sum_{\lambda=-S}^S D_{SO(2k)}(\lambda) \cdot \left(1 + \frac{\lambda}{S}r\right) \cdot \ln\left(1 + \frac{\lambda}{S}r\right), \quad (6.10a)$$

$$\begin{aligned} B^{2k} : S_{vN}(r) &= \ln(2D_{SO(2k)}(1/2)) \\ &\quad - \frac{1}{2D_{SO(2k)}(1/2)}\sum_{\lambda=-S}^S D_{SO(2k-1)}(|\lambda|) \cdot \left(1 + \frac{2\lambda + \text{sgn}(\lambda)}{2S+1}r\right) \cdot \ln\left(1 + \frac{2\lambda + \text{sgn}(\lambda)}{2S+1}r\right), \end{aligned} \quad (6.10b)$$

where we used (5.13) again. The core of the Bloch hyper-ball ( $r = 0$ ) signifies the maximally mixed ensemble:

$$\rho = \frac{1}{N}\mathbf{1}_N, \quad \text{Max}(S_{vN}) = \ln N \quad (N = D_{SO(2k+1)}(S), \quad 2D_{SO(2k)}(1/2)). \quad (6.11)$$

The von Neumann entropy (6.10) decreases monotonically as  $r$  increases regardless of the parity of dimensions (see the left of Fig.18).

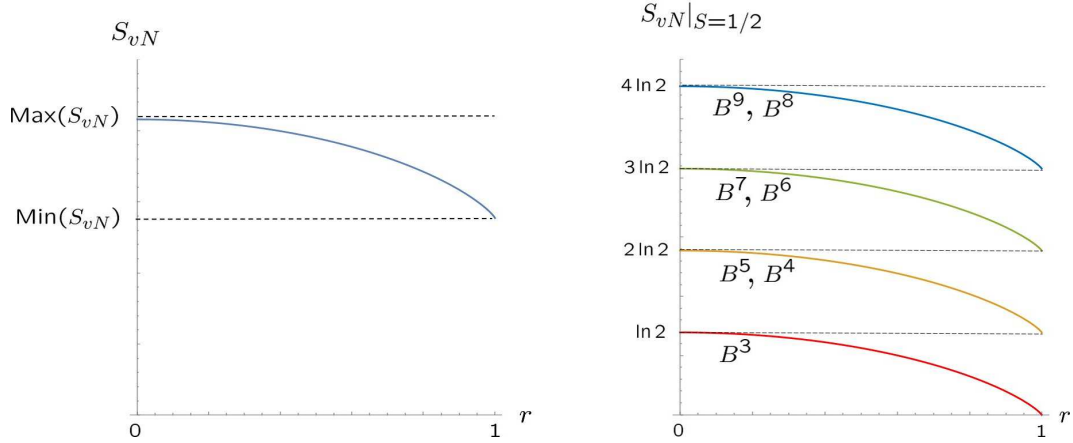


Figure 18: (Left) General behavior of the von Neumann entropy for a Bloch hyper-ball. (Right) The von Neumann entropies for the minimal Bloch  $d + 1$ -balls ( $k = \lfloor (d + 1)/2 \rfloor$ ).

For the Bloch balls with minimal spin  $S = 1/2$ , the density matrices are given by

$$B^{2k+1} : \rho|_{S=1/2} = \frac{1}{2^k} (\mathbf{1}_{2^k} + r \sum_{a=1}^{2k+1} x_a \gamma_a), \quad B^{2k} : \rho|_{S=1/2} = \frac{1}{2^k} (\mathbf{1}_{2^k} + r \sum_{\mu=1}^{2k} x_\mu \gamma_\mu), \quad (6.12)$$

where  $\gamma_a$  and  $\gamma_\mu$  denote the  $SO(2k + 1)$  and the  $SO(2k)$  gamma matrices (E.1), respectively. Both of them are diagonalized as

$$\rho|_{S=1/2} \rightarrow \frac{1}{2^k} \begin{pmatrix} (1+r)\mathbf{1}_{2^{k-1}} & 0 \\ 0 & (1-r)\mathbf{1}_{2^{k-1}} \end{pmatrix}, \quad (6.13)$$

and so the von Neumann entropies for  $B^{2k+1}$  and  $B^{2k}$  take the same value (see the right of Fig.18),

$$S_{vN}(r)|_{S=1/2} = k \ln 2 - \frac{1}{2}(1+r) \ln(1+r) - \frac{1}{2}(1-r) \ln(1-r). \quad (6.14)$$

Their maximum and minimum values are respectively given by

$$\text{Max}(S_{vN})|_{S=1/2} = S_{vN}(0)|_{S=1/2} = k \ln 2, \quad \text{Min}(S_{vN})|_{S=1/2} = S_{vN}(1)|_{S=1/2} = (k-1) \ln 2. \quad (6.15)$$

The maximum value  $\ln(2^k)$  is due to the  $2^k$  matrix dimension of the minimal Hamiltonian, while the minimum value  $\ln(2^{k-1})$  comes from the  $2^{k-1}$  degeneracy of the upper eigenvalue of the density matrix (6.13).

### 6.3 Quantum statistical geometry

We discuss quantum statistical geometries. First let us examine the trace distance  $L \equiv \frac{1}{2} \text{tr}(\sqrt{(\rho - \rho')^2})$  between two density matrices  $\rho$  and  $\rho'$ . From (6.9), the trace distance is easily derived as<sup>30</sup>

$$L = c(S, d+1) \cdot \sqrt{\sum_{\alpha=1}^{d+1} (rx_\alpha - r'x'_\alpha)^2}, \quad (6.16)$$

<sup>30</sup>In the derivation of (6.16), we used the formula,  $\text{tr}(\sqrt{H^2}) = \sum_h |h| \cdot D(h)$ , which holds for arbitrary Hermitian matrix  $H$  with eigenvalues  $h$  of degeneracy  $D(h)$ .

where

$$c(S, 2k+1) \equiv \sum_{\lambda=-S}^S \frac{|\lambda|}{4S} \frac{D_{SO(2k)}(\lambda)}{D_{SO(2k+1)}(S)}, \quad c(S, 2k) \equiv \sum_{\lambda=1/2}^S \frac{2\lambda+1}{2S+1} \frac{D_{SO(2k-1)}(\lambda)}{D_{SO(2k)}(1/2)}. \quad (6.17)$$

In particular, for  $S = 1/2$ ,  $c_S$  (6.17) do not depend on  $k$ ,  $c(1/2, 2k+1) = 1/4$  and  $c'(1/2, 2k) = 1$ . In general,  $c_S$  decrease monotonically as  $S$  and  $k$  increase. The trace distance (6.16) is proportional to the distance between the vectors  $rx_\alpha$  and  $r'x'_\alpha$  in the  $d+1$  dimensional flat Euclidean space.

Next, let us discuss the Bures metric [94, 95]. We will see that various curved spaces with  $SO(d+1)$  rotational symmetry emerge as Bures geometries for  $B^{d+1}$ , corresponding to the gamma matrices with different spins. From the formula of [96], we can evaluate the Bures metrics

$$B^{2k+1} : B_{ab} = \sum_{\lambda, \lambda'=-S}^S \frac{1}{2(\rho_\lambda + \rho_{\lambda'})} \text{tr} \left( \Psi^{(\lambda)\dagger} \frac{\partial \rho}{\partial X_a} \Psi^{(\lambda')} \Psi^{(\lambda')\dagger} \frac{\partial \rho}{\partial X_b} \Psi^{(\lambda)} \right), \quad (6.18a)$$

$$B^{2k} : B_{\mu\nu} = \sum_{\lambda, \lambda'=-S}^S \frac{1}{2(\rho_\lambda + \rho_{\lambda'})} \text{tr} \left( (\tilde{\Psi}^{(\lambda)})^\dagger \frac{\partial \rho}{\partial X_\mu} \tilde{\Psi}^{(\lambda')} (\tilde{\Psi}^{(\lambda')})^\dagger \frac{\partial \rho}{\partial X_\nu} \tilde{\Psi}^{(\lambda)} \right). \quad (6.18b)$$

While the Bures metrics (6.18) may take various forms depending on the functional forms of the spin-coherent states, they generally take the  $SO(d+1)$  spherically symmetric form

$$B_{\alpha\beta} = f(r)\delta_{\alpha\beta} + g(r)x_\alpha x_\beta, \quad (6.19)$$

or<sup>31</sup>

$$\sum_{\alpha, \beta=1}^{d+1} B_{\alpha\beta} d(rx_\alpha) d(rx_\beta) = (f(r) + g(r))dr^2 + f(r)r^2 dl_{S^d}^2 \quad (dl_{S^d}^2 \equiv \sum_{\alpha=1}^{d+1} dx_\alpha dx_\alpha), \quad (6.23)$$

where  $dl_{S^d}$  denotes the line element of  $S^d$ , and  $f(r)$  and  $g(r)$  are some functions that depend on both  $S$  and  $d$ . (Several examples are shown in Table 1.) We find that various  $SO(d+1)$  symmetric curved geometries emerge for different values of  $S$  and  $k$ . The (1/4 of) Ricci scalar curvatures are shown in Fig.19 and they exhibit qualitatively distinct behavior depending on the parity of the dimensions. These Ricci scalars do not have any singularities. We also evaluated the Kretschmann scalars  $R_{\mu\nu\rho\sigma}R^{\mu\nu\rho\sigma}$  and confirmed that they have no singularities either.

In the case  $S = 1/2$ , the Bures geometry of  $B^{d+1}$  is simply illustrated by the hemi-sphere geometry of the hyper-sphere  $S^{d+1}$ . It is not difficult to calculate (6.18) explicitly, using the results of Appendix E. Either (6.18a) or (6.18b) yields

$$B_{\alpha\beta}|_{S=1/2} = \frac{1}{4} \left( \delta_{\alpha\beta} + \frac{r^2}{1-r^2} x_\alpha x_\beta \right) \quad (\alpha, \beta = 1, 2, \dots, d+1) \quad (6.24)$$

or

$$B_{\alpha\beta}|_{S=1/2} d(rx_\alpha) d(rx_\beta) = \frac{1}{4} \left( \frac{1}{1-r^2} dr^2 + r^2 dl_{S^d}^2 \right). \quad (6.25)$$

---

<sup>31</sup>Utilizing the re-parametrization of the radial coordinate,

$$r' = \sqrt{f(r)} r, \quad (6.20)$$

we can further transform (6.23) into the standard form [97]

$$ds^2 = h(r') dr'^2 + r'^2 dl_{S^d}^2, \quad (6.21)$$

where

$$h(r') \equiv \left( 1 + \frac{g(r)}{f(r)} \right) \left( 1 + \frac{f'(r)}{2f(r)} r \right)^{-2} \Big|_{r=r(r')}. \quad (6.22)$$

Information of the spherical space metric can be incorporated in the single function  $h$ .

	$S = 1/2$		$S = 1$		$S = 3/2$	
	$f(r) + g(r)$	$f(r)$	$f(r) + g(r)$	$f(r)$	$f(r) + g(r)$	$f(r)$
$B^3$	$\frac{1}{4(1-r^2)}$	$\frac{1}{4}$	$\frac{1}{6(1-r^2)}$	$\frac{2}{3(4-r^2)}$	$\frac{5-r^2}{4(1-r^2)(9-r^2)}$	$\frac{45-8r^2}{36(9-4r^2)}$
$B^4$	$\frac{1}{4(1-r^2)}$	$\frac{1}{4}$	/	/	$\frac{27-4r^2}{4(9-r^2)(9-4r^2)}$	$\frac{324-65r^2}{972(4-r^2)}$
$B^5$	$\frac{1}{4(1-r^2)}$	$\frac{1}{4}$	$\frac{3}{20(1-r^2)}$	$\frac{3}{5(4-r^2)}$	$\frac{21-5r^2}{20(1-r^2)(9-r^2)}$	$\frac{21-4r^2}{20(9-4r^2)}$

Table 1: Explicit functional forms of  $f(r)$  and  $g(r)$  for the low dimensional Bloch balls and the small spin magnitudes. For  $S = 1/2$ ,  $f(r)$  and  $g(r)$  are universal regardless of the dimensions, but for other  $S$ s, they are not.

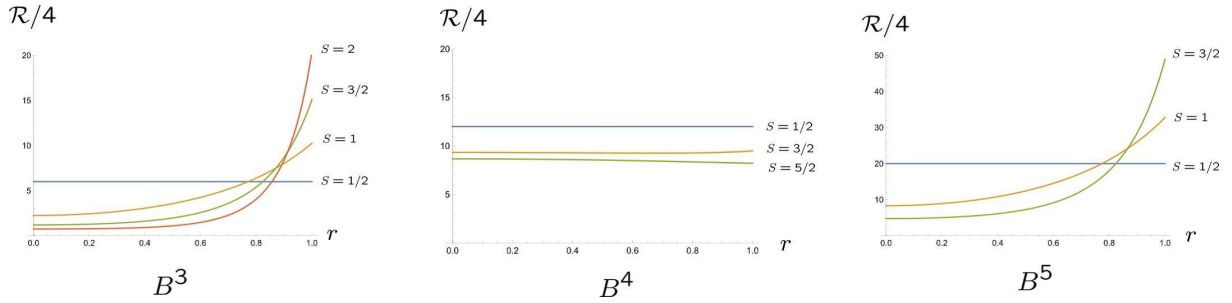


Figure 19: The Ricci scalar curvatures  $\mathcal{R}$  for the low dimensional Bures geometries for the metrics in Table 1. There is no singularity in the Ricci scalar curvatures. As  $r$  increases, the scalar curvatures ( $S \neq 1/2$ ) increase monotonically and grow rapidly near the surfaces ( $r = 1$ ) for  $d+1 = 3$  and 5, but not for  $d+1 = 4$ . In the case of  $S = 1/2$ , we find  $\mathcal{R}/4 = d(d+1)$ , *i.e.*, the Ricci scalar curvature of  $S^{d+1}$ . (See also the discussions around Eq.(6.28).)

The corresponding Bures volume is evaluated as

$$V|_{S=1/2} \equiv \int_{S^d} d\Omega_d \int_0^1 dr r^d \overbrace{\sqrt{\det(B_{\alpha\beta}|_{S=1/2})}}^{= \frac{1}{2^{d+1}} \frac{1}{\sqrt{1-r^2}}} = \left(\frac{\pi}{2}\right)^{[\frac{d}{2}]+1} \frac{1}{d!!} \quad (6.26)$$

where we used  $\int_0^1 dr r^d \frac{1}{\sqrt{1-r^2}} = \left(\frac{\pi}{2}\right)^{\frac{1+(-1)^d}{2}} \frac{(d-1)!!}{d!!}$  and

$$A(S^d) \equiv \int_{S^d} d\Omega_d = \frac{2}{(d-1)!!} (2\pi)^{[\frac{d}{2}]} \pi^{\frac{1-(-1)^d}{2}}. \quad (6.27)$$

The Bures metric (6.24) is exactly equal to the metric of the  $(d+1)$ -sphere of radius  $1/2$ :

$$\sum_{\alpha,\beta=1}^{d+1} B_{\alpha\beta}|_{S=1/2} dX_\alpha dX_\beta = \sum_{A=1}^{d+2} dX_A dX_A, \quad (6.28)$$

where

$$X_{\alpha=1,2,\dots,d+1} \equiv \frac{1}{2} r x_\alpha, \quad X_{d+2} \equiv \frac{1}{2} \sqrt{1-r^2} \quad \left( \sum_{\alpha=1}^{d+1} X_\alpha X_\alpha + X_{d+2} X_{d+2} = \left(\frac{1}{2}\right)^2 \right). \quad (6.29)$$

Due to  $0 \leq r \leq 1$ , the present Bures geometry is equal to the north hemisphere of the  $(d+1)$ -sphere with radius  $1/2$  (Fig.20).<sup>32</sup> The  $SO(d+1)$  symmetry of the Bures geometry corresponds to the rotational symmetry around the  $X_{d+2}$  axis for the northern hemisphere. This is a natural generalization of the known result for  $d=2$  [96]. The Bures distance between  $\rho(X)|_{S=1/2}$  and  $\rho(X')|_{S=1/2}$  coincides with the length of the geodesic curve connecting  $X_A$  and  $X'_A$  on the  $(d+1)$ -hemisphere (Fig.20):

$$D_{X,X'} = \frac{1}{2} \arccos \left( 4 \sum_{A=1}^{d+2} X_A X'_A \right) = \frac{1}{2} \arccos \left( 4 \sum_{\alpha=1}^{d+1} X_\alpha X'_\alpha + \sqrt{(1-r^2)(1-r'^2)} \right), \quad (6.31)$$

where  $r^2 = 4 \sum_{\alpha=1}^{d+1} X_\alpha X_\alpha$  and  $r'^2 = 4 \sum_{\alpha=1}^{d+1} X'_\alpha X'_\alpha$ .

## 7 Summary

Taking advantage of the analogies between the Landau model and the precessing spin system, we explored a higher dimensional generalization of the Zeeman-Dirac model and Bloch sphere with large spins. The  $SO(3)$  Zeeman-Dirac model has  $2S+1$  eigenvalues ranging from  $-S$  to  $+S$  with interval 1. Through the analyses using the concrete matrix realization, we showed that the  $SO(5)$  Zeeman-Dirac model has the same spectrum as the  $SO(3)$  model and that each level accommodates the  $SO(4)$  degeneracy. The  $SO(4)$  Zeeman-Dirac model was similarly analyzed to have  $2S+1$  energy levels, each of which accommodates the degeneracy attributed to the  $SO(3)$  symmetry. These properties are naturally generalized in higher dimensions:

- The  $SO(2k+1)$  Zeeman-Dirac model is defined for any non-negative integer  $2S$ . The  $SO(2k+1)$  Zeeman-Dirac Hamiltonian has the spectrum ranging from  $-S$  to  $+S$  with interval 1. There are  $2S+1$  energy levels with  $SO(2k)$  degeneracies. The distribution of the degeneracies has a peak at the equator of the Bloch  $2k$ -sphere. This peak becomes sharper as the dimension increases.

<sup>32</sup>One can confirm that the scalar curvature  $\mathcal{R}$  for the metric (6.25) and the Bures volume (6.26) are equal to those of the  $d+1$ -hemisphere of radius  $1/2$ :

$$\mathcal{R} = 4d(d+1), \quad V|_{S=1/2} = \frac{1}{2^{d+1}} \cdot \frac{A(S^{d+1})}{2}. \quad (6.30)$$



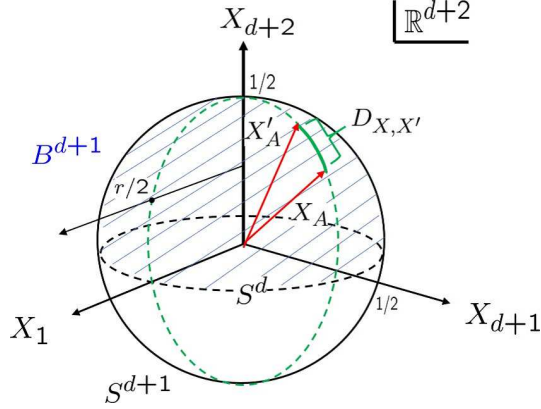


Figure 20: Bures geometry of  $S = 1/2$  is equal to the hyper-hemisphere.

- The  $SO(2k)$  Zeeman-Dirac model is defined only for odd non-negative integer  $2S$ . The  $SO(2k)$  Zeeman-Dirac Hamiltonian exhibits the spectrum ranging from  $-\frac{S}{2} - \frac{1}{4}$  to  $+\frac{S}{2} + \frac{1}{4}$  with interval  $1/2$  excluding the zero energy level. There are  $2S + 1$  energy levels with  $SO(2k - 1)$  degeneracies. The distribution of the degeneracies has two peaks at the opposite latitudes of the two hemispheres of the Bloch  $2k - 1$ -sphere. These two peaks become sharper and approach the equator as the dimension increases.

The  $d$  dimensional Bloch hyper-sphere geometry exists behind the  $SO(d + 1)$  Zeeman-Dirac model and accounts for the particular properties of this model: The  $SO(d)$  stabilizer group symmetry of this Bloch hyper-sphere endows the energy levels with the  $SO(2k)$  degeneracies. The  $SO(d)$  holonomy group of the Bloch hyper-sphere induces the Wilczek-Zee connection, which is identical to the  $SO(d)$  non-Abelian monopole. We investigated the density matrices described by the Bloch hyper-balls and the corresponding von Neumann entropies and Bures metrics. As one moves from the core of the Bloch hyper-ball to its hyper-sphere surface, the von Neumann entropy decreases monotonically and reaches its minimum value at the surface. The Bures statistical geometries of these density matrices represent various curved spherical geometries depending on the dimensions and spin magnitudes. These Bures geometries are rotationally spherical like the corresponding Bloch hyper-balls and have no singularities. They also show qualitatively different behavior depending on the parity of the dimensions. The Bures geometries for  $S = 1/2$  were explicitly evaluated and identified as the simple hyper-hemispheres with the same dimensions as the Bloch hyper-balls.

It may be worthwhile to emphasize that the quantum Nambu matrix geometry serves as the underlying geometry of M(atric) theory [98, 99]. This line of research thus provides an intersection where the exotic concept of non-commutative geometry and string theory meets the quantum information and quantum matter. It is also highly anticipated that the ingenuity of upcoming experiments with artificial gauge fields and synthetic dimensions will further facilitate access to novel physical phenomena of higher dimensional physics.

## Acknowledgments

This work was supported by JSPS KAKENHI Grant No. 21K03542.

## A Examples of the generalized gamma matrices

For a better understanding, we present a concrete matrix realization of the  $SO(5)$  generalized gamma matrices for  $S = 1$  and the  $SO(4)$  generalized gamma matrices for  $S = 3/2$ .

### A.1 $SO(5)$ $\Gamma_a$ for $S = 1$

The  $SO(5)$  gamma matrices with  $S = 1$  are given by the following  $10 \times 10$  matrices,

$$\begin{aligned}
\Gamma_1 = & \begin{pmatrix} 0 & 0 & 0 & 0 & \sqrt{2}i & 0 & 0 & 0 & 0 & 0 \\ 0 & 0 & 0 & i & 0 & 0 & i & 0 & 0 & 0 \\ 0 & 0 & 0 & 0 & 0 & \sqrt{2}i & 0 & 0 & 0 & 0 \\ 0 & -i & 0 & 0 & 0 & 0 & 0 & 0 & i & 0 \\ -\sqrt{2}i & 0 & 0 & 0 & 0 & 0 & 0 & 0 & 0 & \sqrt{2}i \\ 0 & 0 & -\sqrt{2}i & 0 & 0 & 0 & 0 & \sqrt{2}i & 0 & 0 \\ 0 & -i & 0 & 0 & 0 & 0 & 0 & 0 & i & 0 \\ 0 & 0 & 0 & 0 & 0 & -\sqrt{2}i & 0 & 0 & 0 & 0 \\ 0 & 0 & 0 & -i & 0 & 0 & -i & 0 & 0 & 0 \\ 0 & 0 & 0 & 0 & -\sqrt{2}i & 0 & 0 & 0 & 0 & 0 \end{pmatrix}, \quad \Gamma_2 = \begin{pmatrix} 0 & 0 & 0 & 0 & \sqrt{2} & 0 & 0 & 0 & 0 & 0 \\ 0 & 0 & 0 & -1 & 0 & 0 & 1 & 0 & 0 & 0 \\ 0 & 0 & 0 & 0 & 0 & -\sqrt{2} & 0 & 0 & 0 & 0 \\ 0 & -1 & 0 & 0 & 0 & 0 & 0 & 0 & 1 & 0 \\ \sqrt{2} & 0 & 0 & 0 & 0 & 0 & 0 & 0 & 0 & \sqrt{2} \\ 0 & 0 & -\sqrt{2} & 0 & 0 & 0 & 0 & -\sqrt{2} & 0 & 0 \\ 0 & 1 & 0 & 0 & 0 & 0 & 0 & 0 & -1 & 0 \\ 0 & 0 & 0 & 0 & 0 & -\sqrt{2} & 0 & 0 & 0 & 0 \\ 0 & 0 & 0 & 1 & 0 & 0 & -1 & 0 & 0 & 0 \\ 0 & 0 & 0 & 0 & \sqrt{2} & 0 & 0 & 0 & 0 & 0 \end{pmatrix}, \\
\Gamma_3 = & \begin{pmatrix} 0 & 0 & 0 & \sqrt{2}i & 0 & 0 & 0 & 0 & 0 & 0 \\ 0 & 0 & 0 & 0 & -i & i & 0 & 0 & 0 & 0 \\ 0 & 0 & 0 & 0 & 0 & 0 & -\sqrt{2}i & 0 & 0 & 0 \\ -\sqrt{2}i & 0 & 0 & 0 & 0 & 0 & 0 & \sqrt{2}i & 0 & 0 \\ 0 & i & 0 & 0 & 0 & 0 & 0 & 0 & i & 0 \\ 0 & -i & 0 & 0 & 0 & 0 & 0 & 0 & -i & 0 \\ 0 & 0 & \sqrt{2}i & 0 & 0 & 0 & 0 & 0 & 0 & -\sqrt{2}i \\ 0 & 0 & 0 & -\sqrt{2}i & 0 & 0 & 0 & 0 & 0 & 0 \\ 0 & 0 & 0 & 0 & -i & i & 0 & 0 & 0 & 0 \\ 0 & 0 & 0 & 0 & 0 & 0 & \sqrt{2}i & 0 & 0 & 0 \end{pmatrix}, \quad \Gamma_4 = \begin{pmatrix} 0 & 0 & 0 & \sqrt{2} & 0 & 0 & 0 & 0 & 0 & 0 \\ 0 & 0 & 0 & 0 & 1 & 1 & 0 & 0 & 0 & 0 \\ 0 & 0 & 0 & 0 & 0 & 0 & \sqrt{2} & 0 & 0 & 0 \\ \sqrt{2} & 0 & 0 & 0 & 0 & 0 & 0 & \sqrt{2} & 0 & 0 \\ 0 & 1 & 0 & 0 & 0 & 0 & 0 & 0 & 1 & 0 \\ 0 & 1 & 0 & 0 & 0 & 0 & 0 & 0 & 1 & 0 \\ 0 & 0 & \sqrt{2} & 0 & 0 & 0 & 0 & 0 & 0 & \sqrt{2} \\ 0 & 0 & 0 & \sqrt{2} & 0 & 0 & 0 & 0 & 0 & 0 \\ 0 & 0 & 0 & 0 & 1 & 1 & 0 & 0 & 0 & 0 \\ 0 & 0 & 0 & 0 & 0 & 0 & \sqrt{2} & 0 & 0 & 0 \end{pmatrix}, \\
\Gamma_5 = & \begin{pmatrix} 2 & 0 & 0 & 0 & 0 & 0 & 0 & 0 & 0 & 0 \\ 0 & 2 & 0 & 0 & 0 & 0 & 0 & 0 & 0 & 0 \\ 0 & 0 & 2 & 0 & 0 & 0 & 0 & 0 & 0 & 0 \\ 0 & 0 & 0 & 0 & 0 & 0 & 0 & 0 & 0 & 0 \\ 0 & 0 & 0 & 0 & 0 & 0 & 0 & 0 & 0 & 0 \\ 0 & 0 & 0 & 0 & 0 & 0 & 0 & 0 & 0 & 0 \\ 0 & 0 & 0 & 0 & 0 & 0 & 0 & 0 & 0 & 0 \\ 0 & 0 & 0 & 0 & 0 & 0 & -2 & 0 & 0 & 0 \\ 0 & 0 & 0 & 0 & 0 & 0 & 0 & -2 & 0 & 0 \\ 0 & 0 & 0 & 0 & 0 & 0 & 0 & 0 & -2 & 0 \end{pmatrix}, \tag{A.1}
\end{aligned}$$

which satisfy

$$\sum_{a=1}^5 \Gamma_a \Gamma_a = 12 \cdot \mathbf{1}_{10}, \quad [\Gamma_a, \Gamma_b, \Gamma_c, \Gamma_d] = -32 \sum_{e=1}^5 \epsilon_{abcde} \Gamma_e. \tag{A.2}$$

The corresponding  $SO(5)$  generators,  $\Sigma_{ab} = -i\frac{1}{4}[\Gamma_a, \Gamma_b]$ , satisfy  $\sum_{a < b=1}^5 \Sigma_{ab} \Sigma_{ab} = 6 \cdot \mathbf{1}_6$ . The  $SO(4)$  decomposition

$$(p, q) = (2, 0) \rightarrow (s_L, s_R) = (1, 0) \oplus (1/2, 1/2) \oplus (0, 1) \tag{A.3}$$

implies that the  $SO(4)$  matrices of  $\Sigma_{ab}$  take the following form

$$\Sigma_{\mu\nu} = \begin{pmatrix} \Sigma_{\mu\nu}^{(1,0)} & 0 & 0 \\ 0 & \Sigma_{\mu\nu}^{(1/2,1/2)} & 0 \\ 0 & 0 & \Sigma_{\mu\nu}^{(0,1)} \end{pmatrix}, \tag{A.4}$$

where

$$\Sigma_{\mu\nu}^{(1,0)} = \eta_{\mu\nu}^i S_i^{(1)}, \quad \Sigma_{\mu\nu}^{(1/2,1/2)} = \frac{1}{2} \eta_{\mu\nu}^{(+i)} \sigma_i \otimes \mathbf{1}_2 + \mathbf{1}_2 \otimes \frac{1}{2} \eta_{\mu\nu}^{(-i)} \sigma_i, \quad \Sigma_{\mu\nu}^{(0,1)} = \eta_{\mu\nu}^{(-i)} S_i^{(1)}. \tag{A.5}$$

We can confirm (A.4) using (A.1) explicitly.

## A.2 $SO(4)$ $\Gamma_\mu$ for $S = 3/2$

The  $SO(5)$  gamma matrices with  $S = 3/2$  are given by  $20 \times 20$  matrices. According to the  $SO(4)$  subgroup decomposition

$$(p, q) = (3, 0) \longrightarrow (s_L, s_R) = (3/2, 0) \oplus (1, 1/2) \oplus (1/2, 1) \oplus (0, 3/2) \quad (\text{A.6})$$

or

$$\mathbf{20} \longrightarrow \mathbf{4} \oplus \mathbf{6} \oplus \mathbf{6} \oplus \mathbf{4}, \quad (\text{A.7})$$

the  $SO(4)$  subspace of our interest  $(1, 1/2) \oplus (1/2, 1)$  corresponds to  $\mathbf{6} \oplus \mathbf{6}$  in (A.7). Thus, the  $SO(4)$  gamma matrices with  $S = 3/2$  are given by the following  $12 \times 12$  matrices:

$$\Gamma_\mu = \begin{pmatrix} 0 & Y_\mu \\ Y_\mu^\dagger & 0 \end{pmatrix}, \quad \Gamma_5 = \begin{pmatrix} \mathbf{1}_6 & 0 \\ 0 & -\mathbf{1}_6 \end{pmatrix}, \quad (\text{A.8})$$

where

$$Y_1 \equiv \begin{pmatrix} 0 & \sqrt{2}i & 0 & 0 & 0 & 0 \\ 0 & 0 & 2i & 0 & 0 & 0 \\ \sqrt{2}i & 0 & 0 & 0 & i & 0 \\ 0 & i & 0 & 0 & 0 & \sqrt{2}i \\ 0 & 0 & 0 & 2i & 0 & 0 \\ 0 & 0 & 0 & 0 & \sqrt{2}i & 0 \end{pmatrix}, \quad Y_2 \equiv \begin{pmatrix} 0 & \sqrt{2} & 0 & 0 & 0 & 0 \\ 0 & 0 & 2 & 0 & 0 & 0 \\ -\sqrt{2} & 0 & 0 & 0 & 1 & 0 \\ 0 & -1 & 0 & 0 & 0 & \sqrt{2} \\ 0 & 0 & 0 & -2 & 0 & 0 \\ 0 & 0 & 0 & 0 & -\sqrt{2} & 0 \end{pmatrix},$$

$$Y_3 \equiv \begin{pmatrix} 2i & 0 & 0 & 0 & 0 & 0 \\ 0 & \sqrt{2}i & 0 & 0 & 0 & 0 \\ 0 & -i & 0 & \sqrt{2}i & 0 & 0 \\ 0 & 0 & -\sqrt{2}i & 0 & i & 0 \\ 0 & 0 & 0 & 0 & -\sqrt{2}i & 0 \\ 0 & 0 & 0 & 0 & 0 & -2i \end{pmatrix}, \quad Y_4 \equiv \begin{pmatrix} 2 & 0 & 0 & 0 & 0 & 0 \\ 0 & \sqrt{2} & 0 & 0 & 0 & 0 \\ 0 & 1 & 0 & \sqrt{2} & 0 & 0 \\ 0 & 0 & \sqrt{2} & 0 & 1 & 0 \\ 0 & 0 & 0 & 0 & \sqrt{2} & 0 \\ 0 & 0 & 0 & 0 & 0 & 2 \end{pmatrix}. \quad (\text{A.9})$$

The matrices (A.8) satisfy

$$\sum_{\mu=1}^4 \Gamma_\mu \Gamma_\mu = 12 \cdot \mathbf{1}_{12}, \quad [[\Gamma_\mu, \Gamma_\nu, \Gamma_\rho]] = 40 \sum_{\sigma=1}^4 \epsilon_{\mu\nu\rho\sigma} \Gamma_\sigma. \quad (\text{A.10})$$

We can diagonalize  $\Gamma_4$  as

$$\mathcal{V}^\dagger \Gamma_4 \mathcal{V} = \begin{pmatrix} 2 \cdot \mathbf{1}_4 & 0 & 0 & 0 \\ 0 & 1 \cdot \mathbf{1}_2 & 0 & 0 \\ 0 & 0 & -1 \cdot \mathbf{1}_2 & 0 \\ 0 & 0 & 0 & -2 \cdot \mathbf{1}_4 \end{pmatrix}, \quad (\text{A.11})$$

where

$$\mathcal{V} = \frac{1}{\sqrt{6}} \begin{pmatrix} \sqrt{3} & 0 & 0 & 0 & 0 & 0 & | & 0 & 0 & -\sqrt{3} & 0 & 0 & 0 \\ 0 & 1 & 0 & 0 & -\sqrt{2} & 0 & | & \sqrt{2} & 0 & 0 & -1 & 0 & 0 \\ 0 & \sqrt{2} & 0 & 0 & 1 & 0 & | & -1 & 0 & 0 & -\sqrt{2} & 0 & 0 \\ 0 & 0 & \sqrt{2} & 0 & 0 & -1 & | & 0 & 1 & 0 & 0 & -\sqrt{2} & 0 \\ 0 & 0 & 1 & 0 & 0 & \sqrt{2} & | & 0 & -\sqrt{2} & 0 & 0 & -1 & 0 \\ 0 & 0 & 0 & \sqrt{3} & 0 & 0 & | & 0 & 0 & 0 & 0 & 0 & -\sqrt{3} \\ \hline \sqrt{3} & 0 & 0 & 0 & 0 & 0 & | & 0 & 0 & \sqrt{3} & 0 & 0 & 0 \\ 0 & \sqrt{2} & 0 & 0 & -1 & 0 & | & -1 & 0 & 0 & \sqrt{2} & 0 & 0 \\ 0 & 0 & 1 & 0 & 0 & -\sqrt{2} & | & 0 & -\sqrt{2} & 0 & 0 & 1 & 0 \\ 0 & 1 & 0 & 0 & \sqrt{2} & 0 & | & \sqrt{2} & 0 & 0 & 1 & 0 & 0 \\ 0 & 0 & \sqrt{2} & 0 & 0 & 1 & | & 0 & 1 & 0 & 0 & \sqrt{2} & 0 \\ 0 & 0 & 0 & \sqrt{3} & 0 & 0 & | & 0 & 0 & 0 & 0 & 0 & \sqrt{3} \end{pmatrix}. \quad (\text{A.12})$$

The  $SO(4)$  matrix generators,  $\Sigma_{\mu\nu}$ , are represented as

$$\Sigma_{\mu\nu} = \begin{pmatrix} \Sigma_{\mu\nu}^{(1, \frac{1}{2})} & 0 \\ 0 & \Sigma_{\mu\nu}^{(\frac{1}{2}, 1)} \end{pmatrix} = \begin{pmatrix} \eta_{\mu\nu}^{(+i)} S_i^{(1)} \otimes \mathbf{1}_2 + \mathbf{1}_3 \otimes \eta_{\mu\nu}^{(-i)} \frac{1}{2} \sigma_i & 0 \\ 0 & \eta_{\mu\nu}^i \frac{1}{2} \sigma_i \otimes \mathbf{1}_3 + \mathbf{1}_2 \otimes \eta_{\mu\nu}^{(-i)} S_i^{(1)} \end{pmatrix}. \quad (\text{A.13})$$

Note that  $\Sigma_{\mu\nu} \neq -i \frac{1}{4} [\Gamma_\mu, \Gamma_\nu]$ .

## B Matrix-valued quantum geometric tensor

Here, we consider  $N$ -fold degenerate quantum states represented by a  $M \times N$  rectangular matrix  $\Psi$ . This subject has been addressed in [100, 101]. We assume that  $\Psi$  satisfies the normalization condition,

$$\Psi^\dagger \Psi = \mathbf{1}_N. \quad (\text{B.1})$$

In terms of the rectangular matrix  $\Psi$ , the quantum geometric tensor [73] may be generalized as a matrix-valued quantity

$$\chi_{\mu\nu} = \partial_\mu \Psi^\dagger \partial_\nu \Psi - \partial_\mu \Psi^\dagger \Psi \cdot \Psi^\dagger \partial_\nu \Psi, \quad (\text{B.2})$$

which satisfies

$$\chi_{\mu\nu}^\dagger = \chi_{\nu\mu}. \quad (\text{B.3})$$

It is straightforward to show that the matrix quantum geometric tensor (B.2) is covariant under the gauge transformation:

$$\Psi \rightarrow \Psi \cdot g \quad (g^\dagger g = \mathbf{1}_N), \quad \chi_{\mu\nu} \rightarrow g^\dagger \chi_{\mu\nu} g. \quad (\text{B.4})$$

A field theoretical model of rectangular matrix-valued field with gauge symmetry is discussed in [102]. The target space of this model is the Grassmannian manifold,  $Gr(M, N) \simeq U(M)/(U(N) \otimes U(M-N))$ , which naturally realizes a matrix extension of the  $\mathbb{C}P^{N-1} = Gr(N, 1)$  with the Fubini-Study metric. We adopt the same procedure to explore the matrix version of the quantum geometric tensor. We introduce the auxiliary gauge field and the covariant derivative as

$$A_\mu = -i\Psi^\dagger \partial_\mu \Psi = A_\mu^\dagger, \quad D_\mu \Psi \equiv \partial_\mu \Psi - i\Psi A_\mu, \quad (D_\mu \Psi)^\dagger = \partial_\mu \Psi^\dagger + iA_\mu \Psi^\dagger, \quad (\text{B.5})$$

which transform as

$$A_\mu \rightarrow g^\dagger A_\mu g - ig^\dagger \partial_\mu g, \quad D_\mu \Psi \rightarrow (D_\mu \Psi) \cdot g, \quad (D_\mu \Psi)^\dagger \rightarrow g^\dagger \cdot (D_\mu \Psi)^\dagger. \quad (\text{B.6})$$

The matrix  $\chi_{\mu\nu}$  is simply represented as

$$\chi_{\mu\nu} = (D_\mu \Psi)^\dagger D_\nu \Psi. \quad (\text{B.7})$$

Equation (B.7) manifestly shows that  $\chi_{\mu\nu}$  is not generally gauge invariant, but rather covariant under the transformation (B.4). The matrix-valued quantum geometric tensor is decomposed into its symmetric (Hermitian) part and its antisymmetric (anti-Hermitian) part as

$$\chi_{\mu\nu} = G_{\mu\nu} + i\frac{1}{2}F_{\mu\nu}, \quad (\text{B.8})$$

where

$$G_{\mu\nu} \equiv \frac{1}{2}(\chi_{\mu\nu} + \chi_{\nu\mu}) = \frac{1}{2}((D_\mu \Psi)^\dagger D_\nu \Psi + (D_\nu \Psi)^\dagger D_\mu \Psi), \quad (\text{B.9a})$$

$$F_{\mu\nu} \equiv -i(\chi_{\mu\nu} - \chi_{\nu\mu}) = -i((D_\mu \Psi)^\dagger D_\nu \Psi - (D_\nu \Psi)^\dagger D_\mu \Psi). \quad (\text{B.9b})$$

Equation (B.3) implies that both  $G_{\mu\nu}$  and  $F_{\mu\nu}$  are Hermitian:

$$G_{\mu\nu}^\dagger = G_{\mu\nu}, \quad F_{\mu\nu}^\dagger = F_{\mu\nu}. \quad (\text{B.10})$$

It is obvious that both  $G_{\mu\nu}$  and  $F_{\mu\nu}$  transform as covariantly

$$G_{\mu\nu} \rightarrow g^\dagger G_{\mu\nu} g, \quad F_{\mu\nu} \rightarrow g^\dagger F_{\mu\nu} g. \quad (\text{B.11})$$

Using  $A_\mu$ , we can represent  $G_{\mu\nu}$  and  $F_{\mu\nu}$  as

$$G_{\mu\nu} = \frac{1}{2}(\partial_\mu \Psi^\dagger \partial_\nu \Psi + \partial_\nu \Psi^\dagger \partial_\mu \Psi) - \frac{1}{2}(A_\mu A_\nu + A_\nu A_\mu), \quad (\text{B.12a})$$

$$F_{\mu\nu} = \partial_\mu A_\nu - \partial_\nu A_\mu + i[A_\mu, A_\nu]. \quad (\text{B.12b})$$

Note that  $F_{\mu\nu}$  (B.12b) stand for the field strength of the gauge field  $A_\mu$ ,<sup>33</sup> while  $G_{\mu\nu}$  (B.12a) cannot be expressed only in terms of  $A_\mu$ . The matrix  $G_{\mu\nu}$  may be considered as a matrix-valued version of the quantum metric, because its trace gives rise to the quantum metric,

$$g_{\mu\nu} \equiv \text{tr}(G_{\mu\nu}). \quad (\text{B.14})$$

For groups with traceless generators, such as a special unitary group or a special orthogonal group, the trace of the quantum geometric tensor directly yields the quantum metric,

$$\text{tr}(\chi_{\mu\nu}) = \text{tr}(G_{\mu\nu}) + i \frac{1}{2} \overbrace{\text{tr}(F_{\mu\nu})}^{=0} = g_{\mu\nu} \quad \text{for } SU(N), SO(N), \text{ etc.} \quad (\text{B.15})$$

## C $SO(4)$ monopole harmonics from the $SO(4)$ non-linear realization

We revisit the analysis of the  $SO(4)$  Landau model [57, 81] from the perspective of non-linear realization.

### C.1 $SO(3)$ decomposition of the $SO(4)$ matrix generators

Due to  $SO(4) \simeq SU(2)_L \otimes SU(2)_R$ , the  $SO(4)$  irreducible representation is indexed by  $SU(2)$  bi-spin,  $s_L$  and  $s_R$ . The  $SO(4)$  matrix generators for an irreducible representation are generally given by

$$\Sigma_{\mu\nu}^{(s_L, s_R)} = \eta_{\mu\nu}^{(+i)} S_i^{(s_L)} \otimes \mathbf{1}_{2s_R+1} + \eta_{\mu\nu}^{(-i)} \mathbf{1}_{2s_L+1} \otimes S_i^{(s_R)}, \quad (\text{C.1})$$

where  $\eta_{\mu\nu}^{(\pm)i}$  are the 't Hooft tensors (3.5) and  $S_i^{(s_L)}$  and  $S_i^{(s_R)}$  signify the  $SU(2)$  matrices with spins  $s_L$  and  $s_R$ , respectively ( $\sum_{i=1}^3 S_i^{(s_{L/R})} S_i^{(s_{L/R})} = s_{L/R}(s_{L/R} + 1) \mathbf{1}_{2s_{L/R}+1}$ ). In detail,

$$\Sigma_{ij}^{(s_L, s_R)} = \epsilon_{ijk} (S_k^{(s_L)} \otimes \mathbf{1}_{2s_R+1} + \mathbf{1}_{2s_L+1} \otimes S_k^{(s_R)}), \quad (\text{C.2a})$$

$$\Sigma_{i4}^{(s_L, s_R)} = -\Sigma_{4i}^{(s_L, s_R)} = S_i^{(s_L)} \otimes \mathbf{1}_{2s_R+1} - \mathbf{1}_{2s_L+1} \otimes S_i^{(s_R)}. \quad (\text{C.2b})$$

The sum of their squares gives

$$\sum_{\mu > \nu = 1}^4 \Sigma_{\mu\nu}^{(s_L, s_R)} \Sigma_{\mu\nu}^{(s_L, s_R)} = 2(s_L(s_L + 1) + s_R(s_R + 1)) \mathbf{1}_{(2s_L+1)(2s_R+1)}. \quad (\text{C.3})$$

Note that  $\Sigma_{ij}^{(s_L, s_R)}$  (C.2a) represents the tensor product of two  $SU(2)$  spins, which is irreducibly decomposed by the  $SU(2)$  group as

$$O \Sigma_{ij}^{(s_L, s_R)} O^t = \epsilon_{ijk} \bigoplus_{J=|s_L-s_R|}^{s_L+s_R} S_k^{(J)}, \quad (\text{C.4})$$

<sup>33</sup>From (B.5), we obtain the field strength (B.12b) as

$$-i[D_\mu, D_\nu]\Psi = \Psi F_{\mu\nu}. \quad (\text{B.13})$$

where  $O$  denotes an orthogonal matrix of the Clebsch-Gordan coefficients,

$$O_{\alpha\beta} \equiv C_{s_L, m_L; s_R, m_R}^{(JM)} \quad (\alpha, \beta = 1, 2, \dots, (2s_L + 1)(2s_R + 1)), \quad (\text{C.5})$$

with identification

$$\begin{aligned} \alpha &\equiv (J, M) & (J = s_L + s_R, s_L + s_R - 1, \dots, |s_L - s_R|, \quad M = J, J - 1, \dots, -J), \\ \beta &\equiv (m_L, m_R) & (m_L = s_L, s_L - 1, \dots, -s_L, \quad m_R = s_R, s_R - 1, \dots, -s_R). \end{aligned} \quad (\text{C.6})$$

## C.2 $SO(4)$ monopole harmonics

Using the parameterization of  $x_\mu$  (4.2), we introduce the non-linear realization matrix

$$\Psi^{(s_L, s_R)} \equiv e^{-i \sum_{i=1}^3 \chi y_i \Sigma_i^{(s_L, s_R)}} = e^{(-i\chi \sum_{i=1}^3 y_i S_i^{(s_L)}) \otimes \mathbf{1}_{2s_R+1} + \mathbf{1}_{2s_L+1} \otimes (i\chi \sum_{i=1}^3 y_i S_i^{(s_R)})}, \quad (\text{C.7})$$

or

$$\Psi^{(s_L, s_R)} = D^{(s_L)}(\chi) \otimes D^{(s_R)}(-\chi) \quad (\text{C.8})$$

where

$$D^{(s_L)}(\chi) \equiv e^{-i\chi \sum_{i=1}^3 y_i S_i^{(s_L)}}, \quad D^{(s_R)}(-\chi) \equiv e^{i\chi \sum_{i=1}^3 y_i S_i^{(s_R)}}. \quad (\text{C.9})$$

The covariant derivative is defined as

$$D_\mu^{(s_L, s_R)} = \partial_\mu + iA_\mu^{(s_L, s_R)} \quad (\text{C.10})$$

where

$$A_\mu^{(s_L, s_R)} dx_\mu = -\frac{1}{1+x_4} \sum_{ij}^{(s_L, s_R)} x_j dx_i = -\frac{1}{1+x_4} \epsilon_{ijk} (S_k^{(s_L)} \otimes \mathbf{1}_{2s_R+1} + \mathbf{1}_{2s_L+1} \otimes S_k^{(s_R)}) x_j dx_i. \quad (\text{C.11})$$

The matrix  $\Psi^{(s_L, s_R)}$  satisfies

$$L_{\mu\nu}^{(s_L, s_R)} \Psi^{(s_L, s_R)} = \Psi^{(s_L, s_R)} \Sigma_{\mu\nu}^{(s_L, s_R)}, \quad (\text{C.12})$$

where

$$L_{\mu\nu}^{(s_L, s_R)} = -ix_\mu D_\nu^{(s_L, s_R)} + ix_\nu D_\mu^{(s_L, s_R)} + F_{\mu\nu}^{(s_L, s_R)}. \quad (\text{C.13})$$

Therefore, with

$$\Psi^{(s_L, s_R)} = \left( \Psi_1^{(s_L, s_R)} \quad \Psi_2^{(s_L, s_R)} \quad \Psi_3^{(s_L, s_R)} \quad \dots \quad \Psi_{(2s_L+1)(2s_R+1)}^{(s_L, s_R)} \right), \quad (\text{C.14})$$

we have

$$L_{\mu\nu}^{(s_L, s_R)} \Psi_\alpha^{(s_L, s_R)} = \Psi_\beta^{(s_L, s_R)} (\Sigma_{\mu\nu}^{(s_L, s_R)})_{\beta\alpha}. \quad (\text{C.15})$$

From (C.4), we can obtain the  $SU(2)$  irreducible decomposition of Eq.(C.15)

$$OL_{\mu\nu}^{(s_L, s_R)} O^t \cdot O \Psi_\alpha^{(s_L, s_R)} = O \Psi_\beta^{(s_L, s_R)} (\Sigma_{\mu\nu}^{(s_L, s_R)})_{\beta\alpha} \quad (\text{C.16})$$

as

$$\left( \bigoplus_{J=|s_L-s_R|}^{s_L+s_R} L_{\mu\nu}^{(J)} \right) \Phi_\alpha^{(s_L, s_R)} = \Phi_\beta^{(s_L, s_R)} (\Sigma_{\mu\nu}^{(s_L, s_R)})_{\beta\alpha}, \quad (\text{C.17})$$

where

$$\Phi_\alpha^{(s_L, s_R)} \equiv O \Psi_\alpha^{(s_L, s_R)}, \quad L_{\mu\nu}^{(J)} \equiv -ix_\mu D_\nu^{(J)} + ix_\nu D_\mu^{(J)} + F_{\mu\nu}^{(J)}, \quad (\text{C.18})$$

with

$$A_\mu^{(J)} dx_\mu \equiv -\frac{1}{1+x_4} \epsilon_{ijk} x_j S_k^{(J)} dx_i. \quad (\text{C.19})$$

Assume that  $J$  includes  $S$ ,

$$J = s_L + s_R, s_L + s_R - 1, \dots, S, \dots, |s_L - s_R|. \quad (\text{C.20})$$

We introduce the  $(2S+1)$  component ‘‘vector’’  $\phi_\alpha^{(s_L, s_R)}$  with its Ath component being

$$(\phi_\alpha^{(s_L, s_R)})_A \equiv C_{s_L, m_L; s_R, m_R}^{S, A} (\Psi_\alpha^{(s_L, s_R)})_{m_L, m_R} \quad (\alpha = 1, 2, \dots, (2s_L+1)(2s_R+1), \quad A = S, S-1, \dots, -S), \quad (\text{C.21})$$

or

$$(\phi_{m_L, m_R}^{(s_L, s_R)})_A \equiv C_{s_L, m'_L; s_R, m'_R}^{S, A} D^{(s_L)}(\chi)_{m'_L, m_L} D^{(s_R)}(-\chi)_{m'_R, m_R} \quad (-s_L \leq m_L \leq s_L, \quad -s_R \leq m_R \leq s_R), \quad (\text{C.22})$$

which is consistent with the expression in Refs.[57, 81]. These  $SO(4)$  monopole harmonics satisfy

$$L_{\mu\nu}^{(S)} \phi_{m_L, m_R}^{(s_L, s_R)} = \phi_{m_L, m_R}^{(s_L, s_R)} \Sigma_{\mu\nu}^{(s_L, s_R)} \quad (\text{C.23})$$

where

$$L_{\mu\nu}^{(S)} = -ix_\mu D_\nu^{(S)} + ix_\nu D_\mu^{(S)} + F_{\mu\nu}^{(S)}, \quad (\text{C.24})$$

with

$$A_\mu^{(S)} dx_\mu = -\frac{1}{1+x_4} \epsilon_{ijk} x_j S_k^{(S)} dx_i. \quad (\text{C.25})$$

Consequently,

$$\sum_{\mu > \nu} L_{\mu\nu}^{(S)2} \phi_{m_j, m_k}^{(s_L, s_R)} = 2(s_L(s_L+1) + s_R(s_R+1)) \phi_{m_j, m_k}^{(s_L, s_R)}. \quad (\text{C.26})$$

The ortho-normal relations of the  $SO(4)$  monopole harmonics are given by

$$\int_{S^3} d\Omega_3 \phi_\alpha^{(s_L, s_R)\dagger} \phi_\beta^{(s_L, s_R)} = A(S^3) \frac{D_{SO(3)}(S)}{D_{SO(4)}(s_L, s_R)} \delta_{\alpha\beta} = 2\pi^2 \frac{2S+1}{(2s_L+1)(2s_R+1)} \delta_{\alpha\beta}, \quad (\text{C.27})$$

where  $d\Omega_3 = \sin^2 \chi \sin \theta d\chi d\theta d\phi$ ,  $A(S^3) = \int_{S^3} d\Omega_3 = 2\pi^2$  and  $D_{SO(4)}(s_L, s_R) = (2s_L+1)(2s_R+1)$ .

## D Nested Bloch four-spheres from higher Landau levels

Here, we extend the analysis of the  $SO(5)$  lowest Landau level (Sec.3.2) to higher Landau levels. Since the quantum matrix geometry exhibits a nested structure in higher Landau levels [66, 61], the corresponding Zeeman-Dirac model also exhibits a nested structure. The Landau level  $N$  and the spin index  $S$  of the  $SU(2)$  monopole are identified with the  $SO(5)$  Casimir indices as

$$(p, q) = (N + 2S, N) \quad (\text{D.1})$$

or  $[l_1, l_2] = [\frac{1}{2}(p+q), \frac{1}{2}(p-q)] = [N+S, S]$ . The degeneracy of the  $N$ th Landau level is given by

$$D(N, S) \equiv \frac{1}{6}(N+1)(2S+1)(N+2S+2)(2N+2S+3). \quad (\text{D.2})$$

Evaluating the matrix coordinates with the  $N$ th Landau level eigenstates

$$(\Gamma_a)_{\alpha\beta} \propto \langle \psi_\alpha | x_a | \psi_\beta \rangle, \quad (\text{D.3})$$

we can derive  $D(N, S) \times D(N, S)$  generalized gamma matrices  $\Gamma_{a=1,2,3,4,5}$  [66], which satisfy

$$\sum_{a=1}^5 \Gamma_a \Gamma_a = 4 \frac{(N+S+2)S(S+1)}{N+S+1} \mathbf{1}_{D(N,S)} \propto \mathbf{1}. \quad (\text{D.4})$$

The matrix  $\Gamma_5$  is a diagonal matrix (see Fig.21 also)

$$\Gamma_5 = \frac{2}{N+S+1} \bigoplus_{n=0}^N (n+S+1) \left( \bigoplus_{\lambda=-S}^S \lambda \cdot \mathbf{1}_{(n+S+1+\lambda)(n+S+1-\lambda)} \right). \quad (\text{D.5})$$

With the  $SO(5)$  matrix generators  $\Sigma_{ab}$  of the representation (D.1),  $\Gamma_a$  transform as an  $SO(5)$  vector [66]<sup>34</sup>

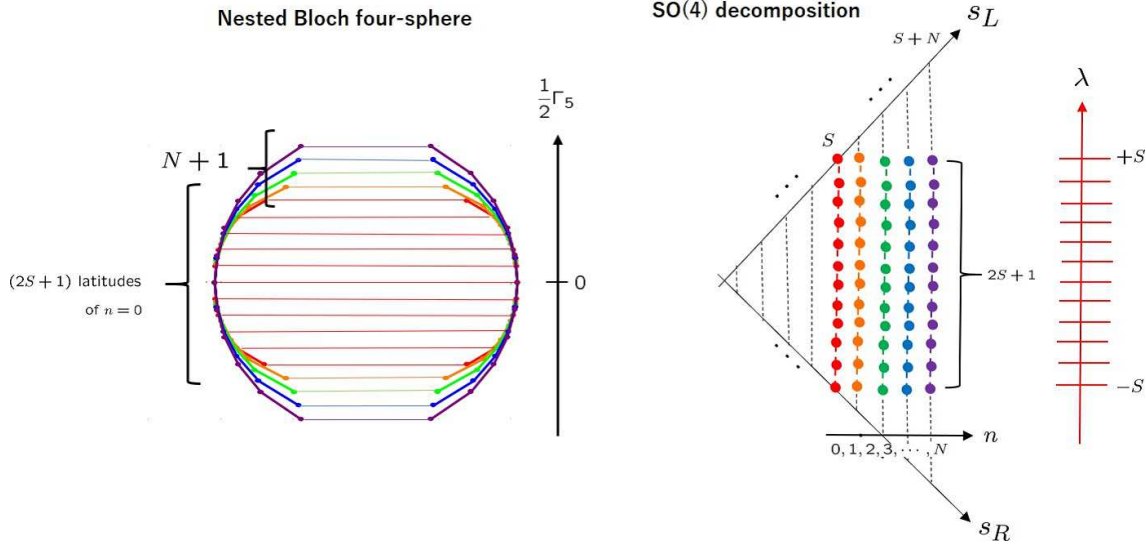


Figure 21: The  $SO(5)$  Zeeman-Dirac model for  $(p, q) = (2S + N, N)$ . Taken from [66].

$$[\Sigma_{ab}, \Gamma_c] = i\delta_{ac}\Gamma_b - i\delta_{bc}\Gamma_a. \quad (\text{D.7})$$

The  $SO(5)$  Zeeman-Dirac Hamiltonian is constructed as

$$H = \sum_{a=1}^5 x_a \cdot \frac{1}{2} \Gamma_a. \quad \left( \sum_{a=1}^5 x_a x_a = 1 \right) \quad (\text{D.8})$$

Since  $\Gamma_a$  transform as an  $SO(5)$  vector (D.7),  $\Psi = e^{i\xi \sum_{\mu=1}^4 y_\mu \Sigma_{\mu 5}}$  diagonalizes this Hamiltonian:

$$\Psi^\dagger \sum_{a=1}^5 (x_a \cdot \frac{1}{2} \Gamma_a) \Psi = \frac{1}{2} \Gamma_5. \quad (\text{D.9})$$

Therefore, the eigenvalues of the Hamiltonian (D.8) are given by

$$\frac{n+S+1}{N+S+1} \lambda \quad (n = 0, 1, 2, \dots, N, \quad \lambda = S, S-1, S-2, \dots, -S). \quad (\text{D.10})$$

<sup>34</sup>Unlike the generalized  $SO(5)$  gamma matrices in Sec.3.2, the commutators of the present  $\Gamma_a$  ( $N \geq 1$ ) do not yield the  $SO(5)$  matrix generators:

$$[\Gamma_a, \Gamma_b] \not\propto 4i\Sigma_{ab}. \quad (\text{D.6})$$



Notice that the energy levels are indexed by two quantities,  $n$  and  $\lambda$ , and the degeneracies are given by  $(n + S + \lambda + 1)(n + S - \lambda + 1)$ . Consequently, there are  $(N + 1)(2S + 1)$  energy levels (Fig.21). The Wilczek-Zee connection for the energy level (D.10) is equal to the  $SO(4)$  monopole gauge field:

$$A^{(s_L, s_R)} = -\frac{1}{1 + x_5} \Sigma_{\mu\nu}^{(s_L, s_R)} x_\nu dx_\mu, \quad (\text{D.11})$$

where  $\Sigma_{\mu\nu}^{(s_L, s_R)}$  are given by (C.1) with

$$(s_L, s_R) \equiv \left( \frac{n}{2} + \frac{S}{2} + \frac{\lambda}{2}, \frac{n}{2} + \frac{S}{2} - \frac{\lambda}{2} \right). \quad (\text{D.12})$$

The correspondence to the Landau model eigenstates is given as follows. For the  $SO(5)$  Landau model in the  $SO(4)$  monopole background with bi-spin index  $(I_+/2, I_-/2)$ , the Landau level  $L$  and the  $l$ th sector are related to the  $SO(5)$  and  $SO(4)$  Casimir indices as

$$(p, q) = (L + I_+ + I_- - l, L + l), \quad (\text{D.13a})$$

$$(s_L, s_R) = \left( \frac{I_+}{2}, \frac{I_-}{2} \right). \quad (\text{D.13b})$$

For the  $SO(5)$  Zeeman-Dirac model, the relations are given by (D.1) and (D.12). Consequently, their identification is given by

$$L = N - n, \quad l = n, \quad (\text{D.14a})$$

$$\frac{I_+}{2} = \frac{n}{2} + \frac{S}{2} + \frac{\lambda}{2}, \quad \frac{I_-}{2} = \frac{n}{2} + \frac{S}{2} - \frac{\lambda}{2}. \quad (\text{D.14b})$$

Let  $\Psi_\sigma$  denote the degenerate  $SO(5)$  spin-coherent states, all of which are aligned to the direction of the  $\lambda$ -latitude on the  $n$ th shell of the nested Bloch four-sphere (see the left of Fig.21), and  $\psi_{\alpha, N-n}^{(n)}$  stand for the  $(N - n)$ th Landau level eigenstates of the  $n$ -sector in the  $SO(4)$  monopole background with the bi-spin index,  $(\frac{n}{2} + \frac{S}{2} + \frac{\lambda}{2}, \frac{n}{2} + \frac{S}{2} - \frac{\lambda}{2})$ . They are related as

$$(\Psi_1 \quad \Psi_2 \quad \cdots \quad \Psi_{(n+S+\lambda+1)(n+S-\lambda+1)}) = \begin{pmatrix} \psi_{1, N-n}^{(n) \dagger} \\ \psi_{2, N-n}^{(n) \dagger} \\ \psi_{3, N-n}^{(n) \dagger} \\ \vdots \\ \psi_{D(N, S), N-n}^{(n) \dagger} \end{pmatrix}. \quad (\text{D.15})$$

## E $SO(d + 1)$ minimal Zeeman-Dirac models

We investigate the  $SO(d + 1)$  Zeeman-Dirac models made of the spinor representation gamma matrices. This minimal version of the  $SO(2k + 1)$  Zeeman-Dirac models has been analyzed in [103, 100, 104].

### E.1 $SO(d + 1)$ spinor representation matrices

The  $SO(2k + 1)$  gamma matrices  $\gamma_{a=1, 2, \dots, 2k+1}$  are given by

$$\gamma_{\mu=1, 2, \dots, 2k} = \begin{pmatrix} 0 & \bar{g}_\mu \\ g_\mu & 0 \end{pmatrix}, \quad \gamma_{2k+1} = \begin{pmatrix} \mathbf{1}_{2^{k-1}} & 0 \\ 0 & -\mathbf{1}_{2^{k-1}} \end{pmatrix}, \quad (\text{E.1})$$

where

$$g_\mu \equiv \{-i\gamma'_i, \mathbf{1}_{2^{k-1}}\}, \quad \bar{g}_\mu \equiv \{i\gamma'_i, \mathbf{1}_{2^{k-1}}\}, \quad (\text{E.2})$$

with  $SO(2k-1)$  gamma matrices  $\gamma'_{i=1,2,\dots,2k-1}$ . The matrices (E.1) satisfy

$$\{\gamma_a, \gamma_b\} = 2\delta_{ab}\mathbf{1}_{2^k}, \quad (\text{E.3})$$

and their commutators provide the  $SO(2k+1)$  matrix generators,

$$\sigma_{ab} \equiv -i\frac{1}{4}[\gamma_a, \gamma_b]. \quad (\text{E.4})$$

The matrices  $\sigma_{\mu\nu}$  are the matrix generators of the  $SO(2k)$  group:

$$\sigma_{\mu\nu} = \begin{pmatrix} \sigma_{\mu\nu}^{[+1/2]} & 0 \\ 0 & \sigma_{\mu\nu}^{[-1/2]} \end{pmatrix}, \quad (\text{E.5})$$

where

$$\sigma_{ij}^{[+1/2]} = \sigma_{ij}^{[-1/2]} \equiv \sigma'_{ij} \equiv -i\frac{1}{4}[\gamma'_i, \gamma'_j], \quad \sigma_{i,2k}^{[+1/2]} = -\sigma_{i,2k}^{[-1/2]} \equiv \frac{1}{2}\gamma'_i. \quad (\text{E.6})$$

## E.2 $SO(2k+1)$ minimal spin model

The spinor representation of the  $SO(2k+1)$  is specified by

$$[1/2, 1/2, \dots, 1/2]_{SO(2k+1)}. \quad (\text{E.7})$$

We construct the  $SO(2k+1)$  minimal Zeeman-Dirac Hamiltonian as

$$H = \sum_{a=1}^{2k+1} x_a \cdot \frac{1}{2}\gamma_a. \quad \left( \sum_{a=1}^{2k+1} x_a x_a = 1 \right), \quad (\text{E.8})$$

Using the non-linear realization matrix

$$\begin{aligned} \Psi &= e^{i\theta_{2k} \sum_{\mu=1}^{2k} y_\mu \sigma_{\mu,2k+1}} = \cos\left(\frac{\theta_{2k}}{2}\right) \mathbf{1}_{2^k} + 2i \sin\left(\frac{\theta_{2k}}{2}\right) \sum_{\mu=1}^{2k} y_\mu \sigma_{\mu,2k+1} \\ &= \frac{1}{\sqrt{2(1+x_{2k+1})}} \begin{pmatrix} (1+x_{2k+1})\mathbf{1}_{2^{k-1}} & -\sum_{\mu=1}^{2k} x_\mu \bar{g}_\mu \\ \sum_{\mu=1}^{2k} x_\mu g_\mu & (1+x_{2k+1})\mathbf{1}_{2^{k-1}} \end{pmatrix} = (\Psi^{(1/2)} \quad \Psi^{(-1/2)}), \end{aligned} \quad (\text{E.9})$$

we can diagonalize the Hamiltonian (E.8) as

$$\Psi^\dagger H \Psi = \frac{1}{2}\gamma_{2k+1}. \quad (\text{E.10})$$

The energy levels are  $\pm 1/2$  with degeneracy  $2^{k-1}$  for each. Equation (E.10) is invariant under the  $SO(2k)$  transformation,

$$\Psi \rightarrow \Psi \cdot e^{i\frac{1}{2}\omega_{\mu\nu}\sigma_{\mu\nu}}. \quad (\text{E.11})$$

We can derive the Bloch vector as

$$\Psi^{(\pm 1/2)\dagger} \gamma_a \Psi^{(\pm 1/2)} = \pm x_a \mathbf{1}_{2^{k-1}}. \quad (\text{E.12})$$

The matrix-valued quantum geometric tensor is given by

$$\chi_{\theta_\mu \theta_\nu}^{(\pm 1/2)} = \partial_{\theta_\mu} \Psi^{(\pm 1/2)\dagger} \partial_{\theta_\nu} \Psi^{(\pm 1/2)} - \partial_{\theta_\mu} \Psi^{(\pm 1/2)\dagger} \Psi^{(\pm 1/2)} \Psi^{(\pm 1/2)\dagger} \partial_{\theta_\nu} \Psi^{(\pm 1/2)} \quad (\theta_\mu, \theta_\nu = \theta_{2k}, \theta_{2k-1}, \dots, \theta, \phi). \quad (\text{E.13})$$

The trace of (E.13) provides the metric of the  $2k$ -sphere:

$$g_{\theta_\mu\theta_\nu}^{(\pm 1/2)} = \frac{1}{2} \text{tr}(\chi_{\theta_\mu\theta_\nu}^{(\pm 1/2)} + \chi_{\theta_\nu\theta_\mu}^{(\pm 1/2)}) = 2^{k-3} \text{diag}(1, \sin^2 \theta_{2k}, \sin^2 \theta_{2k} \sin^2 \theta_{2k-1}, \dots, \prod_{i=3}^{2k} \sin^2 \theta_i, \sin^2 \theta \prod_{i=3}^{2k} \sin^2 \theta_i). \quad (\text{E.14})$$

The Wilczek-Zee connections are derived as

$$A^{(\pm 1/2)} = -i\Psi^{(\pm 1/2)\dagger} d\Psi^{(\pm 1/2)} = -\frac{1}{1+x_{2k+1}} \sigma_{\mu\nu}^{[\pm 1/2]} x_\nu dx_\mu, \quad (\text{E.15})$$

which coincide with the gauge fields of the  $SO(2k)$  monopoles for  $\text{ch}_k^{(\pm 1/2)} = \pm 1$ . The corresponding curvature  $F_{\theta_\mu\theta_\nu} = \partial_{\theta_\mu} A_{\theta_\nu} - \partial_{\theta_\nu} A_{\theta_\mu} + i[A_{\theta_\mu}, A_{\theta_\nu}]$  represents the antisymmetric part of the matrix-valued quantum geometric tensor:

$$F_{\theta_\mu\theta_\nu}^{(\pm 1/2)} = -i(\chi_{\theta_\mu\theta_\nu}^{(\pm 1/2)} - \chi_{\theta_\nu\theta_\mu}^{(\pm 1/2)}) = \frac{1}{2} e_{\theta_\mu}^{\mu'} \wedge e_{\theta_\nu}^{\nu'} \sigma_{\mu'\nu'}^{[\pm 1/2]}, \quad (\text{E.16})$$

where  $e_{\theta_\mu}^{\mu'}$  denote the vielbein of  $S^{2k}$ .

### E.3 $SO(2k)$ minimal spin model

The spinor representation of the  $SO(2k)$  is designated by

$$[1/2, 1/2, \dots, \pm 1/2]_{SO(2k)}. \quad (\text{E.17})$$

We introduce the  $SO(2k)$  minimal Zeeman-Dirac Hamiltonian as

$$H = \sum_{\mu=1}^{2k} x_\mu \cdot \frac{1}{2} \gamma_\mu \quad \left( \sum_{\mu=1}^{2k} x_\mu x_\mu = 1 \right), \quad (\text{E.18})$$

and the non-linear realization matrix as

$$\Psi = e^{i\theta_{2k-1} \sum_{i=1}^{2k-1} y_i \sigma_{i,2k}} = \cos\left(\frac{\theta_{2k-1}}{2}\right) \mathbf{1}_{2k} + 2i \sin\left(\frac{\theta_{2k-1}}{2}\right) \sum_{i=1}^{2k-1} y_i \sigma_{i,2k} = \begin{pmatrix} U & 0 \\ 0 & U^\dagger \end{pmatrix}, \quad (\text{E.19})$$

where

$$\sigma_{i,2k} \equiv \begin{pmatrix} \sigma_{i,2k}^{[+1/2]} & 0 \\ 0 & \sigma_{i,2k}^{[-1/2]} \end{pmatrix} = \frac{1}{2} \begin{pmatrix} \gamma'_i & 0 \\ 0 & -\gamma'_i \end{pmatrix}, \quad (\text{E.20a})$$

$$U = e^{i\theta_{2k-1} \sum_{i=1}^{2k-1} y_i \sigma_{i,2k}^{[+1/2]}} = \frac{1}{\sqrt{2(1+x_{2k})}} ((1+x_{2k}) \mathbf{1}_{2^{k-1}} + i x_i \gamma'_i). \quad (\text{E.20b})$$

The Hamiltonian (E.18) is diagonalized as

$$\tilde{\Psi}^\dagger H \tilde{\Psi} = \frac{1}{2} \gamma_{2k+1} \quad (\text{E.21})$$

where

$$\tilde{\Psi} = \Psi V = \frac{1}{\sqrt{2}} \begin{pmatrix} U & -U \\ U^\dagger & U^\dagger \end{pmatrix} = (\tilde{\Psi}^{(1/2)} \tilde{\Psi}^{(-1/2)}) \quad (\text{E.22})$$

with

$$V = \frac{1}{\sqrt{2}} \begin{pmatrix} \mathbf{1}_{2^{k-1}} & -\mathbf{1}_{2^{k-1}} \\ \mathbf{1}_{2^{k-1}} & \mathbf{1}_{2^{k-1}} \end{pmatrix}. \quad (\text{E.23})$$

The energy levels are  $\pm 1/2$  with degeneracy  $2^{k-1}$  for each. Equation (E.21) is invariant under the  $SO(2k-1)$  transformation,

$$\tilde{\Psi} \rightarrow \tilde{\Psi} \cdot e^{i\frac{1}{2}\omega_{ij}\tilde{\sigma}_{ij}} \quad (\tilde{\sigma}_{ij} \equiv \mathcal{V}^\dagger \sigma_{ij} \mathcal{V}). \quad (\text{E.24})$$

We can derive the Bloch vector as

$$(\tilde{\Psi}^{(\pm 1/2)})^\dagger \gamma_\mu \tilde{\Psi}^{(\pm 1/2)} = \pm x_\mu \mathbf{1}_{2^{k-1}}. \quad (\text{E.25})$$

The matrix-valued quantum geometric tensor is given by

$$\chi_{\theta_i \theta_j}^{(\pm 1/2)} = \partial_{\theta_i} (\tilde{\Psi}^{(\pm 1/2)})^\dagger \partial_{\theta_j} \tilde{\Psi}^{(\pm 1/2)} - \partial_{\theta_j} (\tilde{\Psi}^{(\pm 1/2)})^\dagger \partial_{\theta_i} \tilde{\Psi}^{(\pm 1/2)} \quad (\tilde{\Psi}^{(\pm 1/2)})^\dagger \partial_{\theta_j} \tilde{\Psi}^{(\pm 1/2)} \quad (\theta_i, \theta_j = \theta_{2k-1}, \dots, \theta_3, \theta, \phi). \quad (\text{E.26})$$

Its symmetric part of  $\chi_{\theta_i \theta_j}^{(\lambda)}$  provides the metric of  $(2k-1)$ -sphere:

$$g_{\theta_i \theta_j}^{(\pm 1/2)} = \frac{1}{2} \text{tr}(\chi_{\theta_i \theta_j}^{(\pm 1/2)} + \chi_{\theta_j \theta_i}^{(\pm 1/2)}) = 2^{k-3} \text{diag}(1, \sin^2 \theta_{2k-1}, \sin^2 \theta_{2k-1} \sin^2 \theta_{2k-2}, \dots, \prod_{i=3}^{2k-1} \sin^2 \theta_i, \sin^2 \theta \prod_{i=3}^{2k-1} \sin^2 \theta_i). \quad (\text{E.27})$$

The Wilczek-Zee connections are derived as

$$-i\tilde{\Psi}^\dagger d\tilde{\Psi} = V^\dagger (-i\Psi^\dagger d\Psi) V = \begin{pmatrix} A^{(+1/2)} & * \\ * & A^{(-1/2)} \end{pmatrix}, \quad (\text{E.28})$$

where  $A^{(+1/2)} = A^{(-1/2)}$  is equal to the gauge field of the  $SO(2k-1)$  monopole:

$$\begin{aligned} A^{(+1/2)} &= -i(\tilde{\Psi}^{(1/2)})^\dagger d\tilde{\Psi}^{(1/2)} = -i\frac{1}{2}(U^\dagger dU + U dU^\dagger) = -\frac{1}{1+x_{2k}} \sigma'_{ij} x_j dx_i \\ &= -i(\tilde{\Psi}^{(-1/2)})^\dagger d\tilde{\Psi}^{(-1/2)} = A^{(-1/2)}. \end{aligned} \quad (\text{E.29})$$

The corresponding curvature  $F_{\theta_i \theta_j} = \partial_{\theta_i} A_{\theta_j} - \partial_{\theta_j} A_{\theta_i} + i[A_{\theta_i}, A_{\theta_j}]$  represents the antisymmetric part of (E.26):

$$F_{\theta_i \theta_j}^{(1/2)} = -i(\chi_{\theta_i \theta_j}^{(1/2)} - \chi_{\theta_j \theta_i}^{(1/2)}) = \frac{1}{2} e^{i'}_{\theta_i} \wedge e^{j'}_{\theta_j} \sigma'_{i'j'} = F_{\theta_i \theta_j}^{(-1/2)}, \quad (\text{E.30})$$

where  $e^{i'}_{\theta_i}$  denote the vielbein of  $S^{2k-1}$ .

## References

- [1] Ingemar Bengtsson, Karol Zyczkowski, “*Geometry of Quantum States*”, Cambridge University Press (2006).
- [2] Michael A. Nielsen, Issac L. Chuang, “*Quantum Computation and Quantum Information*”, Cambridge University Press (2005).
- [3] Dariusz Chruściński, Andrzej Jamiolkowski, “*Geometric Phases in Classical and Quantum Mechanics*”, Birkhäuser (2004).
- [4] Arno Bohm, Ali Mostafazadeh, Hiroyasu Koizumi, Qian Niu, Joseph Zwanziger, “*The Geometric Phase in Quantum Systems*”, Springer (2003).
- [5] Päivi Törmä, “*Essay: Where Can Quantum Geometry Lead Us?*”, Phys. Rev. Lett. 131 (2023) 240001; arXiv:2312.11516.

- [6] J. Lambert, E. S. Sorensen, “*From Classical to Quantum Information Geometry: A Guide for Physicists*”, New J. Phys. 25 (2023) 081201; arXiv:2302.13515.
- [7] Felix Bloch, “*Nuclear Induction*”, Phys. Rev. 70 (1946) 460.
- [8] M. V. Berry, “*Quantum phase factors accompanying adiabatic changes*”, Proc. R. Soc. Lond. A 392 (1984) 45-57.
- [9] G. Herzberg, H. C. Longuet-Higgins, “*Intersection of potential energy surfaces in polyatomic molecules*”, Disc. Faraday Soc. 35 (1963) 77.
- [10] Frank Wilczek, A. Zee, “*Appearance of Gauge Structure in Simple Dynamical Systems*”, Phys. Rev. Lett. 52 (1984) 2111.
- [11] Frank Wilczek, “*Introduction to quantum matter*”, Phys. Scr. B T146 (2012) 014001.
- [12] H.M. Price, O. Zilberberg, T. Ozawa, I. Carusotto, N. Goldman, “*Four-Dimensional Quantum Hall Effect with Ultracold Atoms*”, Phys. Rev. Lett. 115 (2015) 195303.
- [13] H.M. Price, O. Zilberberg, T. Ozawa, I. Carusotto, N. Goldman, “*Measurement of Chern numbers through center-of-mass responses*”, Phys. Rev. B 93 (2016) 245113.
- [14] T. Ozawa, H.M. Price, N. Goldman, O. Zilberberg, I. Carusotto, “*Synthetic dimensions in integrated photonics: From optical isolation to four-dimensional quantum Hall physics*”, Phys. Rev. A 93 (2016) 043827.
- [15] You Wang, Hannah M. Price, Baile Zhang, Y. D. Chong, “*Circuit implementation of a four-dimensional topological insulator*”, Nature Communications, 11 (2020) 2356; arXiv:2001.07427.
- [16] Shaojie Ma, Hongwei Jia, Yangang Bi, Shangqiang Ning, Fuxin Guan, Hongchao Liu, Chenjie Wang, Shuang Zhang, “*Gauge Field Induced Chiral Zero Mode in Five-Dimensional Yang Monopole Metamaterials*”, Phys.Rev.Lett. 130 (2023) 243801; arXiv:2305.13566.
- [17] Xingen Zheng, Tian Chen, Weixuan Zhang, Houjun Sun, Xiangdong Zhang, “*Exploring topological phase transition and Weyl physics in five dimensions with electric circuits*”, Phys.Rev.Res. 4 (2022) 033203; arXiv:2209.08492.
- [18] S. Sugawa, F. Salces-Carcoba, A. R. Perry, Y. Yue, I. B. Spielman, “*Second Chern number of a quantum-simulated non-Abelian Yang monopole*”, Science 360 (2018) 1429-1434.
- [19] Sh. Ma, Y. Bi, Q. Guo, B. Yang, O. You, J. Feng, H.-B. Sun, Sh. Zhang, “*Linked Weyl surfaces and Weyl arcs in photonic metamaterials*”, Science 373 (2021) 572-576.
- [20] Tracy Li, Lucia Duca, Martin Reitter, Fabian Grusdt, Eugene Demler, Manuel Endres, Monika Schleier-Smith, Immanuel Bloch, Ulrich Schneider, “*Bloch state tomography using Wilson lines*”, Science 352 (2016) 1094; arXiv:1509.02185.
- [21] John R. Klauder, “*The action option and a Feynman quantization of spinor fields in terms of ordinary c-numbers*”, Ann. Phys. 11 (1960) 123-168.
- [22] J. M. Radcliffe “*Some properties of coherent spin states*”, J. Phys. A 4 (1971) 313.
- [23] A. M. Perelomov, “*Coherent States for Arbitrary Lie Group*”, Commun. Math. Phys. 26 (1972) 222-236.

- [24] F. A. Arecchi, Eric Courtens, Robert Gilmore, Harry Thomas, “*Atomic coherent states in quantum optics*”, Phys. Rev. A 6 (1972) 2211.
- [25] P.A.M. Dirac, “*Quantized singularities in the electromagnetic field*”, Proc. Royal Soc. London, A133 (1931) 60-72.
- [26] T.T. Wu, C.N. Yang, “*Dirac Monopoles without Strings: Monopole Harmonics*”, Nucl.Phys. B107 (1976) 365-380.
- [27] F. T. Hioe and J. H. Eberly, “*N-Level Coherence Vector and Higher Conservation Laws in Quantum Optics and Quantum Mechanics*”, Phys. Rev. Lett. 47 (1981) 838.
- [28] Gen Kimura, “*The Bloch Vector for N-Level Systems*”, Phys. Lett. A 314 (2003) 339; arXiv:quant-ph/0301152.
- [29] Mark S. Byrd, Navin Khaneja, “*Characterization of the positivity of the density matrix in terms of the coherence vector representation*”, Phys. Rev. A 68 (2003) 062322; arXiv:quant-ph/0302024.
- [30] Ansgar Graf and Frédéric Piéchon, “*Berry Curvature and Quantum Metric in N-band systems : an Eigenprojector Approach*”, Phys. Rev. B 104 (2021) 085114; arXiv:2102.09899.
- [31] Cameron J.D. Kemp, Nigel R. Cooper and F. Nur Ünal, “*Nested-sphere description of the N-level Chern number and the generalized Bloch hypersphere*”, Phys. Rev. Research 4 (2022) 023120; arXiv:2110.06934.
- [32] J. Anandan, L. Stodolsky, “*Some geometrical considerations of Berry’s phase*”, Phys. Rev. D 35 (1987) 2597-2600.
- [33] D M Gitman and A L Shelepin, “*Coherent states of SU(N) groups*”, J. Phys. A: Math. Theor. 26 (1993) 313-327; hep-th/9208017.
- [34] Sven Gnutzmann and Marek Kuś, “*Coherent states and the classical limit on irreducible SU<sub>3</sub> representations*”, J. Phys. A: Math. Gen. 31 (1998) 9871-9896.
- [35] A. V. Gorshkov, M. Hermele, V. Gurarie, C. Xu, P. S. Julienne, J. Ye, P. Zoller, E. Demler, M. D. Lukin, A. M. Rey, “*Two-orbital SU(N) magnetism with ultracold alkaline-earth atoms*”, Nature Physics (2010) 289 - 295; arXiv:0905.2610.
- [36] Mark S. Byrd, Luis J. Boya, Mark Mims, E. C. G. Sudarshan, “*Geometry of n-state systems, pure and mixed*”, Journal of Physics: Conference Series 87 (2007) 012006.
- [37] D. Uskov, A.R.P. Rau, “*Geometric phase and Bloch-sphere construction for SU(N) groups with a complete description of the SU(4) group*”, Phys. Rev. A 78 (2008) 022331; arXiv:0801.2091.
- [38] A. R. P. Rau, “*Symmetries and Geometries of Qubits, and Their Uses*”, Symmetry 13 (2021) 1732; arXiv:2103.14105.
- [39] Zhifeng Zhang, Haoqi Zhao, Shuang Wu, Tianwei Wu, Xingdu Qiao, Zihe Gao, Ritesh Agarwal, Stefano Longhi, Natalia M. Litchinitser, Li Ge, Liang Feng, “*Spin orbit microlaser emitting in a four-dimensional Hilbert space*”, Nature 612 (2022) 246.
- [40] C. Alden Mead, “*Molecular Kramers Degeneracy and Non-Abelian Adiabatic Phase Factors*”, Phys. Rev. Lett. 59 (1987) 161.

- [41] J.E. Avron, L. Sadun, J. Segert, and B. Simon, “*Topological Invariants in Fermi Systems with Time-Reversal Invariance*”, Phys.Rev.Lett.61 (1988) 1329.
- [42] J.E. Avron, L. Sadun, J. Segert, and B. Simon, “*Chern Numbers, Quaternions, and Berry’s Phases in Fermi Systems*”, Commun.Math.Phys.124 (1989) 124.
- [43] C. Alden Mead, “*The geometric phase in molecular systems*”, Rev.Mod.Phys. 64 (1992) 51.
- [44] S.E. Apsel, C.C. Chancey, M.C.M. O’Brien, “*Berry phase and the  $\Gamma_8 \otimes (\tau_2 \oplus \epsilon)$  Jahn-Teller system*”, Phys.Rev. B 45 (1992) 5251.
- [45] Congjun Wu, Jiang-ping Hu, Shou-cheng Zhang, “*Exact  $SO(5)$  Symmetry in the Spin-3=2 Fermionic System*”, Phys.Rev. Lett. 91 (2003) 186402.
- [46] Jonas Larson, Erik Sjöqvist, Patrik Öhberg, “*Conical Intersections in Physics*”, Springer (2020).
- [47] Shinsei Ryu, Andreas P. Schnyder, Akira Furusaki, Andreas W. W. Ludwig, “*Topological insulators and superconductors: ten-fold way and dimensional hierarchy*”, New J. Phys. 12 (2010) 065010; arXiv:0912.2157.
- [48] Péter Lévy, “*Geometrical description of  $SU(2)$  Berry phases*”, Phys. Rev. A 41, 2837 (1990).
- [49] Péter Lévy, “*Quaternionic gauge fields and the geometric phase*”, J. Math. Phys. 32, 2347 (1991).
- [50] M.T. Johnsson, J.R. Aitchison, “*The  $SU(2)$  instanton and the adiabatic evolution of two Kramers doublets*”, Jour. Phys. A: Math. Gen. 30 (1997) 2085.
- [51] Chen Ning Yang, “*Generalization of Dirac’s monopole to  $SU2$  gauge fields*”, J. Math. Phys. 19 (1978) 320.
- [52] Chen Ning Yang, “ *$SU2$  monopole harmonics*”, J. Math. Phys. 19 (1978) 2622.
- [53] A.A. Belavin, A.M. Polyakov, A.S. Schwartz and Yu. S. Tyupkin, “*Pseudoparticle solutions of the Yang-Mills equations*”, Phys. Lett. B 59 (1975) 85-87.
- [54] F.D.M. Haldane, “*Fractional quantization of the Hall effect: a hierarchy of incompressible quantum fluid states*”, Phys. Rev. Lett. 51 (1983) 605-608.
- [55] Kazuki Hasebe, “*Relativistic Landau Models and Generation of Fuzzy Spheres*”, Int.J.Mod.Phys.A 31 (2016) 1650117; arXiv:1511.04681.
- [56] Goro Ishiki, Takaki Matsumoto, Hisayoshi Muraki, “*Kähler structure in the commutative limit of matrix geometry*”, JHEP 08 (2016) 042; arXiv:1603.09146.
- [57] Kazuki Hasebe, “ *$SO(4)$  Landau Models and Matrix Geometry*”, Nucl.Phys. B 934 (2018) 149-211; arXiv:1712.07767.
- [58] G. Ishiki, T. Matsumoto, H. Muraki, “*Information metric, Berry connection, and Berezin-Toeplitz quantization for matrix geometry*”, Phys. Rev. D 98 (2018) 026002; arXiv:1804.00900.
- [59] Kaho Matsuura, Asato Tsuchiya, “*Matrix geometry for ellipsoids*”, Prog. Theor. Exp. Phys. 2020, 033B05.
- [60] V. P. Nair, “*Landau-Hall states and Berezin-Toeplitz quantization of matrix algebras*”, Phys.Rev. D 102 (2020) 025015; arXiv:2001.05040.

- [61] Kazuki Hasebe, “*SO(5) Landau models and nested matrix geometry*”, Nucl.Phys. B 956 (2020) 115012; arXiv:2002.05010.
- [62] Hiroyuki Adachi, Goro Ishiki, Takaki Matsumoto, Kaishu Saito, “*The matrix regularization for Riemann surfaces with magnetic fluxes*”, Phys. Rev. D 101 (2020) 106009; arXiv:2002.02993.
- [63] Kazuki Hasebe, “*SO(5) Landau Model and 4D Quantum Hall Effect in The SO(4) Monopole Background*”, Phys. Rev. D 105 (2022) 065010; arXiv:2112.03038.
- [64] Harold C. Steinacker, “*Quantum (Matrix) Geometry and Quasi-Coherent States*”, J. Phys. A: Math. Theor. 54 (2021) 055401; arXiv:2009.03400.
- [65] Hiroyuki Adachi, Goro Ishiki, Satoshi Kanno, “*Vector bundles on fuzzy Kähler manifolds*”, arXiv:2210.01397.
- [66] Kazuki Hasebe, “*Generating Quantum Matrix Geometry from Gauge Quantum Mechanics*”, Phys. Rev. D 108 (2023) 126023; arXiv:2310.01051.
- [67] Wei Zhu, Chao Han, Emilie Huffman, Johannes S. Hofmann, and Yin-Chen He, “*Uncovering Conformal Symmetry in the 3D Ising Transition: State-Operator Correspondence from a Quantum Fuzzy Sphere Regularization*”, Phys.Rev. X 13 (2023) 021009; arXiv:2210.13482.
- [68] Yale Fan, Willy Fischler, and Eric Kubischta, “*Quantum error correction in the lowest Landau level*”, Phys.Rev. A 107 (2023) 032411; arXiv:2210.16957.
- [69] Gabriel Cuomo, Zohar Komargodski, Márk Mezei, Avia Raviv-Moshe, “*Spin Impurities, Wilson Lines and Semiclassics*”, JHEP 06 (2022) 112; arXiv:2202.00040.
- [70] Gabriel Cuomo, Anton de la Fuente, Alexander Monin, David Pirtskhalava, Riccardo Rattazzi, “*Rotating superfluids and spinning charged operators in conformal field theory*”, Phys.Rev. D 97 (2018) 045012; arXiv:1711.02108.
- [71] Gabriel Cuomo, Luca V. Delacretaz, Umang Mehta, “*Large Charge Sector of 3d Parity-Violating CFTs*”, JHEP 05 (2021) 115; arXiv:
- [72] J. J. Sakurai, Jim Napolitano, “*Modern Quantum Mechanics*”, Cambridge University Press (2020).
- [73] J. P. Provost and G. Vallee, “*Riemannian Structure on Manifolds of Quantum States*”, Commun. Math. Phys. 76 (1980) 289-301.
- [74] Balázs Hetényi and Péter Lévy, “*Fluctuations, uncertainty relations, and the geometry of quantum state manifolds*”, Phys. Rev. A 108 (2023) 032218.
- [75] Alexander Avdoshkin, Fedor K. Popov, “*Extrinsic geometry of quantum states*”, Phys. Rev. B 107 (2023) 245136.
- [76] Kazuki Hasebe, “*A Unified Construction of Skyrme-type Non-linear sigma Models via The Higher Dimensional Landau Models*”, Nucl.Phys. B 961 (2020) 115250; arXiv:2006.06152.
- [77] S.C. Zhang and J.P. Hu, “*A four dimensional generalization of the quantum Hall effect*”, Science 294 (2001) 823; cond-mat/0110572.
- [78] Judith Castelino, Sangmin Lee, Washington Taylor, “*Longitudinal 5-branes as 4-spheres in Matrix theory*”, Nucl.Phys.B526 (1998) 334-350; hep-th/9712105.



- [79] H. Grosse, C. Klimcik, P. Presnajder, “*On Finite 4D Quantum Field Theory in Non-Commutative Geometry*”, Commun.Math.Phys. 180 (1996) 429-438; hep-th/9602115.
- [80] Kazuki Hasebe, “*Chiral topological insulator on Nambu 3-algebraic geometry*”, Nucl.Phys. B 886 (2014) 681-690; arXiv:1403.7816.
- [81] V.P. Nair, S. Randjbar-Daemi, “*Quantum Hall effect on  $S^3$ , edge states and fuzzy  $S^3/\mathbf{Z}_2$* ”, Nucl.Phys. B679 (2004) 447-463; hep-th/0309212.
- [82] Z. Guralnik, S. Ramgoolam, “*On the Polarization of Unstable D0-Branes into Non-Commutative Odd Spheres*”, JHEP 0102 (2001) 032; hep-th/0101001.
- [83] Sanjaye Ramgoolam, “*Higher dimensional geometries related to fuzzy odd-dimensional spheres*”, JHEP 0210 (2002) 064; hep-th/0207111.
- [84] Anirban Basu, Jeffrey A. Harvey, “*The M2-M5 Brane System and a Generalized Nahm’s Equation*”, Nucl.Phys. B713 (2005) 136-150; hep-th/0412310.
- [85] M. M. Sheikh-Jabbari, M. Torabian, “*Classification of All 1/2 BPS Solutions of the Tiny Graviton Matrix Theory*”, JHEP 0504 (2005) 001; hep-th/0501001.
- [86] K. Hasebe and Y. Kimura, “*Dimensional Hierarchy in Quantum Hall Effects on Fuzzy Spheres*”, Phys.Lett. B 602 (2004) 255; hep-th/0310274.
- [87] Kazuki Hasebe, “*Higher Dimensional Quantum Hall Effect as A-Class Topological Insulator*”, Nucl.Phys. B 886 (2014) 952-1002; arXiv:1403.5066.
- [88] Kazuki Hasebe, “*Higher (Odd) Dimensional Quantum Hall Effect and Extended Dimensional Hierarchy*”, Nucl.Phys. B 920 (2017) 475-520; arXiv:1612.05853.
- [89] See for instance, F. Iachello, “*Lie Algebras and Applications*”, (Lecture Notes in Physics) Springer (2006).
- [90] Kazuki Hasebe, “*Hopf Maps, Lowest Landau Level, and Fuzzy Spheres*”, SIGMA 6 (2010) 071; arXiv:1009.1192.
- [91] Joshua DeBellis, Christian Saemann, Richard J. Szabo, “*Quantized Nambu-Poisson Manifolds and n-Lie Algebras*”, J.Math.Phys.51 (2010) 122303; arXiv:1001.3275.
- [92] Takehiro Azuma, Maxime Bagnoud, “*Curved-space classical solutions of a massive supermatrix model*”, Nucl.Phys. B 651 (2003) 71-86; hep-th/0209057.
- [93] Takehiro Azuma, “*Matrix models and the gravitational interaction*”, hep-th/0401120.
- [94] Donald Bures, “*An extension of Kakutani’s theorem on infinite product measures to the tensor product of semifinite  $w^*$ -algebras*”, Trans. Am. Math. Soc. 135 (1969) 199.
- [95] Armin Uhlmann, “*The Metric of Bures and the Geometric Phase*”, in Gielerak et al. (ed.), “*Quantum Groups and Related Topics*”, Dordrecht: Kluwer Academic Pub.
- [96] Matthias Hübner, “*Explicit computation of the Bures distance for density matrices*”, Phys. Lett. A 163 (1992) 239.
- [97] See for instance, Chap.8 in Steven Weinberg, “*Gravitation and cosmology*”, Wiley (1972).

- [98] Pei-Ming Ho, Yutaka Matsuo, “*Nambu bracket and M-theory*”, Prog. Theo. Exp. Phys. (2016) 06A104; arXiv:1603.09534.
- [99] Jonathan Bagger, Neil Lambert, Sunil Mukhi, Constantinos Papageorgakis, “*Multiple Membranes in M-theory*”, Phys. Rep. 527 (2013) 1-100; arXiv:1203.3546.
- [100] Péter Lévy, “*Non-abelian Born-Oppenheimer electric gauge force and the natural metric on Hilbert subspaces*”, Phys. Rev. A 45 (1992) 1339.
- [101] Jerzy Nowakowski, Andrzej Trautman, “*Natural connections on Stiefel bundles are sourceless gauge fields*”, Jour. Math, Phys. 19 (1978) 1100.
- [102] A.J. MacFarlane, “*Generalizations of  $\sigma$ -models and  $Cp^N$  models, and instantons*”, Phys. Lett. B 82 (1979) 239.
- [103] M.G. Benedict, L.G. Fehér, Z. Horváth, “*Monopoles and instantons from Berry’s phase*”, Jour. Math. Phys. 30 (1989) 1727.
- [104] Péter Lévy, “*Modified symmetry generators and the geometric phase*”, Jour. Phys. A 27 (1994) 2875.